CHEMICAL REVIEWS

Review

pubs.acs.org/CR

Recent Development of Polymer Electrolyte Membranes for Fuel Cells

Hongwei Zhang and Pei Kang Shen*

State Key Laboratory of Optoelectronic Materials and Technologies and Key Laboratory of Low-Carbon Chemistry & Energy Conservation of Guangdong Province, School of Physics and Engineering, Sun Yat-sen University, Guangzhou 510275, P.R. China

CONTENTS

1. INTRODUCTION

Polymer electrolyte membrane fuel cells (PEMFCs) have increasingly received worldwide attention because of their potential application in transportation and in stationary and portable electronics. PEMFC technology already provides sufficient performance and durability to be competitive with alternative technologies in some of these applications. Commercialization of fuel cells and deployment in these early market applications is expected to lead to further improvement in performance, durability, and cost. It is clear from the publication list, as shown in Figure 1, that the PEMFCs are objects of intent interest. During

Received: January 29, 2011
Published: February 16, 2012

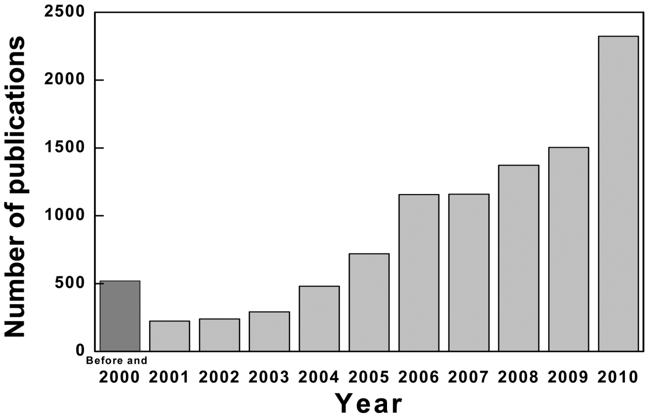

Figure 1. Summary of the number of publications found in four scientific databases (ScienceDirect, ACS Publications, Wiley InterScience, and SpringerLink). The search keywords were "membrane fuel cell" and "membrane fuel cells" in all fields.

the past 5 years, the number of publications concerning PEMFCs has risen steeply. In particular, research on polymer electrolyte membranes (PEMs) is very active.

Current PEMFCs containing state-of-the-art perfluorosulfonic acid ionomer (PFSI)-based membranes require humidification of the inlet gas. The necessary humidification system is a major part of the fuel cell system cost. The development of high-temperature membranes capable of operating at low relative humidity with sufficiently high ionic conductivity is a challenge but will decrease the cost and system complexity associated with humidification. Therefore, it is no exaggeration to say that improvement in the properties of the membrane would significantly improve the performance of the PEMFCs.

A fuel cell is an electrochemical device that directly converts the chemical energy of a fuel (e.g., hydrogen or methanol) into electrical energy. Figure 2 is a schematic view of a hydrogen-fueled PEMFC with a proton-conducting membrane. Two plates sandwich a membrane to form a "membrane electrode assembly" (MEA), which is the core component of a PEMFC. A PEM functions as (i) a separator to prevent mixing of reactants; (ii) a conductor for protons from anode to cathode; (iii) an electrical insulator to drive electrons through an external path to the cathode; and (iv) a structural framework to support the electrocatalysts (in the case of catalyst-coated membrane (CCM)). When such a H_2/O_2 PEMFC is operating, the anode side is supplied with hydrogen and the cathode side is fed with oxygen or air. Under the electrocatalysis, hydrogen is split into protons and electrons through an oxidation reaction at the anode. The protons travel across the PEM, and the electrons transfer in an external circuit to the cathode. At the cathode, oxygen combines with protons and electrons to form water through a reduction reaction. Thus, a closed circuit that generates electrical energy is formed.

To be applied in PEMFCs, the advanced membrane materials should meet the following requirements: (i) high ionic conductivity; (ii) low fuel permeability; (iii) good thermal and hydrolytic stability; (iv) excellent electrochemical stability in an aggressive environment; (v) substantial morphological and dimensional stability; (vi) outstanding mechanical properties in both the dry and hydrated states; (vii) sufficient water uptake and moderate swelling; (viii) suppressed water transport through diffusion and electroosmosis; (ix) easy fabrication to form the MEA, and finally, more importantly from a practical point of view, (x) a competitive low-cost and sufficient long-term durability.

Although considerable progress in PEMs has been made in the last several decades, the durability and cost are still two major obstacles hindering widespread application. The purpose of this review is to sum up the recent progress on PEMs as a whole. Polyphosphazene, a fascinating material, is excluded from this review because of few reports about polyphosphazene-based PEMs in the past 5 years and the existence of recent excellent reviews.[1−3] Computer simulations and theoretical considerations of PEMs are also not included because they have already been extensively reviewed in a book series and in topical reviews.[4−17]

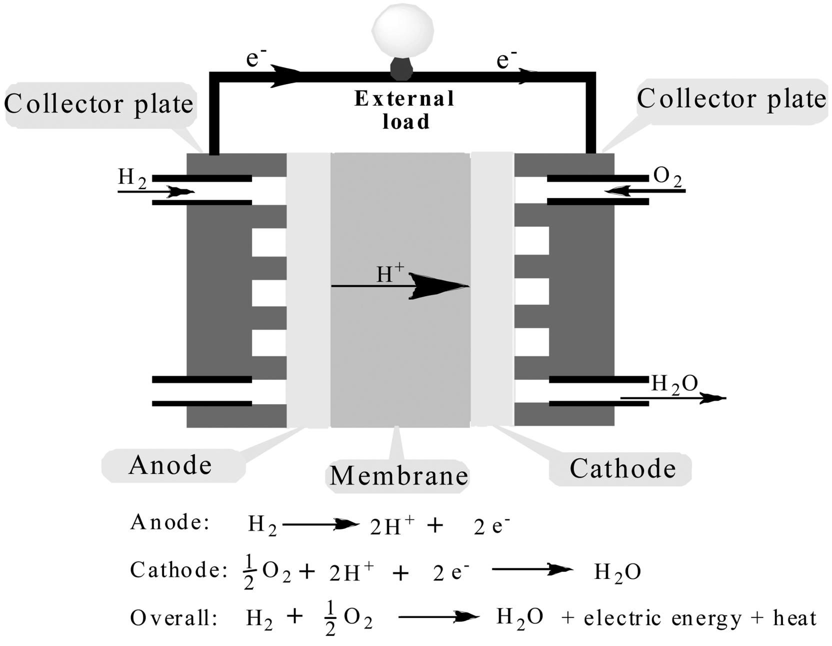

$$\text{Anode:}\quad H_2 \longrightarrow 2H^+ + 2e^-$$

$$\text{Cathode:}\quad \frac{1}{2}O_2 + 2H^+ + 2e^- \longrightarrow H_2O$$

$$\text{Overall:}\quad H_2 + \frac{1}{2}O_2 \longrightarrow H_2O + \text{electric energy} + \text{heat}$$

Figure 2. Schematic diagram of a PEMFC.

This article focuses on five different types of membranes organized according to their main chain composition and functional groups. These types are PFSI membranes, partially fluorinated acid ionomer membranes, nonfluorinated acid ionomer membranes, polybenzimidazole (PBI)/H_3PO_4 membranes, and alkaline ionomer membranes. The properties and applications of those membranes are described one after another and compared in the following sections. The synthesis strategies for these membrane materials are briefly reviewed and discussed. The future directions for PEM research and development in fuel cell applications and the possible approaches for the synthesis and modification of "future" PEMs are discussed.

2. PERFLUOROSULFONIC ACID IONOMER MEMBRANES

The perfluorosulfonic acid ionomer membranes, represented by Nafion (a registered trademark of DuPont Co.), are the most commonly used PEMs and have served as benchmarks for membrane performances because of their excellent chemical and electrochemical stabilities as well as outstanding proton conductivity. They have unique structures that consist of poly(tetra-fluoroethylene)-like hydrophobic main backbones and pendant side chains with hydrophilic terminated sulfonic groups. The former endows them with superior properties of structural integrity, and the latter gives them desirable proton conductivity when fully hydrated. Water plays an important role in the proton conductivity by impacting the formation, dimensions, and connectivity of ionic pathways in PEMs. With increasing water content, the PEM constituents are characteristically separated into hydrophobic regions and water-filled hydrophilic cluster phase domains. These cluster phase domains are connected by short narrow nanochannels that form random water-containing cluster networks embedded in the continuous, spongelike fluorocarbon phases.[18,19] Consider, for example, Nafion117 membranes, in which the total exchangeable proton sites are estimated to be 2.5×10^{19} sites cm^{-2} or 4.2×10^{-5} mol cm^{-2}.[20] The total number of water molecules per sulfonate group (denoted as λ) is often used to describe the hydration extent of a PEM. The possible evolution of Nafion from the dry state to a fully hydrated state may be described as follows.[21−42] For $\lambda < 2$, only isolated small water clusters are formed and Nafion behaves like an insulator. As λ reaches ~2, a percolation threshold of proton conductivity occurs. But at this time, the water molecules are bound tightly to the sulfonate groups on the inner surface of the channels and clusters to form solvation shells, which leads to a higher activation energy for proton transfer and lower proton mobility, resulting in very low proton conductivity. As λ increases from 2 to 5, the water clusters become increasingly bigger and the channels become broader. Some of the water molecules exist as free water, but the majority of them are confined through the coordination of hydronium ions by multiple sulfonate groups via the strong electrostatic interaction between them. This impedes a structural transport (Grotthuss) mechanism and results in a predominantly vehicular transport mechanism. At this stage, proton mobility is the major factor determining proton conductivity.

For λ between 5 and 7, the Nafion membrane undergoes a morphology transition and structural reorganization. The water clusters and channels are further expanded and become partially interconnected. A continuous path for proton conduction begins to be developed. Furthermore, the proton conductivity and the percentage of free water in PEM increase gradually. The structural transport mechanism coexists with the vehicular transport mechanism and becomes more significant. Finally, for λ from 7 to a water-saturated hydration level, the average distance between sulfonate groups becomes larger due to obvious Nafion swelling, and a well-developed percolated network is formed. Moreover, the percentage of free water increases markedly. The proton conductivity shows an apparently monotonic increase and finally approaches a value similar to that of bulk water when the proton transfer in Nafion is mostly through a structural transport mechanism.

Because water plays a vital role for proton transportation in Nafion, the dependence of the conductivity on water makes Nafion unsuitable at temperatures lower than 0 °C and at temperatures higher than 100 °C because of the decrease of conductivity induced by the inherent properties of water (freezing or boiling).[43,44] Besides this shortcoming, Nafion also suffers from other drawbacks, such as (i) insufficient resistance to methanol crossover; (ii) poor mechanical and chemical stability at elevated temperatures; and, most prominently, (iii) high cost resulting from the complicated manufacturing process required. To overcome these disadvantages, considerable efforts have been devoted to modification of conventional polymers or new alternative membranes. There have been no new PFSI membranes synthesized, but many modified conventional PFSI membranes were reported in the last several years. Several different approaches for the modification of PFSI membranes have been explored, including (i) physical or chemical treatment; (ii) reinforcement by porous support materials; and (iii) addition of organic or inorganic compounds. Table 1 provides a summary of modified PFSI membranes.

2.1. PFSI Membranes Treated by Physical or Chemical Methods

The main strategy for simple physical or chemical treatment is to form a heterogeneous ultrathin layer on the Nafion surface or to adjust the nanostructure of the Nafion membrane. Heterogeneous ultrathin layers formed by preparing bifunctional carboxylate/sulfonate PFSI membrane,[45,46] by immersing Nafion membrane into dopamine aqueous solution,[47] by treating Nafion membrane under perfluoroheptane (C_7F_{16}) and argon (Ar) plasma,[48,49] or by depositing Pd or Pd alloy ultrathin layers onto Nafion surfaces[50−56] are aimed at suppressing methanol crossover. But Nafion membranes with deposited Pd or Pd alloy ultrathin layers do not work well because of the cracks caused by the different swelling ratios of the sputtered metal layer and Nafion membrane, although there does exist a so-called "pseudo-proton conducting" phenomenon in Pd membranes.[57] Treatment by uniaxial prestretching,[58] by application of an electric field,[59] by ion irradiation,[60] by thermal annealing,[61,62] and with Sc-CO_2[63,64] all aim at adjusting the nanostructure in Nafion membranes, and they all do result in improvements in the modified PFSI membranes. However, there is no reduction in cost because the PFSI membranes modified by these methods are even more costly.

2.2. PFSI Membranes Reinforced with Porous Supporting Materials

To reduce the costs of PFSI membranes, an efficient method of reinforcement by impregnating PFSI into low-cost sub-μm porous support materials is widely employed (Figure 3). The porous PTFE membrane is most often selected as a reinforcing material owing to its excellent chemical stability and good mechanical strength. The reinforced PFSI membranes, having a thinner membrane thickness by virtue of their higher strength, have a lower membrane resistance and need less of the expensive

Table 1. Summary of Modified PFSI Membranes

base membrane	modified methods	main conclusions and comments	reference
PFSI membranes treated by physical or chemical methods			
Nafion	carboxylate/sulfonate bifunctional treatment	dramatically reduced water permeability and modestly decreased proton conductivity	45, 46
Nafion	depositing polydopamine nanolayer	about 50% decrease of methanol permeability and slightly decreased proton conductivity	47
PFSI membrane	perfluoroheptane and argon plasma deposition	greatly improved mechanical strength and greatly decreased methanol permeability	48, 49
Nafion	depositing ultrathin palladium or its alloy layer	improvements in methanol permeability are often weakened by the cracks deriving from the different swelling ratios between the ultrathin metal layer and Nafion membrane	50−57
recast Nafion	uniaxially prestretched treatment	shows 44.8% higher direct methanol fuel cell (DMFC) power density than that of Nafion117	58
Nafion solution	applying an electric field during casting	better PEMFC performance than Nafion117	59
Aciplex	ion irradiation	conductivity increased 3 orders of magnitude in dry conditions	60
Nafion	thermal annealing treatment	dependent on annealing temperature and not always resulting in improvement	61, 62
PFSI membrane	supercritical carbon dioxide treatment	decreases methanol permeability 41.8% without sacrificing proton conductivity	63, 64
Nafion	dissolving in dimethylsulfoxide (DMSO) at 190 °C and recasting	properties similar to Nafion115	65
Nafion	adopting modified Pt electrocatalyst supports	increases power density of a H_2/air PEMFC from 345 to 456 mW cm^{-2} at 100 °C and 30% RH	66, 67
Reinforced PFSI membranes by porous supporting materials			
Nafion/PTFE	conventional impregnation process	better PEMFC performance than that of pure Nafion membrane	68−70
Nafion/ePTFE	impregnation process employing surfactant under low inner gas pressure	rather better durability and stability with an open circuit voltage (OCV) degradation rate of 3.3 mV h^{-1}	71, 72
Nafion/ultrahigh molecular weight polyethylene (UHMWPE)	conventional impregnation process	significantly lowered methanol crossover and thin membrane thickness	73
Nafion/poly(vinylidene fluoride) (PVDF)	conventional impregnation process	good improvements in DMFC performance over plain Nafion	74
Nafion/poly(tetrafluoroethylene (PTFE)/hygroscopic particles	in situ incorporation of a third composition (nanosilicate or nano-ZrP particles) combined with conventional impregnation process	possesses a self-humidified functionality suitable for low relative humidity (RH) and elevated temperature operation	75−80
PFSI composite membranes incorporated with organic or inorganic compounds			
Nafion/organic methanol-blocking fillers	impregnating Nafion membranes into the solution of organic fillers or their precursors (e.g., PANI, PVI, PPV, chitosan (CS), PEDOT, SSt, sulfonated poly(tetrafluoroethylene-*co*-hexafluoropropylene) (FEP), etc.)	improvements in methanol permeation are mostly offset by reduced proton conductivity	81−98
Nafion/polypyrrole/Pt	in situ polymerization of pyrrole monomers with Pt precursors in Nafion membrane	significantly enhanced PEMFC performance; large reduction in methanol permeability with moderate sacrifice of proton conductivity	99
Nafion/PVI/Pd	complexation followed by impregnation	better performance of DMFC fed with 5 M methanol and oxygen only at 30 °C	100
Nafion/organic polymer constituents	direct blending of solution between Nafion and sulfonated poly(aryl ether ketone) (SPAEK), sulfonated poly(ether ether ketone) (SPEEK), nitrated SPEEK, or PBI	reduction in proton conductivity and improved methanol crossover; readily undergoes phase separation due to the differences in specific gravity and solvent concentration profile	101−105
Nafion/PAH-PSS layer by later (LbL) film	LbL technique	very small methanol permeation improvements with large reduction in proton conductivity	106
Nafion/inert hygroscopic inorganic fillers	blending method or sol−gel process using Nafion and inert hygroscopic inorganic particles or their precursors (e.g., fullerene, WO_3, SiO_2, TiO_2, $Sr(OH)_2$, zeolite, MMT, ORMOSIL, PVOS, zirconia, GPTMS, TEOS, etc.)	enhancing the water retention property, improving thermal stability, and reducing methanol crossover; however, often decreasing proton conductivity due to negative effects of these inert hygroscopic fillers such as insulation for proton and poor compatibility between fillers and Nafion	107−138

Table 1. continued

base membrane	modified methods	main conclusions and comments	reference
PFSI composite membranes incorporated with organic or inorganic compounds			
Nafion/inorganic proton-conductive fillers	blending method or impregnation process using Nafion and proton-conductive particles or their precursors (e.g., α-ZrP, heteropoly acid (HPA), BPO_4, ErTfO)	proton conductivity similar to Nafion; improved MEA and methanol crossover, but HPA leaching often occurs	139−152
Nafion/inorganic binary component fillers	incorporating two kinds of inorganic particles such as zeolite-Pt, $SiO_2-Cs_{2.5}H_{0.5}PWO_{40}$, SiO_2−SZ, ZrO_2-SiO_2, TiO_2-WO_3	better water management and reasonable proton conductivity at high temperatures and low humidity	153−162
Nafion/bifunctional fillers	incorporating inorganic particles with both hydrophilic and proton-conductive functions (e.g., acid-functionalized multiwalled carbon nanotubes (MWCNTs), acid- or CS- functionalized methylcyclopentadienyl manganese tricarbonyl (MMT), sulfonic acid-functionalized zeolite beta, sulfonic acid-functionalized silica and polysiloxanes)	great improvements in methanol permeability without a large conductivity sacrifice, some of them providing reasonable proton conductivity above 100 °C	163−185
Pt-SiO_2/SPEEK/PTFE/Nafion/Pt-SiO_2	PTFE-reinforced SPEEK/Nafion composite membrane containing SiO_2-supported platinum catalyst	self-humidifying function, OCV of 0.98 V; maximum power density value of 0.8 W cm^{-2} with dry H_2/O_2 at 60 °C	186
PFSI composite membrane	NA	operating >6000 h at 120 °C and 50% RH fed with H_2/air and only 1% to 1‰ degradation rate of conventional Nafion MEA	187

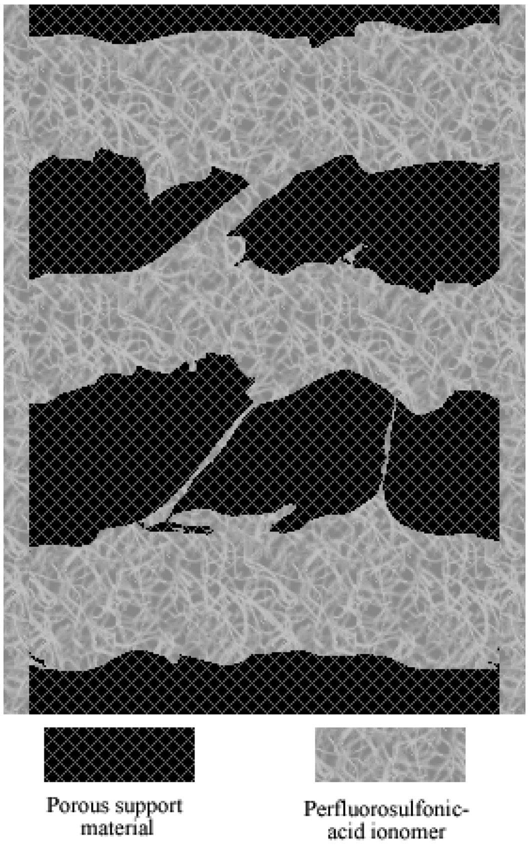

Figure 3. Schematic representation of the cross-sectional morphology of a reinforced PFSI membrane.

PFSI. In addition, they have other advantages such as improved dimensional stability, remarkable durability, chemical stability, and reduced methanol permeability resulting from suppressed swelling of the PFSI in porous PTFE membranes.

However, the great difference of hydrophilicity between the hydrophilic PFSI solution and the hydrophobic pores of the PTFE often induces the formation of voids and bubbles in the reinforced PFSI/PTFE membranes. When the impregnation process is done under negative pressure, the problem is greatly alleviated because the gas pressure in the capillaries of the porous substrate matrix is the most important factor for solution impregnation. The PFSI/PTFE PEM fabricated from a PFSI solution with 5 vol % surfactant concentration under a pressure of 5 × 10^2 Pa shows high resistance to hydrogen gas permeability over 4500 dry/wet cycles, indicating better durability and stability caused by the improved interface contact.[71] An improved method proposed on this basis for the preparation of reinforced PFSI/PTFE PEM with high durability and high chemical stability consisted of impregnating PTFE frame micropores into the Na^+ form of the surfactant-containing Nafion ionomers under a pressure of 5 × 10^2 Pa. These Nafion/PTFE PEMs are then heat-treated at 270 °C to induce cross-linking of the Nafion ionomer. In an in situ accelerating RH cyclic experiment at 90 °C, the degradation in the OCV of the fuel cell assembled with the PEM as-prepared above is 3.3 mV h^{-1}, which is significantly lower than that of 13.2 mV h^{-1} for a fuel cell assembled with the commercial Nafion membrane.[72] Similarly, impregnating PFSI into the alternative substrates such as microporous UHMWPE[73] and electrospun PVDF[74] for DMFC also leads to better performance than plain Nafion membrane because the reduction of proton conductivity can be compensated by decreased membrane thickness and significantly reduced methanol crossover.

Some attempts at incorporating a third component into reinforced PFSI membranes have been made. When hygroscopic nanosilicate particles[75−77] or ZrP nanoparticles[78−80] are incorporated in situ into reinforced Nafion/PTFE membranes, the reinforced Nafion/PTFE membranes so prepared are endowed with a self-humidification functionality by the excellent water-retention property of these third-component particles, which may make the membranes suitable for application at low RH and elevated temperature.

Moreover, at 110−130 °C under low humidity, the reinforced Nafion/PTFE membranes containing ZrP particles have higher conductivity and better PEMFC performance than reinforced Nafion/PTFE membranes containing silicate particles because ZrP particles can provide additional routes for proton transport.

2.3. PFSI Composite Membranes with Incorporated Organic or Inorganic Compounds

PFSI composite membranes include macrocomposite, nanocomposite, and/or hybrid organic−inorganic membranes with organic or inorganic materials incorporated as a modifier. Two strategies have been considered to incorporate organic or inorganic materials into Nafion-based PEMs. One of these strategies is the impregnation of commercial Nafion membrane with organic or inorganic materials or their precursors followed by in situ synthesis, and the other is solution-casting a Nafion solution mixed with organic or inorganic particles. The modifiers will block the methanol transport channel and increase the twist of the channel in PEMs. For the impregnation method, the hydrophilic regions of Nafion membrane provide the reaction cage for the modifiers, so the original structure of Nafion membrane is maintained. On the other hand, for the blending method, the modifiers participate in forming the membrane structure.[188]

2.3.1. PFSI Composite Membranes with Incorporated Organic Compounds. Composite membranes containing organic materials having a sulfonic acid group often show higher methanol permeability and proton conductivity than do composite membranes containing organic materials without a sulfonic acid group because the sulfonic acid groups on the fillers can provide additional transport channels for methanol and protons.[81−98] All these composite membranes do indeed have reduced methanol permeability because fillers block the methanol transport channels and increase the channel zigzag. But only a few modified Nafion membranes have demonstrated sufficiently low methanol permeability to offset the reduction of proton conductivity.

Sulfonated FEP/Nafion blend membranes prepared through mixing Nafion solution with sulfonated FEP powder show moderate charge transfer resistances and produce well-laminated interfaces between the PEM and the electrodes. The maximum power density observed for a fuel cell using this blend membrane supplied with humidified H_2 and dry O_2 under 0.2 MPa is 861 mW cm^{-2}.[98] The Nafion/polypyrrole/Pt composite membranes synthesized by chemical in situ polymerization of pyrrole monomers with platinum (Pt) precursors in the hydrophilic region of Nafion possess higher thermal stabilities of sulfonic groups and side chains than the pristine Nafion due to the interaction between Nafion−SO_3^-··· polypyrrole−NH_2^+ and the presence of thermally stable Pt. The cell performance of this composite membrane is significantly enhanced compared with that of Nafion due more to the reduction of methanol crossover than to the reduction in proton conductivity.[99]

However, the Nafion composite membranes made by blending Nafion solution and organic polymer solutions must often face the problem of phase separation arising from differences in specific gravity and in solvent concentration profile.[101−104] These problems can be greatly alleviated by ionic interactions. Nafion/PBI blend membrane doped with phosphoric acid shows better durability. Its lifetime in a H_2/O_2 single fuel cell is increased by 55% as compared to phosphoric acid-doped PBI at 150 °C without humidification.[105]

2.3.2. PFSI Composite Membranes with Incorporated Inorganic Compounds. More intensive efforts have been made to modify Nafion with inorganic materials than with organic materials. All inorganic materials used in Nafion modification can be classified under three categories: (i) inert hygroscopic fillers, (ii) proton-conductive fillers, and (iii) hydrophilic and proton-conductive bifunctional fillers.

2.3.2.1. PFSI Composite Membranes with Incorporated Inert Hygroscopic Fillers. Incorporating these inert hygroscopic fillers into Nafion membranes can reduce the methanol crossover, improve the thermal stability, and enhance the water-retention properties of the Nafion composite membranes and consequently increase the efficiency of corresponding fuel cells under low RH or elevated temperature. Adopting the direct blending method for the introduction of inert hygroscopic fillers into Nafion membranes usually results in low proton conductivities arising from proton insulation by these inert hygroscpoic fillers and impaired mechanical properties from the poor compatibility between the hygroscopic fillers and Nafion. Thus, the sol−gel process using Nafion solution and inert hygroscopic filler precursors is the preferred technique. Using high-resolution solid-state NMR, Ye and co-workers showed that either a lower concentration of the tetraethyl orthosilicate (TEOS) or a shorter permeation time in the sol−gel process is necessary to allow complete hydrolysis of the TEOS in Nafion during the preparation of Nafion/SiO_2 composites. Otherwise, incomplete hydrolysis of the TEOS leaves residual ethyl groups on the silica surface, which not only reduces the amount of water adsorbed by the silica but also blocks the proton transport pathways in the Nafion/SiO_2 composites.[189]

Tang and co-workers reported a Nafion/SiO_2 composite membrane based on self-assembled Nafion−SiO_2 nanoparticles (Figure 4) formed through a reformative sol−gel process. The self-assembled Nafion−SiO_2 nanoparticles are uniformly distributed in the Nafion/SiO_2 composite membrane and have an average particle size of 2.8 ± 0.5 nm. With the addition of 5 wt % SiO_2 nanoparticles, the Nafion/SiO_2 composite membrane shows significantly improved performance in terms of stability and durability at cell/humidifying temperatures of 100/60 °C under a current density of 600 mA cm^{-2} and has a degradation rate of 0.12 mV min^{-1}, which is almost 20 times smaller than the 2.33 mV min^{-1} measured on a pristine Nafion212 membrane under the same conditions.[117]

TiO_2 is another inert hygroscopic filler often employed in composite PEMs. The composite membranes based on mesoporous anatase TiO_2 powders (T_{PF6}) and Nafion show large improvements in PEMFC performance under low RH and elevated temperature. For H_2/O_2 PEMFC with 3 wt % of T_{PF6} in the composite membrane, the best power density delivered at a voltage of 0.4 V, a temperatue of 120 °C, and with RH below 50% is 669 mW cm^{-2}, 5.7 times higher than the value

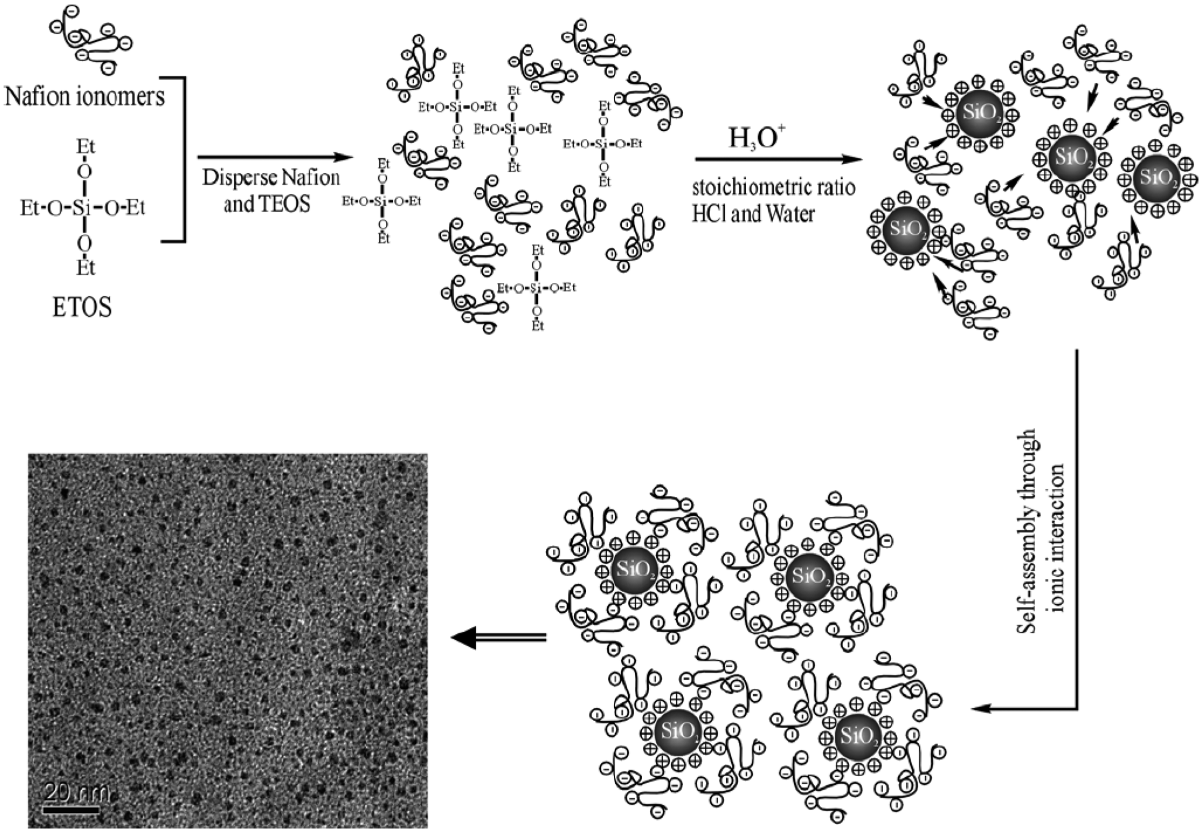

Figure 4. Scheme for the formation of the Nafion−SiO_2 nanoparticles by self-assembly method. The inset shows the transmission electron microscopy (TEM) micrograph of the self-assembled Nafion−SiO_2 nanoparticles.[117] Reprinted with permission from ref 117. Copyright 2007 Elsevier.

obtained under the same conditions from the recast Nafion membrane.[130]

2.3.2.2. PFSI Composite Membranes with Incorporated Proton-Conductive Fillers. Among the proton-conducting fillers used in Nafion composite membranes, α-ZrP is the most investigated compound.[139−151] Particles of α-ZrP, a Bronsted acid with the ability to donate protons, can increase water retention of Nafion composite membranes at elevated temperatures by acting as nanotanks, and thus improve membrane conductivity. Therefore, the α-ZrP-based Nafion composite membranes are expected to have enhanced proton conductivities under high temperature. In a Nafion composite membrane with homogeneously dispersed α-ZrP particles, as is produced by an in situ precipitation of α-ZrP within the Nafion membrane, the particles are 56 nm wide platelets with a thickness of 7 nm, which corresponds to stacking of about 10−13 layers of α-ZrP.[145] The increase in the α-ZrP loading is associated with an enhancement of the elastic modulus and with a decrease in the membrane conductivity, especially at low RH values. As a consequence of the higher elastic modulus values, the conductivity of the composite membranes exhibits an enlarged stability region at higher temperature (up to 140 °C) and RH values in comparison with the parent Nafion membrane.[146] Moreover, this kind of composite membrane can decrease methanol crossover by ~50% so that, for example, the peak power density of DMFC with 10 M methanol as fuel at 75 °C using Nafion/α-ZrP composite membrane is 76.19 mW cm^{-2}, ~2 times higher than that of plain Nafion115.[148] Also, attention should be paid to Nafion/ErTfO composite membranes because it has been reported that ErTfO/Nafion composite membranes exhibit decreased fuel permeability, increased tensile strength, better chemical stability, and decreased membrane swelling without compromising proton conductivity.[149]

Moving a step forward, some inorganic binary component materials are prepared and used as fillers to modify the Nafion membrane.[153−162] Incorporating inorganic binary component materials is an effective method for simultaneously improving proton conductivity and water uptake of Nafion membrane at high temperatures and RH due to synergistic effects.

The actual function of partial inorganic binary component materials is to behave as hydrophilic and proton-conductive bifunctional fillers. Uniformly dispersed $Cs_{2.5}H_{0.5}PWO_{40}$ supported on SiO_2 in a Nafion composite membrane minimizes membrane conductivity loss under dry conditions and obviously improves its cell performance under both humidified and dry conditions at 60 and 80 °C.[155] A single cell employing self-humidifying Nafion/SiO_2−SZ composite membrane exhibits a maximum peak power density of 0.98 W cm^{-2} under dry H_2/O_2 conditions at 60 °C as compared to 0.74 W cm^{-2} of Nafion/SiO_2 membrane and 0.64 W cm^{-2} of recast Nafion membrane, respectively.[158]

The Nafion composite membranes show potential for use in high-temperature operation. For example, the recast Nafion composite membrane containing ZrO_2−SiO_2 binary oxide (Zr/Si = 0.5) gives a cell performance of 683 mW cm^{-2} under conditions of humidified H_2/air gases, 120 °C, 50% RH, and 2 atm.[159] Di Noto and co-workers prepared two nanofillers with core−shell structure consisting of harder core covered by softer shell ("ZrO_2−SiO_2" and "TiO_2−WO_3"). Both of them were used to blend with Nafion solution for preparing Nafion composite membranes. The conductivity and thermal stability of those two kinds of Nafion composite membranes are influenced significantly by the concentration and strength of the dynamic cross-links between the sulfonic anion side groups of Nafion and the oxoclusters of the core–shell nanofillers, R–SO_3H···[“ZrO_2–SiO_2” or “TiO_2–WO_3”]···HSO_3–R. The highest conductivities for these two core–shell nanofillers are 4.3×10^{-2} and 5.0×10^{-2} S cm^{-1}, respectively, at 135 °C, whereas under the same conditions, Nafion only shows a conductivity of 2.8×10^{-2} S cm^{-1}.[161,162]

2.3.2.3. PFSI Composite Membranes with Incorporated Bifunctional Fillers.

To minimize the Nafion composite membrane proton conductivity loss caused by the addition of the inorganic fillers, a particularly interesting approach that serves to increase the net sulfonic acid content has been extensively explored. This approach involves first introducing acidic surface groups onto the inorganic fillers to form bifunctional fillers and then incorporating them into Nafion composite membranes. The most widely used bifunctional fillers include functionalized MWCNT, MMT, zeolite, and silicon.

Usually, the content of acid-functionalized MWCNTs in Nafion composite membranes is very low (<2.0 wt %) because of the risk of short-circuits. Hence, only limited improvements in PEMFC performance can be achieved.[163,164] A novel strategy of deliberate manipulation of hydrophilic domain sizes in Nafion composite membrane by gradually introducing sulfonic acid-functionalized MWCNT into the Nafion can markedly improve the cell performance using a trifle of sulfonic acid-functionalized MWCNTs. The H_2/O_2 fuel cell employing the Nafion composite membrane with 0.05 wt % sulfonic acid-functionalized MWCNT has a maximum power density of 380 mW cm^{-2} at 70 °C, higher than that of Nafion115 (250 mW cm^{-2}).[165] Although functionalized MMT[166−169] and functionalized zeolite beta[170] are also employed to enhance the performance of Nafion, very promising results are still lacking.

More attention has been paid to Nafion composite membranes doped with bifunctional inorganic fillers containing silicon, including silica[171−176] and polysiloxane.[177−184] Most of these reports demonstrate that Nafion composite membranes modified by incorporating the bifunctional particles containing silicon into the Nafion matrix show better membrane properties such as improved water management, a different proton-conducting kinetic mechanism, and a lower methanol permeability than pristine Nafion due to the hygroscopic and proton-conductive properties of bifunctional fillers (Figure 5).

The common method of modifing silica particles is to use the silanol groups on the particle surface (Figure 6).[171−173] Tay and co-workers used a different technique to prepare nanoparticles with a core–shell structure consisting of a silica core (<10 nm) and a densely grafted oligomeric ionomer layer. The resultant Nafion composite membrane can not only improve proton conductivity considerably but also repress methanol permeability by a factor of almost four. However, to obtain the core–shell structured nanoparticles, three steps including silylation, bromination, and atom transfer radical polymerization (ATRP) are required, which makes the synthetic process very complex.[175]

Phosphonic acid-functionalized silica is seldom an alternative to sulfonic acid-functionalized silica. The Nafion nanocomposite membrane containing 3 wt % phosphoric acid-functionalized (3-aminopropyl)triethoxysilane (3-APTES) has a methanol permeability at least 50% lower than that of Nafion and a maximum proton conductivity of 0.07 S cm^{-1}, which is comparable with the conductivity of Nafion. However, the stability of the phosphoric acid group on 3-APTES has not been evaluated.[177]

Polyphenylsilsesquioxane (PPSQ) is a class of polysiloxane which has high heat stability, high crystallinity, and fuel suppressibility.

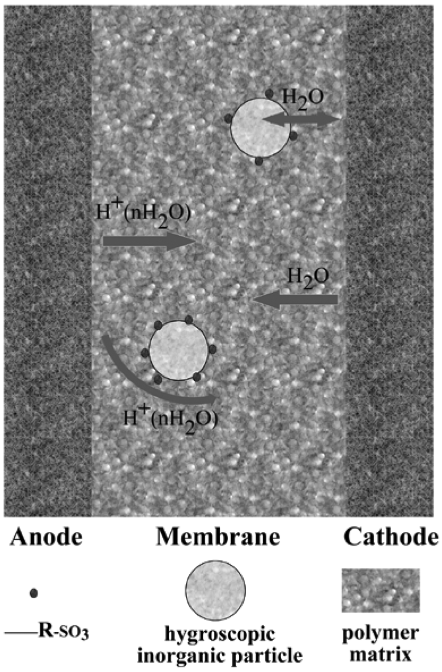

Figure 5. Schematic diagram of water and proton transport in Nafion membrane modified by inorganic fillers with hygroscopic and proton-conductive properties.

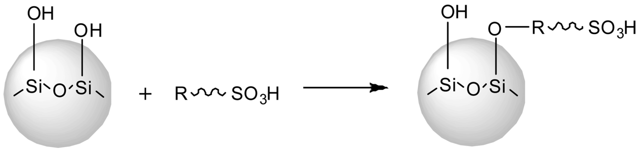

Figure 6. Schematic diagram of the silica particles modified by sulfonic acid groups.

The Nafion composite membranes with 5 wt % sulfonated PPSQ can give a proton conductivity of 1.57×10^{-1} S cm^{-1} at 120 °C and yield better cell performance than Nafion115 at temperatures ranging from 100 to 120 °C and at pressures from 1 to 2 bar.[178]

Polysiloxanes incorporated in Nafion are commonly synthesized by an in situ sol–gel technique within Nafion membranes through corresponding organically functionalized silicon alkoxide precursors containing a thiol (–SH) group (e.g., mercaptopropyltrimethoxysilane (MPTMS) and (3-mercaptopropyl)methyldimethoxysilane (MPMDMS)[180]) to give a Nafion composite membrane that is further treated with H_2O_2 solution to convert the –SH to –SO_3H. The incorporation of polysiloxanes in Sc-CO_2 equipment can also enhance the performance of modified PFSI membranes. The results indicated that poly(MPMDMS) particles with sizes of about 40–70 nm are homogeneously dispersed in the composite membranes and are not restricted in the ion clusters phase due to a low surface tension of Sc-CO_2 and a specific interaction between Sc-CO_2 and the C–F bonds of fluoropolymers. The highest selectivity value of the modified PFSI membrane with 13.9 wt % poly(MPMDMS) is ~5.88 times that of Nafion117 because of its higher proton conductivity and lower methanol permeability.[183,184]

Combining several methods mentioned above, Zhang and co-workers proposed the idea of a PTFE-reinforced SPEEK/Nafion self-humidifying composite membrane containing SiO_2-supported platinum catalyst (Figure 7). This self-humidifying membrane exhibits a higher OCV of 0.98 V and a maximum

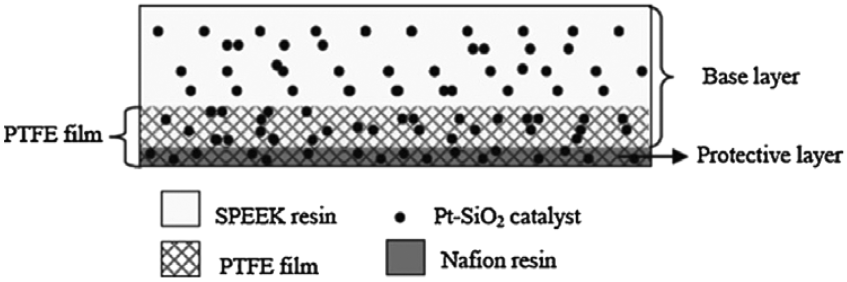

Figure 7. Schematic diagram of the Pt−SiO_2/SPEEK/PTFE/Nafion/Pt-SiO_2 self-humidifying membrane.[186] Reprinted with permission from ref 186. Copyright 2007 Elsevier.

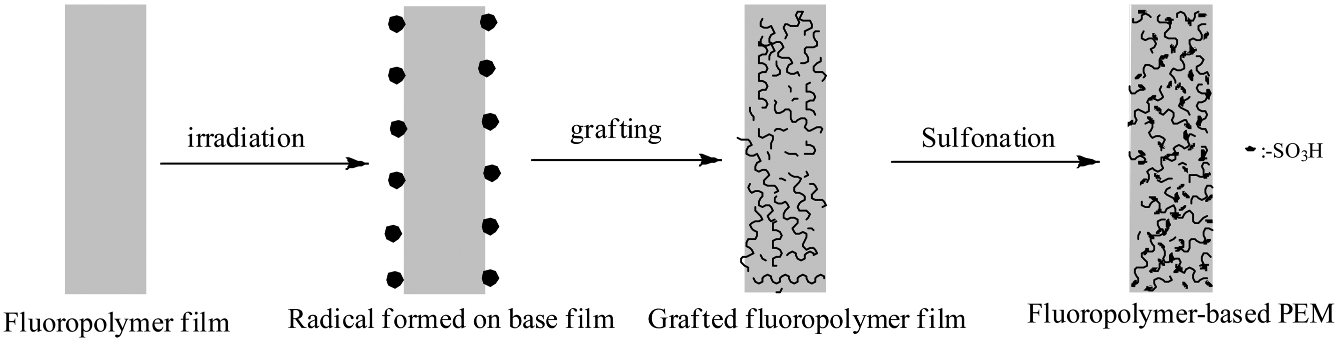

Figure 8. Process for the preparation of PEMs by the radiation-grafting method.

power density value of 0.8 W cm^{-2} with dry H_2/O_2.[186] Apparently, this method can greatly reduce the use of Nafion, but the durability of this composite membrane is still questionable.

The perfluorinated polymer composite membrane developed by Endoh and Hommura showed promising performance. The MEA composed of this perfluorinated polymer composite membrane operated for >6000 h at 120 °C and 50% RH. The degradation rate was reduced to 1/100th to 1/1000th of that of the conventional MEA.[187] Although details of the membrane structure have not been disclosed, it is apparent that their effort opened the door for operating PEMFCs at 120 °C and low RH.

3. PARTIALLY FLUORINATED ACID IONOMER MEMBRANES

In this section, the partially fluorinated acid ionomer membranes that include radiation grafted membranes and blending membranes using commercial fluoropolymers as main body are described in detail. Although it is not easy to obtain PEMs with expected characteristics through modification of existing fluoropolymers using the blending method, the modification of existing fluoropolymers through radiation-grafting polymerization, which has little influence on the most inherent characteristics of the main body, offers a facile route for preparing PEMs with desirable characteristics.

3.1. Partially Fluorinated Acid Ionomer Membranes via Radiation Grafting Polymerization

The membranes fabricated by radiation-induced grafting provide a cost-competitive option because inexpensive commercial materials are used, and the preparation procedure is based on established industrial processes.[190] This methodology has two major advantages: (i) commercial polymer films are modified, thus obviating the need for film formation steps; and (ii) a wealth of adjustable experimental parameters are available (e.g., radiation dose/type, temperature, film thickness), thus allowing a large degree of tailorability and customization.[191] There are three steps involved during the preparation procedure: the preirradiation of the base matrix by ionizing sources, the grafting of a versatile monomer such as styrene onto the matrix, and the sulfonation of the grafted membrane (Figure 8).

The common base fluoropolymer films used for the preparation of radiation-grafted membranes include PTFE, FEP, poly(tetrafluoroethylene)-*co*-perfluorinated alkyl vinyl ethers) (PFA), PVDF, P(VdF-*co*-hexafluoropropylene) (P(VdF-*co*-HFP)), P(VDF-*co*-chlorotrifluoroethylene) (P(VDF-*co*-CTFE)), ethylene-tetrafluoroethylene (ETFE), poly(vinyl fluoride) (PVF), and cPTFE films. Except for PTFE and PVF films, the perfluorinated film-based membranes are promising materials for the hydrogen-fed PEMFCs because of their significant chemical stability, and the partially fluorinated film-based membranes are appropriate for the DMFCs because of their considerable mechanical strength. PTFE and PVF films are not suitable for the preparation of fuel cell membranes by radiation-induced grafting because the former is quite unstable for radiation and the latter only undergoes surface grafting.[192]

One solution of the problem with PTFE is to use UV-induced photografting instead of γ-ray radiation grafting to reduce the damage to the PTFE base film. As an effect of the ionic clusters formed in the membrane, the resulting PTFE-*g*-poly(styrene sulfonic acid) (PTFE-*g*-PSSA) membranes by UV-induced photografting have a conductivity similar to that of Nafion membranes even though the degree of grafting is <10%.[193] In this reference paper, a lake−river−forest mechanism is proposed. The "lake" and "river" are the sulfonated grafted hydrophilic domains, which are distributed in the forest and are responsible for the transport of protons and water, while the "forest" consists of the ungrafted regions. Another solution to the problem with PTFE is the utilization of cPTFE[194,195] or PTFE/PFA polymer alloys,[196] both of which can greatly improve the radiation resistance of PTFE.

FEP is an interesting base material for the membrane because the presence of the fluorinated matrix confers excellent aggressive media resistance on FEP. The un-cross-linked FEP-*g*-PSSA membrane with a thickness of 125 μm shows a high proton conductivity of 0.25 S cm^{-1},[197,198] and the PEMFC using cross-linked FEP-*g*-PSSA membrane with a thickness of around 35 μm shows negligible degradation after a durability test of 4000 h at 80−85 °C.[199] However, the un-cross-linked FEP-*g*-PSSA membrane is susceptible to oxidative degradation, so two alternative grafting monomers, α-methylstyrene (AMS) and methacrylonitrile (MAN), are also employed to graft FEP films. They have a high tendency to form an alternating copolymer chain of AMS and MAN. The resulting un-cross-linked membranes have proton conductivity between 50 and 100 mS cm^{-1} and PEMFC durability ~10 times as long as that of an un-cross-linked FEP-*g*-PSSA membrane at a temperature of 80 °C. Further improvement is possible through the cross-linking of the graft copolymer. Moreover, the cografting of AMS and MAN onto FEP base film leads to a chemical degradation different from that of FEP-*g*-PSSA membranes. The serious degradation region of the former is close to the hydrogen inlet, whereas the serious degradation region of the latter is close to the oxygen inlet.[200]

The ETFE is widely used as base matrix for radiation-induced grafting membranes and has been investigated in detail because of its high radiation stability and superior mechanical properties. Two modified radiation-induced grafting techniques have been used to enhance the performance of ETFE-*g*-PSSA membranes. In the first of these techniques, the ETFE film is subjected to pretreatment by swift heavy ion-beams of ^{129}Xe^{23+} to create latent tracks extending fully through the ETFE film (Figure 9) followed by γ-ray preirradiation grafting of styrene. The ETFE-*g*-PSSA membrane thus-prepared exhibits highly anisotropic proton conductivity, with proton conductivity in the thickness direction 3 times greater than that in the surface direction because the styrene is readily grafted in the latent track region.[201]

In the second technique, the ETFE film is subjected to selective exposure to hard synchrotron X-rays through high aspect ratio Ni-masks to create patterns of free radicals that are used as initiators for grafting of the styrene/divinylbenzene (DVB) (Figure 10). The structured ETFE-*g*-PSSA membranes are more homogenously grafted and have a higher flexibility than the unstructured ones. In fuel cell tests the structured membranes have slightly lower performance due to a 10% lower active area but have a significantly longer lifetime due to confined diffusion of oxidative chemical degradation species by the ungrafted ETFE features.[202]

Table 2 shows a comprehensive collection of partially fluorinated acid ionomer membranes by radiation-grafting polymerization.

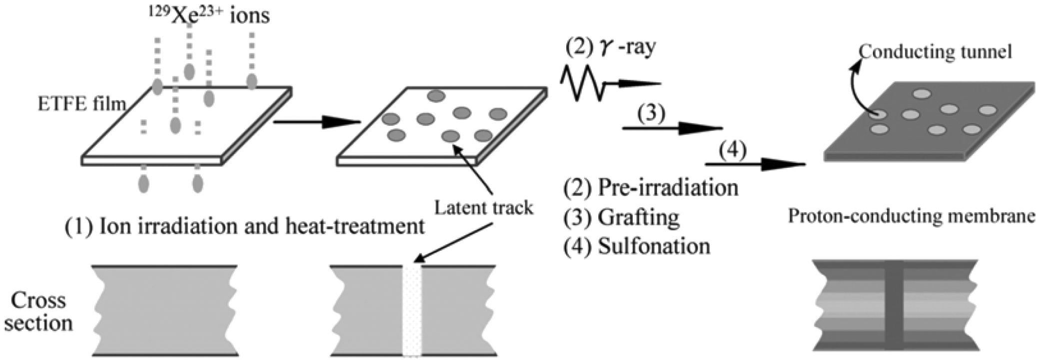

Figure 9. Schematic diagram for the preparation process of Xe-irradiated ETFE-based proton-conducting membranes.[201] Reprinted with permission from ref 201. Copyright 2007 Elsevier.

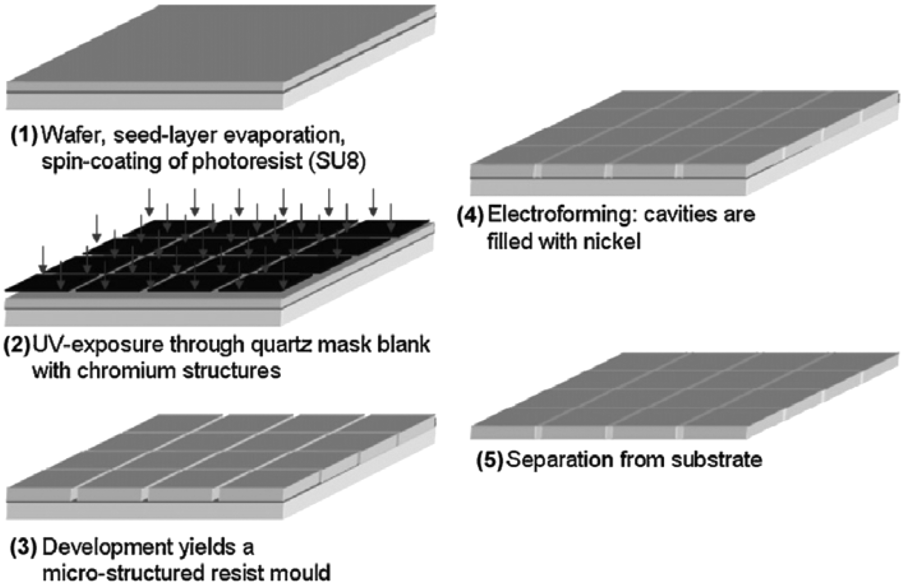

Figure 10. Production process scheme of the nickel shadow masks.[202] Reprinted with permission from ref 202. Copyright 2008 Elsevier.

Table 2. Summary of the Partially Fluorinated Acid Ionomer Membranes by Radiation-Grafting Polymerization

monomers	grafting methods	main conclusions and comments	reference
PTFE base film			
styrene	γ-ray preirradiation grafting	undergoes substantial structural changes; increased ionic sites; enhanced hydrophilicity; reduced hydrophobicity; decreased crystallinity, and without mechanical properties examined	203
styrene	UV-induced photografting	avoids significant degradation of the PTFE main chains; proton conductivity in the thickness direction similar to that of Nafion even if the degree of grafting is <10%	193
cPTFE base film			
styrene	γ-ray preirradiation grafting	improved radiation resistance of PTFE; 50% lower self-diffusion coefficient of water than that of Nafion112; excellent thermal stability up to 200 °C	194, 195
Cross-linked PTFE/PFA polymer-alloy film			
styrene	soft-electron beam (EB)-induced grafting	proton conductivity of 0.17 S cm^{-1} at 60 °C and 95% RH; delamination of the three-phase interface of MEA occurs when operated above 80 °C	196
FEP base film			
styrene or acrylic acid	preirradiation grafting	cross-linking of the FEP matrix leads to remarkable improvements in the thermal durability and mechanical properties, whereas the cross-linking of the polystyrene phase profoundly influences the surface composition of PEM	204−206
styrene	simultaneous irradiation grafting	has a considerably higher value of proton conductivity and less methanol crossover than for the corresponding properties of Nafion; the proton conductivity ranges up to 0.25 S cm^{-1}, but it has a greater susceptibility to oxidative degradation	197, 198
styrene/DVB	EB-induced grafting	PEMFC single-cell durability test over 7900 h at a cell temperature of 80−85 °C at 500 mA cm^{-2} of current density shows negligible degradation during the first 4000 h	199
AMS and MAN	preirradiation grafting	proton conductivity between 50 and 100 mS cm^{-1}; PEMFC durability ~10 times as long as that of a FEP-*g*-PSSA membrane (both are un-cross-linked); different chemical degradation than FEP-*g*-PSSA membranes	200
ETFE base film			
styrene/DVB	γ-ray preirradiation grafting	proton conductivity in thickness direction and the chemical stability of PEM are strongly affected by the choice of grafting solvent; an optimum proton conductivity up to 0.11 S cm^{-1} at 25 °C	207, 208
styrene	- swift heavy ion-beams of $^{129}Xe^{23+}$ creating latent tracks through ETFE films - γ-ray preirradiation grafting	has highly anisotropic proton conductivity: with protons the conductivity in the thickness direction is 3 times higher than that in the surface direction	201
styrene/DVB	- selective exposures of ETFE with hard X-rays to create patterns of free radicals - grafting	slightly lower performance than that of conventional FEP-*g*-PSSA membrane, but significantly longer lifetime	202
styrene/DVB	preirradiation grafting	significantly influenced graft level, conductivity, and water uptake by DVB concentration, while slightly influenced crystallinity and thermal stability	209
styrene	preirradiation grafting	melting temperature (T_m) stays almost constant with increasing irradiation dose, whereas crystallinity increases slightly with irradiation dose; weight loss and crystallinity strongly affected by graft level, while degradation temperatures are independent of graft level	210
MeSt/tBuSt/DVB	preirradiation grafting	significantly improved chemical stability with a durability time of ~200 h in H_2O_2 solution at 60 °C	211, 212
styrene and MAN	preirradiation grafting	proton conductivity is >50 mS cm^{-1} with lower hydration numbers and considerably improved chemical stability with a single fuel cell lifetime exceeding 1000 h	213
• BrTFF • styrene	- simultaneous γ-ray irradiation grafting - ATRP	existing phase separation between hydrocarbon poly(styrene) branches and ETFE-*g*-PBrTFF film; higher proton conductivity than that of Nafion117; a durability time of ~20 h in H_2O_2 solution at 60 °C	214−216
StSi	- γ-ray preirradiation grafting - hydrolysis and condensation - sulfonation	enhanced chemical and thermal stabilities superior to DVB-cross-linked FEP-*g*-PSSA membrane; an optimum membrane shows an appropriate proton conductivity of 0.06 S cm^{-1}; a durability time of ~200 h in H_2O_2 solution at 60 °C; a methanol permeability almost 6 times as low as Nafion	217, 218
• styrene • α-ZrP	- preirradiation grafting - doping	not suited for fuel cells due to instability or brittleness	219

Table 2. continued

monomers	grafting methods	main conclusions and comments	reference
ETFE base film			
4VP or *N*-vinylformamide (NVF) or 1VIm	- electron beam irradiation grafting - doping with phosphoric acid	exceptional flexibility and mechanical stability and a thermal resistance up to at least 160 °C in air; proton conductivity up to 0.10 S cm^{-1} at 120 °C without humidification; power density of a H_2/O_2 fuel cell up to 150 mW cm^{-2} at 120 °C without humidification	220, 221
PVDF base film			
sodium styrene sulfonate (SSS)/*N*,*N*-dimethyl formamide (DMF)/H_2SO_4	EB-induced grafting	grafting level up to 65%; proton conductivity of 0.114 S cm^{-1}; a very good combination of basic physicochemical properties for PEMFC	222
styrene	simultaneous EB-induced grafting[a]	grafting level up to 46%; proton conductivity of 5.59×10^{-2} S cm^{-1} at room temperature	223
• 3-(trimethoxysilyl) propyl methacrylate (TMSPMA) • 3-aminopropyltrimethoxysilane (APTMS)/ phosphotungstic acid (PWA)	- ATRP - hydrolysis and condensation	good mechanical and thermal properties but with low proton conductivity (only 0.01 S cm^{-1} at 70 °C)	224
P(VDF-*co*-CTFE) base film			
• SSS • NaN_3	- ATRP - forming end-functional azide group - cross-linking by UV irradiation	proton conductivity from 0.074 to 0.068 S cm^{-1} at room temperature; improved hydrolytic stability of >200 h in deionized water at 80 °C; a large reduction in swelling	225−229
• poly(hydroxy ethyl acrylate) (PHEA) • 4,5-imidazole dicarboxylic acid (IDA)	- ATRP - cross-linking through esterification - doping with phosphoric acid	good mechanical properties; high thermal stability up to 250 °C; maximum proton conductivity of 0.015 S cm^{-1} at 120 °C under anhydrous conditions	230
styrene	ATRP	properties of PEMs are significantly affected by their nanoarchitectured morphology; interconnected network of small ionic clusters of 2−3 nm in size; ion-exchange capacity (IEC) up to 2.22 mmol g^{-1} without excessive swelling and dissolution	231
P(VDF-*co*-HFP) base film			
• 2-mercaptoethylamine hydrochloride (MEHCl)/SSS	- radical telomerization - grafting	proton conductivity is 100 times lower than that of Nafion; good thermal stability up to 200 °C	232

[a] In the reference paper (ref 223), the PVDF base film is a porous PVDF film (70% porosity, 0.22 μm average pore size, and 110 μm thickness).

Because of the active H atom at the α-hydrogen position on the styrene sulfonic acid group in the PSSA-grafted membrane, these membranes are prone to free radical attack under fuel cell conditions, although substantial efforts have been devoted to remedying this shortcoming. Co-graftings of MeSt and tBuSt[211,212] or styrene and MAN[213] into ETFE films have demonstrated significantly improved chemical stability and rather enhanced lifetime.

Chen and co-workers grafted cross-linkable silane monomer, StSi, into the ETFE film by γ-ray preirradiation to fabricate ETFE-*g*-StSi films. After undergoing hydrolysis, condensation, and sulfonation, ETFE-*g*-StSi membranes with inorganic −Si−O−Si− cross-linking structures are produced. The resultant cross-linked proton-conducting hybrid PEMs possess enhanced chemical and thermal stabilities that are superior to DVB-cross-linked styrene-grafted membranes. An optimum membrane with a trade-off among the proton conductivity, chemical stability, and methanol permeability has an appropriate proton conductivity of 0.06 S cm^{-1}, a durability time of ∼200 h in the 3% H_2O_2 solution at 60 °C, and a methanol permeability almost 6 times as low as Nafion. All the properties of the StSi-grafted cross-linked hybrid PEMs make them promising materials for fuel cells.[217,218]

The PVDF is another representative partially fluorinated polymer with excellent thermal, mechanical, and chemical stability along with low cost compared to Nafion. The PVDF-*g*-PSSA membranes prepared by a single-step synthesis method have grafting levels up to 65% and a higher degree of crystallinity than that in similar PVDF-*g*-PSSA membranes prepared by the conventional multistep method. The PVDF-*g*-PSSA membrane with 65% grafting level shows a proton conductivity of 0.114 S cm^{-1} and a very good combination of basic physicochemical properties for PEMFC.[222]

Kim and co-workers also explored the single-step synthesis of grafted fluoropolymer films via ATRP.[225−229] However, the characteristics of their studies lie on the further modified technique to these grafted fluoropolymer films through ATRP. For example, after P(VDF-*co*-CTFE)-*g*-PSSS films are synthesized using ATRP, the terminal chlorine atoms on them are converted to end-functional azide groups and sequentially cross-linked by UV irradiation (Figure 11). Although the cross-linked P(VDF-*co*-CTFE)-*g*-PSSA membrane with 73 wt % PSSA content exhibits a proton conductivity reduced from 0.074 to 0.068 S cm^{-1} at room temperature compared with the un-cross-linked membrane, it shows water uptake reduced from 300 to

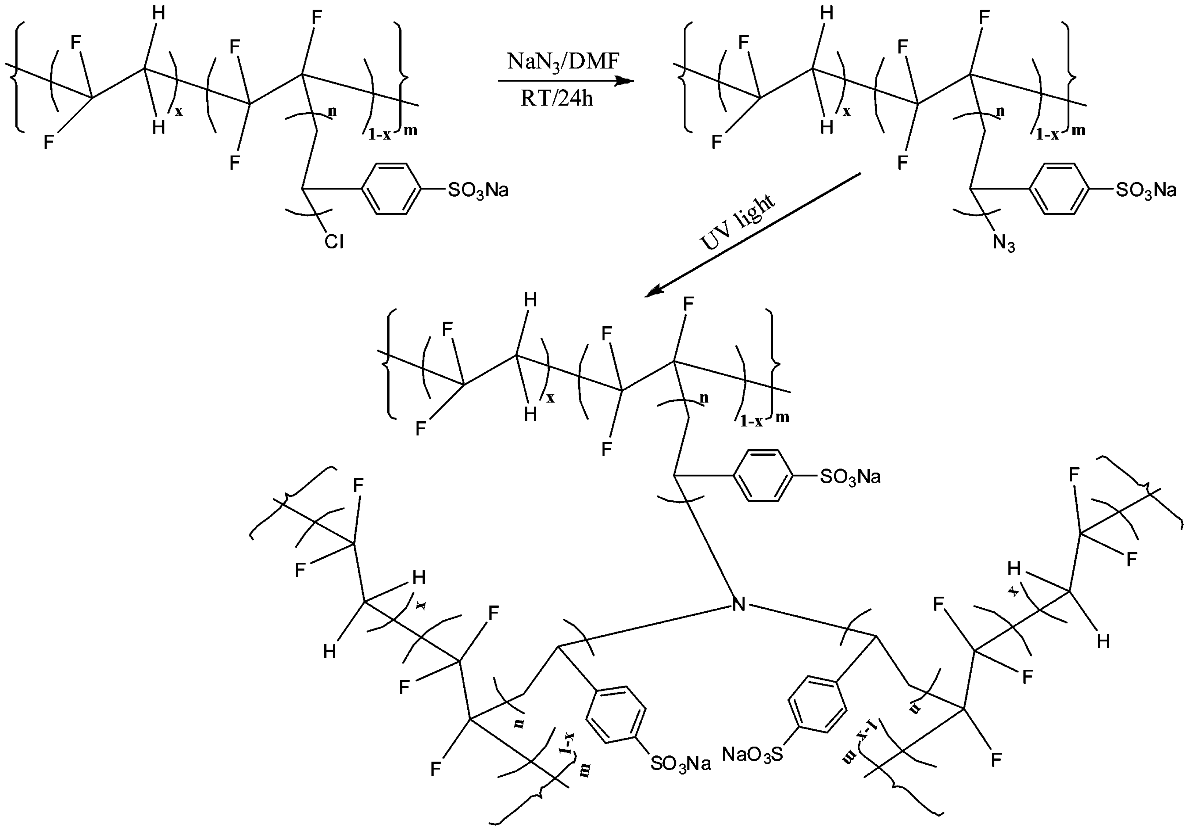

Figure 11. Schematic procedure for the preparation of cross-linked P(VdF-*co*-CTFE)-*g*-PSSA membranes.[225]

83% and tensile strength increased from 21.1 to 26.2 MPa. Furthermore, the cross-linked P(VDF-*co*-CTFE)-*g*-PSSA membrane is stable without breaking >200 h in deionized water at 80 °C, showing good hydrolytic stability.[225]

3.2. Partially Fluorinated Acid Ionomer Membranes via Blending or Doping Method

Polymer blending or doping as a valuable technique is also used to modify and improve the mechanical, thermal, surface, and conductive properties of fluoropolymers. Most of the fluoropolymers using this technique are PVDF or its copolymers as a mechanical support or a binder. The proton-conducting components include sulfuric acid,[233] phosphoric acid,[234−236] room-temperature ionic liquids (RTILs)[237−245] such as 2,3-dimethyl-1-octylimidazolium hexafluorophosphate (DMOImPF$_6$), (1-*n*-butyl-3-methylimidazolium tetrafluoroborate) [C$_4$mim]-[BF$_4$], (1-*n*-butyl-3-methylimidazolium hexafluorophosphate) [C$_4$mim][PF$_6$], (1-*n*-octyl-3-methylimidazolium hexafluorophosphate) [C$_8$mim][PF$_6$], 2,3-dimethyl-1-octylimidazolium tetrafluoroborate (DMOImBF$_4$), 1-ethyl-3-methylimidazolium fluorohydrogenates [EMIm](FH)$_n$F (n = 1.3 and 2.3), *N*-ethylimidazolium bis(trifluoromethanesulfonyl)imide (EImTFSI), *N*-methylimidazolium bis(trifluoromethanesulfonyl)imide (MImTFSI), and 1-methylpyrrolidinium bis(trifluoromethanesulfonyl)imide (MPyTFSI), trifluoroacetic propylamine (TFAPA), zeolite,[246,247] HPA,[248,249] ZrPSPP,[250] silica-containing surface-anchored sulfonic acid,[251,252] sulfonated polystyrene (SPS),[253] SPEEK,[254] poly(styrene-*co*-styrene sulfonic acid)-*b*-poly(methyl methacrylate) [P(S-*co*-SSA)-*b*-PMMA],[255] and PSSA.[256] Unfortunately, few reports described exciting properties of these materials relative to PEMFCs.

3.2.1. Partially Fluorinated Acid Ionomer Membranes without Proton-Conducting Polymer Components.

When phosphoric acid is doped in microporous composite films containing PVDF for protonic conductivity, the resultant composite membranes show a conductivity higher than 0.1 S cm^{-1} under low RH at 80 °C due to the combined effect of the inert filler and the membrane microstructure (tortuosity, pore size, pore interconnection, and size distributions).[234−236] However, the inevitable leaching out of phosphoric acid has a significant negative influence on the durability of these membranes.

It is well-known that RTILs are a kind of room-temperature molten salt (ionic liquid) with unique properties such as high ionic conductivity, negligible vapor pressure, nonflammability, good thermal stability, and a wide electrochemical window. In particular, the protic RTILs have proton-donor and -acceptor sites, which can be used to build up a hydrogen-bonded network.[257] Hence, attempts at incorporating them into inert polymer matrices to yield highly thermal stable proton-conducting membranes have been reported. Regrettably, most of them are not practicable for PEMFCs due to low proton conductivities of 10^{-4}–10^{-3} S cm^{-1}.[237−241,244] The composite membranes based on the protic ionic liquid EImTFSI and P(VDF-*co*-HFP) copolymer achieve desirable conductivities on the order of 10^{-2} S cm^{-1} at room temperature, which remains stable up to 140 °C.[242,243] The proton conductivity of the TFAPA/PVDF composite membranes using a strong acid of trifluoromethanesulfonic acid (TFMSA) as an additive can be increased from 6.1×10^{-4} to 1.2×10^{-2} S cm^{-1} at 150 °C, but the leakage of RTILs and TFMSA is still a severe problem.[245]

Two separate nearly fabulous results are reported by two groups. Both of them are based on blending membranes consisting of silica nanopowders anchored by sulfonic acid groups and P(VDF-*co*-HFP) or PVDF. The former with a loading of 50 wt % P(VDF-*co*-HFP) exhibits power densities above

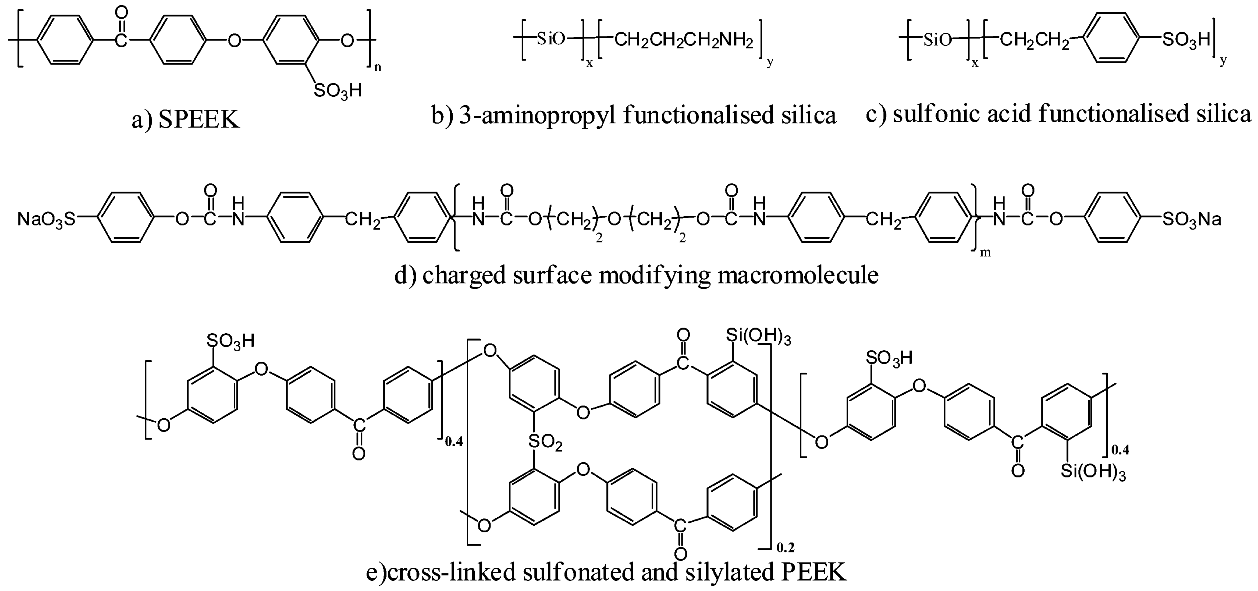

a) SPEEK b) 3-aminopropyl functionalised silica c) sulfonic acid functionalised silica

d) charged surface modifying macromolecule

e)cross-linked sulfonated and silylated PEEK

Figure 12. Chemical structures of several materials: a, b,[284] c,[288] d,[296] and e.[305]

1 W cm^{-2} at 70 °C in single-cell fuel cell tests with nonhydrated H_2/O_2 feeds,[251] whereas the latter with ~100 μm thickness shows maximum power densities of 127, 208, and 290 mW cm^{-2} in DMFC tests with a 1 M methanol solution at 80, 110, and 130 °C, respectively.[252]

3.2.2. Partially Fluorinated Acid Ionomer Membranes with Proton-Conducting Polymer Components. Although polymer blending of low-cost hydrocarbons and partially fluorinated polymers is a very much easier method of fabricating PEMs, it is difficult to obtain highly compatible blend membranes because of the poor compatibility between the two components. Incorporating miscible blocks along with the PVDF in proton-conducting polymer components can improve their compatibility. The blending PEMs based on P(S-*co*-SSA)-*b*-PMMA and PVDF show a well-ordered microphase-separated structure and have better proton conductivity than membranes with randomly ordered morphology.[255] The PVDF/PSSA/DVB composite membranes synthesized in an Sc-CO_2 apparatus are interpenetrating polymer networks (IPNs) that show decreased proton conductivity and methanol permeability with increasing concentration of DVB.[256]

Besides the partially fluorinated acid ionomer membranes mentioned above, there are two composite membranes that use PTFE as a supporting material. One is a sulfonated polyimide (SPI)/PTFE reinforced membrane, which has performance comparable to that of an H_2/O_2 fuel cell based on the commercial NRE-212 membrane at 80 °C under fully humidified conditions.[258] The other is the sulfonated poly(fluorinated arylene ether)s (SDF-F)/VI/PTFE/H_3PO_4 layered membrane, which has good mechanical strength and good high-temperature performance comparable to that of PBI/H_3PO_4 composite membranes.[259]

4. NONFLUORINATED ACID IONOMER MEMBRANES

The nonfluorinated acid ionomer membranes are a very important branch of alternative PEMs. The materials used for these PEMs, which include poly(arylene ether)s, polyimides (PIs), poly(ether imide)s (PEIs), styrene and its derivatives, glass electrolytes, etc., will be discussed in the following section.

4.1. Poly(arylene ether)-Based Membranes

The poly(arylene ether)-based membranes are one of the most promising alternative PEMs because of their availability, processability, excellent thermal and chemical stability, good mechanical properties, and low cost.[260] The sulfonic acid groups are proton-exchange sites in poly(arylene ether)-based membranes and are more readily introduced into aromatic rings than carboxylic acids and phosphonic acids.[261] Because an excellent review[262] has been dedicated to the proton-conducting membranes carrying phosphonic acid groups, this discussion of the poly(arylene ether)-based membranes is mainly focused on the proton-conducting membranes carrying sulfonic acid groups.

4.1.1. Modification of SPEEK Membrane. The most widely used and intensively studied poly(arylene ether)-based membrane is SPEEK (Figure 12a) because its original polymer, poly(ether ether ketone) (PEEK), is commercially available and has important properties similar to those of many classes of aromatic polymers.[263−327] Although the large majority of membranes based on SPEEK does not have the desired lifetime because of the hydroxy radical initiated degradation of SPEEK, there are still some clever routes worthy of being mentioned (Table 3) for improving SPEEK membranes. Large improvements in durability have been attained by double cross-linking[311] or the radiation-grafting[314] method, but further improvements are still needed.

In view of the problems of SPEEK membranes, such as brittleness at elevated temperatures, excessive swelling, and relatively high methanol crossover in membranes with a high degree of sulfonation all leading to insufficient durability, many researchers have investigated other poly(arylene ether)-based membranes with aromatic skeletons different from PEEK.[328−496] With very few exceptions,[379−386] the significant advances in poly(arylene ether)-based membranes are based mainly on four classes of poly(arylene ether)s and their derivatives (Table 4). They are (i) poly(arylene ether)s with cross-linkable groups,[397−417] (ii) poly(arylene ether)s with pendant sulfonated groups or side-chains,[418−435] (iii) poly(arylene ether)s with backbones containing heteroatoms such as F, N, S and P,[442−477] and (iv) multiblock copoly(arylene ether)s synthesized by the coupling reaction of hydrophilic and hydrophobic macromonomers.[478−492]

Table 3. Summary of the Modified SPEEK Membranes

modified methods	new components	main conclusions and comments	reference
blending method	Pt catalyst supported by $Cs_{2.5}H_{0.5}PWO_{40}$	inorganic/organic self-humidifying membrane; PEMFC with dry H_2/air exhibiting peak power density of 540 mW cm^{-2} at 60 °C; no obvious drop of OCV and voltage at 800 mA cm^{-2} lasting at least 100 h	283
blending method	3-aminopropyl functionalized silica (Figure 12b)	decreased water uptake and swelling; PEMFC with humidified H_2 and air at 3 absolute bar showing a maximum power density of 246 mW cm^{-2} at 120 °C	284
blending method	functionalized silica powder with sulfonic acid groups (Figure 12c)	increased proton conductivity and dimensional stability; reduced swelling and methanol permeability; proton conductivity of 0.17 S cm^{-1} at 145 °C and 100% RH	288
modified sol−gel process	phosphonated polysilsesquioxane	proton conductivity of 0.142 S cm^{-1} at 120 °C and 100% RH, higher than that of Nafion117 at the same conditions	289
blending method	charged surface-modifying macromolecule (Figure 12d)	good improvements in methanol permeability with a large conductivity reduction	296
sol−gel process	TiO_2 network	improved mechanical and thermal properties and hydrolytic stability; proton conductivity of 5.8×10^{-2} S cm^{-1} at 120 °C and 100% RH	302
silylation	silylated PEEK (Figure 12e)	significantly improved thermal and mechanical stabilities; proton conductivity of 0.2 S cm^{-1} at 90 °C under wet conditions; well-established correlation among proton conductivity, elastic modulus, and water uptake coefficient	303−310
radiation and thermal cross-linking techniques	doubly cross-linked SPEEK	maintenance more than 200 h in 100 °C water; proton conductivity of 0.11 S cm^{-1} at 100 °C; great improvements in methanol permeability, thermal stability, and mechanical strength	311
radiation grafting	ethyl styrenesulfonate/DVB	good proton conductivity similar to Nafion; much better mechanical strength than Nafion; PEMFC running >1000 h at 95 °C and 80% RH	314
sol−gel process	SiO_2/ZrP	enhanced mechanical properties and a large reduction in methanol permeability with reasonable proton conductivity	280
applying electric field	cross-linked poly(dimethyl siloxane)[a]	forming electric field-induced structure; reduced amount of particles for the percolation threshold of creating proton conductance; low proton conductivity and high fuel permeability	321

[a] The SPEEK particles are dispersed in cross-linked poly(dimethyl siloxane).

The sulfonated poly(arylene ether)s (Figure 13), excluding the four classes of poly(arylene ether)s and their derivatives listed in Table 3, include mainly three series. The first of these series is the microblock ionomers,[380] which among them have similar equivalent weights (EWs) but very different sulfonic acid distributions along the ionomer backbone. During synthesis, the sulfonic acid groups are specifically presented as singlets, doublets, or quadruplets. They are alternately and strictly organized with progressively longer nonionic segments to maintain an approximately constant EW. The results indicated that extending the nonionic spacer length in the repeat unit leads to a progressively higher degree of nanophase separation between hydrophilic and hydrophobic domains in these microblock ionomers, which enables the fabrication of swelling-resistant hydrocarbon membranes with very much higher IEC (>2.0 mmol g^{-1}). However, these microblock ionomer membranes do not present a clear advantage in absolute performance over commercial perfluorinated membranes.

The second of the series included is the sulfonated poly(arylene ether) membranes containing a hydrophobic component of different size (Figure 13, parts a−d). SPE membrane (Figure 13b), for example, provides proton conductivities comparable to that of Nafion at high RH (>80%). However, once the RH is decreased, proton conductivities decrease by several orders of magnitude. Further studies show that small hydrophobic components (i.e., SPE3 and SPE4) are preferable for PEMFC applications because these small hydrophobic components can induce larger and more developed hydrophilic clusters than can the bulky hydrophobic ones (i.e., SPE1 and SPE2).[381,382]

Finally, the third series included is the modified PPO as PEMs, which have been intensively reviewed by Xu and co-workers.[387] In a new solvent-free route for preparing favorable PEMs based on PPO (Figure 13e) proposed by Xu and co-workers, bromomethylated PPO is dissolved in monomer mixtures of styrene and DVB, and then the polymer and monomer mixtures are precast onto a reinforcing material of woven screening fibers, followed in sequence by in situ polymerization and sulfonation. This method can also be applied to other compatible systems of (aromatic) polymers and (aromatic) monomers.[385] Woo and co-workers fabricated an asymmetric porous substrate using bromomethylated PPO through a wet-phase inversion technique and impregnated it with sulfonated PPO to prepare a PEM. Because the porous substrate consisted of a dense top layer and a finger or sponge-type sublayer, the resultant asymmetric PEM had different hydrophilicity on the two sides. When the relatively hydrophilic side of the membrane faces the cathode of PEMFC, the asymmetric membrane can facilitate water management by improving the diffusion of water accumulated in the cathode to the anode, thereby enhancing the overall fuel cell performance under both humidified and nonhumidified conditions.[388]

4.1.2. Poly(arylene ether)s with Cross-Linkable Groups.

To overcome the swelling problem, some groups reported novel acid−base copolymers consisting of sulfonated poly(arylene ether) copolymers containing basic groups.[398−403] These acid−base copolymer membranes exhibit moderate water swelling ratio and obviously improved thermal, oxidative, and dimensional stability due to the strong intermolecular and intramolecular acid−base interactions between the basic groups and the sulfonic acid groups. Contrary to conventional PEMs, which consist of an acid polymer and a base polymer and often swell unacceptably at temperatures above 70−90 °C,[497] some acid−base copolymer membranes with high IEC can be used at temperatures above 100 °C, which shows promise for high-temperature PEMFC applications.[400−405]

Of course, successful efforts in acid−base copolymer synthesis are still rare because of the low reactivity of the relevant monomers. An accessible approach suggested by the cross-linking concept is incorporating aromatic monomers with cross-linkable groups such as an unsaturated propenyl group into sulfonated poly(arylene ether)s. Following this method, the cross-linked sulfonated poly(arylene ether) membranes show greatly decreased methanol crossover, enhanced dimensional stability, and slightly reduced but acceptable proton conductivity.[408]

The cross-linking of allyl-terminated telechelic sulfonated poly(ether sulfone)s (Figure 15, parts b and c) is done using a

Table 4. Summary of the Poly(arylene ether) Membranes with Aromatic Skeletons Different from PEEK

polymers	chemical structures	main conclusions and comments	reference
sulfonated poly(arylene ether ketone ketone sulfone) (SPAEKKS)	Figure 13a	SPAEKKS membrane with IEC of 1.42 mmol g^{-1} showing oxidative stability of 29 h in Fenton's reagent at room temperature and excellent mechanical strength	379
microblock sulfonated poly(arylene ether ketone)	not given	good swelling resistance even for membranes with IEC > 2.0 mmol g^{-1}; favorable durability of the best microblock membrane being superior to that of the perfluorinated membrane at 120 °C and 35% RH; however, no clear advantage in absolute performance over commercial membranes	380
sulfonated poly(arylene ether sulfone)	Figure 13b	proton conductivity comparable to Nafion at high RH (>80%), but markedly decreased proton conductivity at low RH	381, 382
sulfonated poly(fluorenyl ether ketone nitrile) (SPFEKN)	Figure 13c	superior thermal stability, good oxidative stability, and high proton conductivity, but low water uptake; the SPFEKN membrane with degree of sulfonation (DS) of 1.4 shows much better PEMFC performance than that of Nafion117 at 80 and 90 °C	383
sulfonated poly(arylene ether ether nitrile) (SPAEEN)	Figure 13d	good interfacial stability between SPAEEN membranes and substrates of MEA; the power density of DMFC under 90 °C humidified air without back-pressure and 2.0 M methanol feed achieving 125 mW cm^{-2} and exceeding 100 h of stable operation	384
bromomethylated poly(2,6-dimethyl-1,4-phenylene oxide) (PPO)/styrene/DVB/woven screening fibers	Figure 13e	satisfactory thermal and dimensional stability; proton conductivity of 0.07 S cm^{-1} close to that of Nafion117 at 100% RH and room temperature	387
Poly(arylene ether)s with cross-linkable groups			
copolymers bearing sulfonic groups and pendant benzimidazole groups (SPAEK-BI)	Figure 14a	proton conductivity of 0.08 S cm^{-1} at 80 °C; significantly reduced methanol permeability to 1.2×10^{-7} cm^2 s^{-1}	398, 399
Sulfonated poly[(1-(4,4′-diphenyl ether)-5-oxybenzimidazole)benzimidazole] (PBI-OO)	Figure 14b	sulfonated PBI-OO membrane with IEC of 4.3 mmol g^{-1} has a proton conductivity of 0.05 S cm^{-1} at 120 °C and 100% RH	400
copolymers of basic 2,6-bis(benzimidazol-2-yl)yridine and sulfonated poly(arylene sulfones) (DFSBIP-SPAS)	Figure 14c	high proton conductivity from 0.09 to 0.12 S cm^{-1} at room temperature and 100% RH; low swelling of 27.5−35.8% at 100 °C	401
sulfonated poly[bis(benzimidazobenzisoquinolinones)] (SPBIBI)	Figure 14d	excellent dimensional and hydrolytic stabilities, maintenance exceeding 400 h in water at 140 °C; the SPBIBI membrane with IEC of 2.65 mmol g^{-1} has a proton conductivity of 0.174 S cm^{-1} at 100 °C	402−404
cross-linked sulfonated poly(arylene ether sulfone) with propenyl groups	Figure 15a	dramatically reduced swelling and methanol permeability without large sacrifice of proton conductivity	408
cross-linked allyl-terminated telechelic sulfonated poly(ether sulfone)	Figure 15, parts b and c	excellent hydrolytic and oxidative stability; proton conductivity 1.6 times as high as that of Nafion at 100 °C; methanol permeability 80% lower than that of Nafion	411
cross-linked sulfonated poly(ether sulfone) with 4,4′-dihydroxystilbene	Figure 15d	good hydrolytic stability in boiling water; proton conductivity of 0.12 S cm^{-1} at room temperature and 100% RH; humidified H_2/O_2 PEMFC with a power density of 900 mW cm^{-2} at 70 °C	412
cross-linked sulfonated poly(arylene ether ketone) copolymers containing ethynyl moiety	Figure 15e	proton conductivity close to Nafion at room temperature; relatively low water uptake	415
cross-linked multiblock sulfonated poly(aryl ether ketone) containing benzophenone units and methyl moieties	Figure 15, parts f and g	large reduction in methanol permeability without a large proton conductivity sacrifice	409
cross-linked sulfonated poly(bis-A)sulfone	not given	repressed swelling, reduced water uptake, enhanced dimensional stability, and slightly decreased proton conductivity	416
Poly(arylene ether)s with pendant sulfonated groups or side-chains			
poly(arylene ether)s containing sulfofluorenyl groups	Figure 17a	proton conductivity up to 0.3 S cm^{-1} at 80 °C and 93% RH and comparable to that of the Nafion112 under 80−120 °C and from 20 to 93% RH; acceptable proton conductivity after 10 000 h durability test	418−420
poly(ether sulfone)s with highly sulfonated units	Figure 17b	well-defined phase-separated structures and well-connected proton channels; proton conductivity close to that of the Nafion117 over a wide range of RH at 80 °C	422

Table 4. continued

polymers	chemical structures	main conclusions and comments	reference
Poly(arylene ether)s with pendant sulfonated groups or side-chains			
wholly aromatic side-chain-type sulfonated poly(arylene ether)	Figure 17c	excellent oxidative and hydrolytic stability of >4 h in 80 °C Fenton's reagent and at least 1 week in 100 °C water without obvious changes; only 13.6% swell ratio at 80 °C; proton conductivity of 0.14 S cm^{-1} at 100 °C	423
comb-shaped sulfonated poly(arylene ether)s	Figure 17, parts d and e	much higher proton conductivity than that of Nafion in the range 20−120 °C, and near 0.4 S cm^{-1} at120 °C	424, 425
highly fluorinated comb-shaped sulfonated poly(arylene ether) copolymer	Figure 17f	power density of 144.5 mW cm^{-2} at 80 °C by 2 M methanol solution and humidified air, but apparent DMFC performance loss after the 65 h life test	427
branched wholly aromatic poly(ether ketone) bearing clusters of sulfonic acid groups only on the end groups	Figure 17g	significantly phase-separated; wormlike and highly connected morphology; proton conductivity and IEC comparable to those of Nafion	433
Poly(arylene ether)s with backbones containing heteroatoms such as F, N, S, and P			
sulfonated poly(fluorenyl ether) (SPFE-PFCB)	Figure 18a	water content of 25% similar to that of Nafion115 but higher proton conductivity than that of Nafion115 in the range of 25−80 °C	438
highly fluorinated sulfonated poly(arylene ether)	Figure 18b	better thermal stability and a higher proton conductivity of 0.135 S cm^{-1} at 80 °C compared with Nafion	439
partially fluorinated sulfonated poly(arylene ether benzonitrile)	Figure 18c	reduced cell resistance; suppressed methanol permeability and low water uptake; better DMFC cell performance and longer-term durability than Nafion112	440
sulfonated poly(arylene ether sulfone) copolymers/sulfonated poly(arylene ether sulfone) random copolymers	Figure 18d	decreased water uptake from 33 to 24 wt % with little change in proton conductivity	441
phthalazinone-based sulfonated poly(arylene ether)	not given	has relatively lower water uptake and methanol permeability, as well as improved mechanical and thermal properties and oxidative stability	444, 445
sulfonated poly(arylene ether) copolymers containing benzoxazole moiety (SPAEBO)	Figure 19b	oxidative stability and proton conductivity decreases with DS or IEC: the SPAEBO membrane with an IEC of 0.18 mmol g^{-1} shows a proton conductivity of 1.8×10^{-2} S cm^{-1} at 120 °C without external humidification as well as surprisingly long durability (>1200 h) in Fenton's reagent at room temperature	452
sulfonated polyoxadiazole polymers (SPODDPE)	Figure 19c	has proton conductivity on the order of 10^{-2} S cm^{-1} at 80 °C and 20% RH, together with high stability in Fenton's reagent, but mechanical strength is ill-suited for PEM	455
sulfonated poly(oxadiazole triazole) (SPOD-SPT)	Figure 19d	good mechanical properties and high thermal stability; proton conductivity up to 6×10^{-2} S cm^{-1} at 150 °C and 100% RH	459
pyridine-based poly(ether sulfone)[a]	Figure 19e	good mechanical properties; excellent film-forming properties; high oxidative and thermal stability as well as acid-doping ability with high acid uptake; proton conductivity of 1.4×10^{-2} S cm^{-1} at 160 °C; oxidative stability of more than 72 h in Fenton's reagent at 80 °C	460−463
sulfonated poly(arylenethioether sulfone) (SPTES)	Figure 19f	thermal stability, mechanical properties, dimensional stability, and high oxidative stability are all excellent; has good water affinity and enough proton conductivity; peak power density of H_2/O_2 (with back-pressure of 0.2 MPa) PEMFC using SPTES-50 membrane achieves 1.18 W cm^{-2} under 80 °C and 100% RH	466−469
cross-linked SPTES	Figure 19g	significantly reduced OCV decay rate at the cost of negligible PEMFC performance loss compared to un-cross-linked membranes; maximum power density of H_2/O_2 (with back-pressure of 0.2 MPa) reaches 1.32 W cm^{-2} under 80 °C and 100% RH	473
cross-linked sulfonated poly(phenylene sulfide sulfone nitrile)	Figure 19h	large reduction in water swelling and methanol permeability without sacrifice of proton conductivity compared to un-cross-linked membranes	474
sulfonated poly(arylene thioether phosphine oxide) (SPATPO)	Figure 19i	SPATPO membrane with an IEC of 1.14 mmol g^{-1} exhibits a swelling ratio of 11.6% at 80 °C and a proton conductivity of 7.83×10^{-2} S cm^{-1} at 90 °C and 100% RH	476
Multiblock copoly(arylene ether)s synthesized by the coupling reaction of hydrophilic and hydrophobic macromonomers			
sulfonated multiblock poly(arylene ether) copolymers (BisSF-BPSH)	Figure 20	BisSF-BPSH membrane with optimal trade-off between performance (proton conductivity under partially hydrated conditions) and water uptake shows proton conductivity higher than that of Nafion112 while maintaining water uptake of ~40 wt %	491

[a] Doped with 240 wt % H_3PO_4.

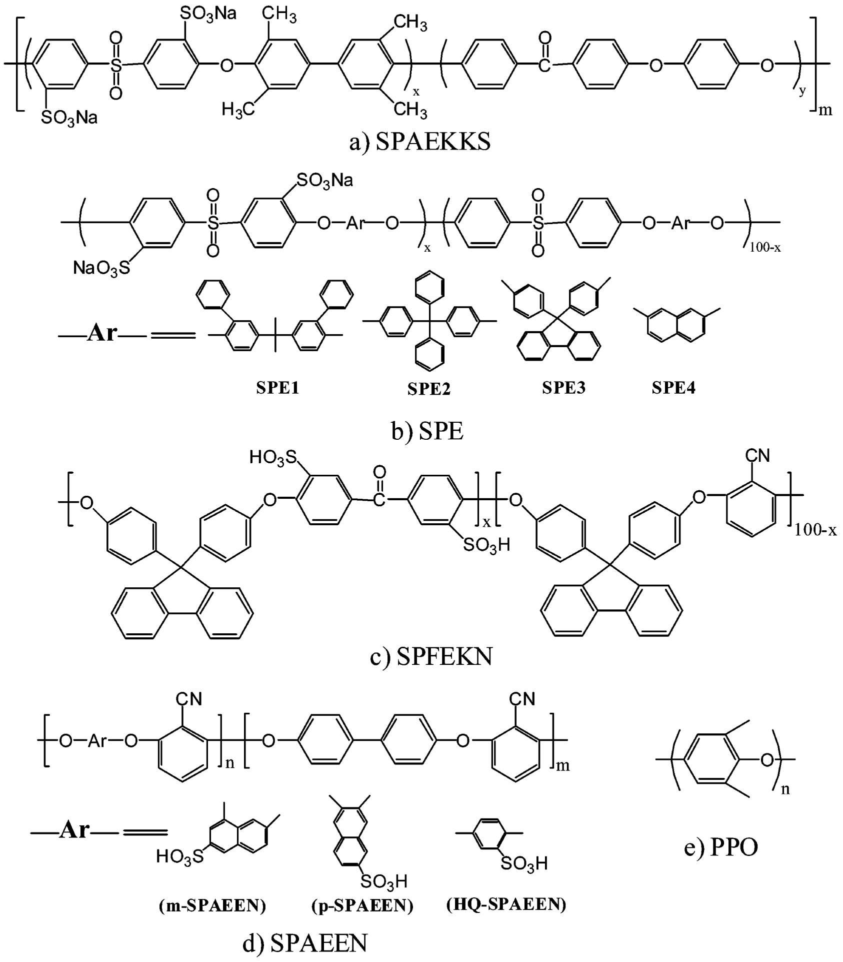

Figure 13. Chemical structures of several poly(arylene ether)s: a,[379] b,[381] c,[383] d,[384] and e.[385]

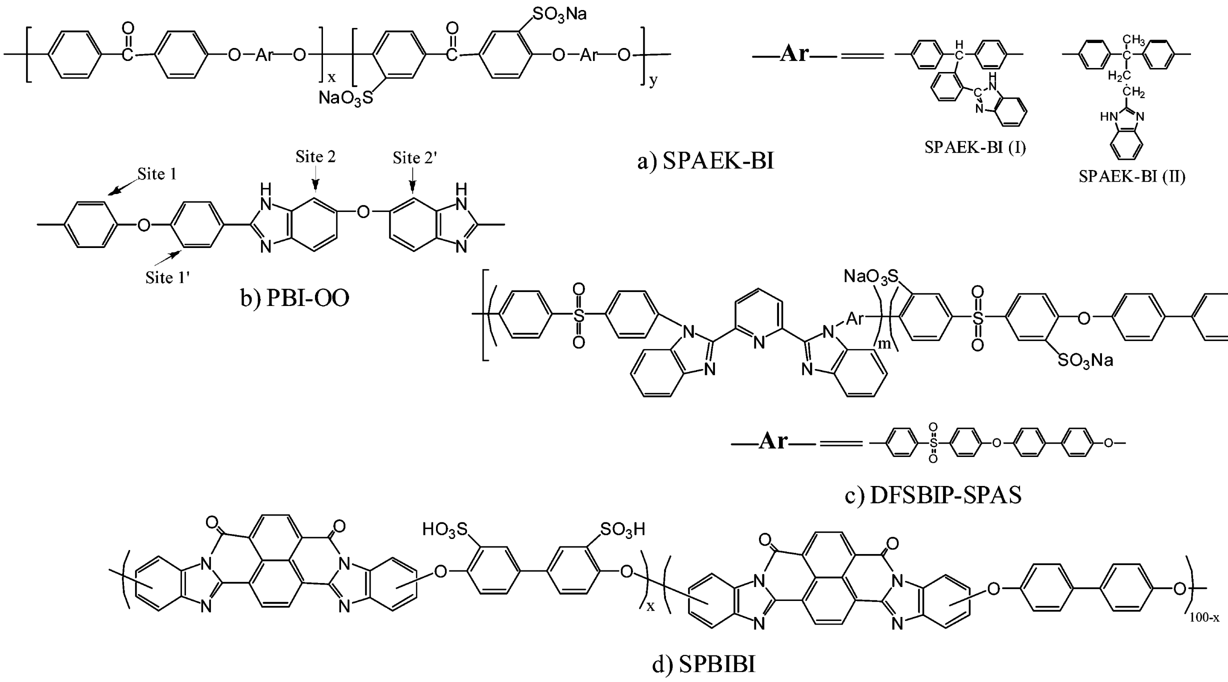

Figure 14. Chemical structures of several acid–base copolymers: a,[398,399] b,[400] c,[401] and d.[403]

bisazide as a cross-linker under thermal curing. The resulting cross-linked membrane offers excellent hydrolytic and oxidative stability, a proton conductivity 1.6 times as high as that of Nafion at 100 °C, and a methanol permeability that is only 17%

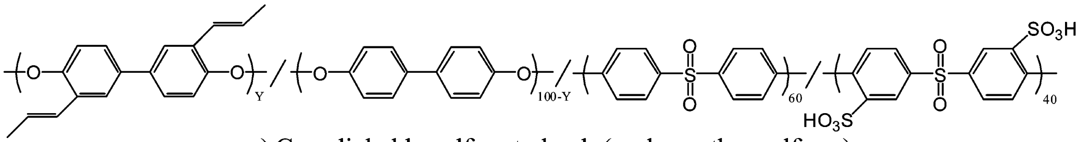

a) Crosslinkable sulfonated poly(arylene ether sulfone)

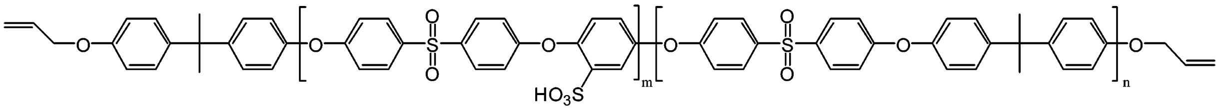

b) Allyl-terminated telechelic sulfonated poly(ether sulfone)

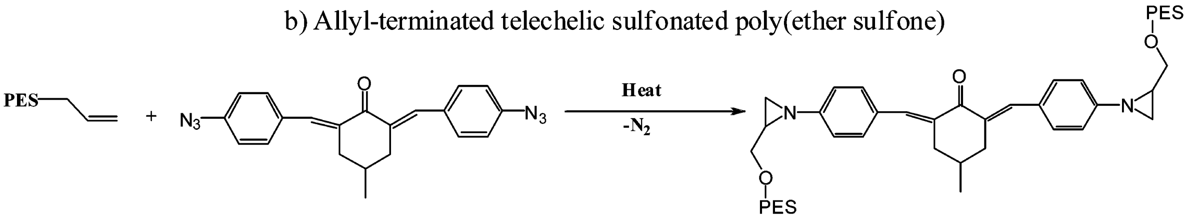

c) Mechanistic representation for the preparation of the crosslinked SPES using a bisazide as a crosslinker

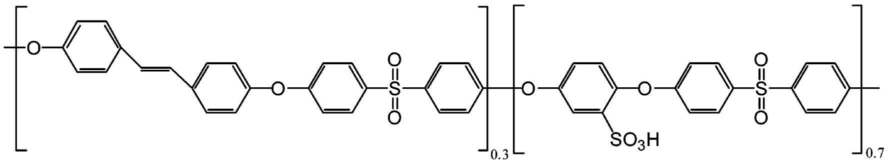

d) Crosslinkable sulfonated poly(ether sulfone) containing stilbene chain segment

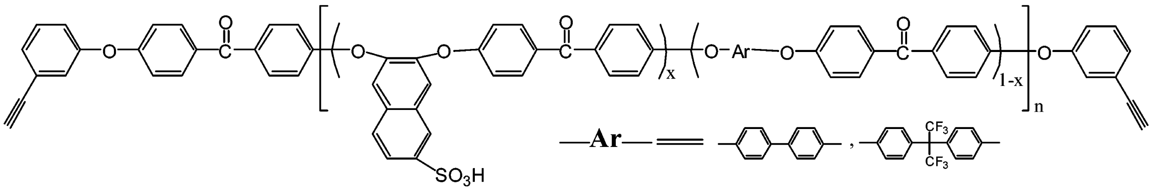

e)Crosslinkable sulfonated poly(arylene ether ketone) containing ethynyl moiety

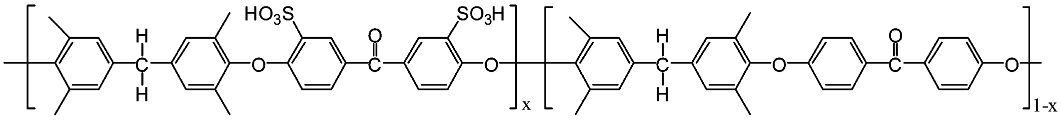

f)Sulfonated poly(aryl ether ketone) containing benzophenone units and methyl moieties

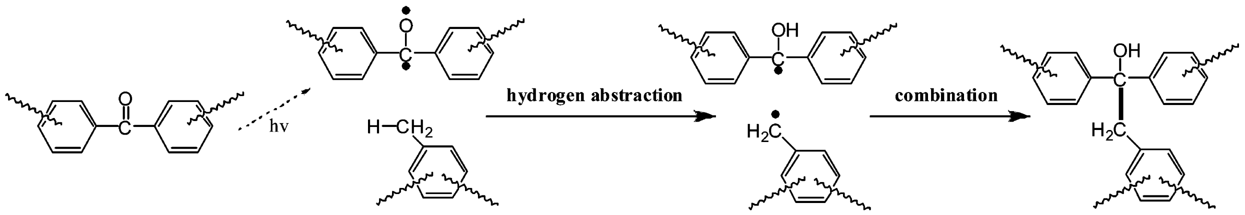

g) Mechanistic representation of the crosslinking between benzophenone units and methyl moieties

Figure 15. Chemical structures of several cross-linkable sulfonated poly(arylene ether) copolymers: a,[408] b,[411] c,[411] d,[412] e,[415] f,[409] and g.[409]

of that of Nafion at room temperature.[411] The cross-linked membrane from cross-linkable sulfonated poly(ether sulfone) (Figure 15d) with 4,4′-dihydroxystilbene and other commercially available monomers is insoluble in boiling water and has a proton conductivity of 0.12 S cm^{-1} at room temperature and 100% RH. The PEMFC based on this cross-linked membrane shows a power density of 900 mW cm^{-2} at 0.6 V with humidified oxygen and hydrogen at 70 °C.[412] The cross-linking of cross-linkable sulfonated poly(arylene ether ketone) containing ethynyl moiety (SPAEK) membrane (Figure 15e) is achieved by forming a benzene ring from the ethynyl moiety. The cross-linked SPAEK membrane with DS of 0.72 exhibits the maximum proton conductivity of 0.072 S cm^{-1} at room temperature and a water uptake of 33 wt %.[415] The cross-linking of multiblock sulfonated poly(aryl ether ketone) containing benzophenone units and methyl moieties (Figure 15f) is completed by UV irradiation to induce cross-linking between benzophenone units and methyl moieties (Figure 15g). On the basis of experimental results, it is concluded that the combination of a multiblock structure and a cross-linking system led to the decreased methanol permeability without decreasing the proton conductivity.[409]

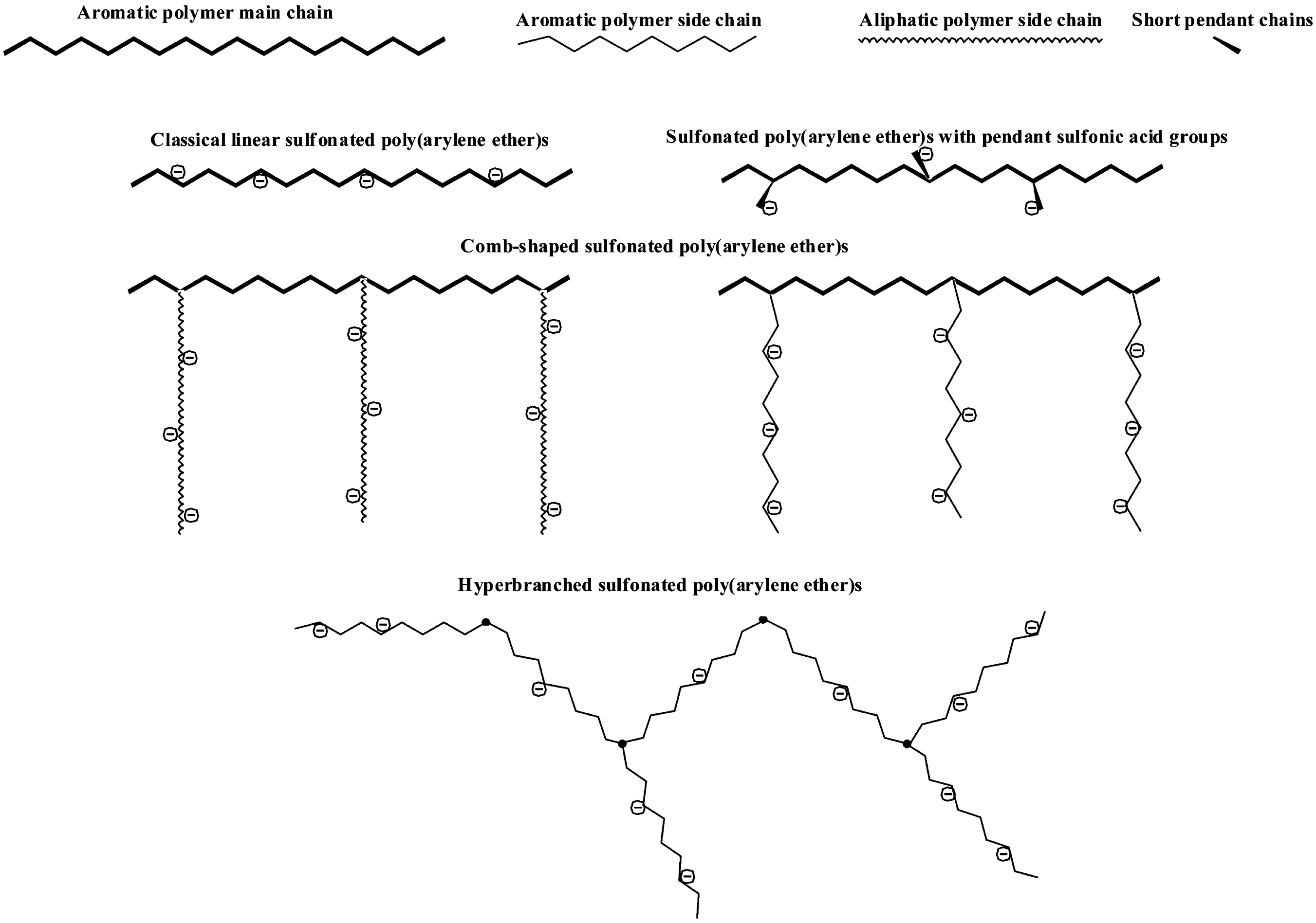

Figure 16. Different macromolecular architectures in poly(arylene ether)s with pendant sulfonated groups or side-chains.

The sulfonated poly(bis-A)sulfone (SPSF) membrane is cross-linked by a method different from those that proceed without the consumption of sulfonic acid groups. It is immersed into a mixture of phosphorus pentoxide/methanesulfonic acid (PPMA) to form cross-links consisting of the very stable sulfonyl group between the sulfonic acid groups and the activated phenyl rings. The cross-linking represses the swelling, reduces the water uptake, and enhances the dimensional stability of SPSF membranes with only a slight sacrifice in proton conductivity. The proton conductivity of cross-linked SPSF membranes remains at the same levels as in Nafion.[416]

4.1.3. Poly(arylene ether)s with Pendant Sulfonated Groups or Side-Chains.

It is generally considered that the polymers with pendant sulfonic acid groups or side-chains are more stable against hydrolysis than those with sulfonic acid groups directly on the backbone of the polymers. The architectures of sulfonated poly(arylene ether)s with pendant sulfonic acid groups or side-chains are shown in Figure 16.

The poly(arylene ether)s containing sulfofluorenyl groups can produce tough, flexible, and transparent membranes by solution casting. The best one (Figure 17a) shows proton conductivity comparable to that of Nafion112 under a wide range of conditions (80−120 °C and 20−93% RH). The highest proton conductivity, 0.3 S cm^{-1}, is achieved at 80 °C and 93% RH. Furthermore, it can still maintain the proton conductivity at acceptable levels for fuel cell operation after a 10 000 h durability test. The scanning transmission electron microscopic (STEM) image shows that the connectivity of ionic clusters in this excellent membrane is similar to that of the Nafion112 membrane.[418−420] These results obviously approach the 2015 technical targets of the Department of Energy (DOE), U.S.A., for membranes.[498] The membranes based on locally sulfonated poly(ether sulfone)s with highly sulfonated units can also be endowed with well-defined phase-separated structures and well-connected proton channels because of the high contrast in polarity between highly sulfonated units and hydrophobic poly(ether sulfone) units. The optimized membrane of this type (Figure 17b) shows proton conductivity comparable to that of Nafion 117 over a wide range of RH at 80 °C. Regrettably, there are no experimental results concerning durability tests on them.[422]

The comb-shaped copolymers attaching sulfonic acid groups on polymer side-chains can decrease the limitation of main-chain rigidity on the mobility of the sulfonic acid groups, enhance their degree of freedom, and thus lead to distinct phase separation and high proton conductivity. A variety of comb-shaped sulfonated polymers have been prepared by chemical grafting, direct copolymerization, or postsulfonation process to introduce sulfonated groups to the polymer side-chains.[423−431] Compared with classical sulfonated arylene main-chain polymer membranes, the comb-shaped copolymer membranes have good dimensional stability, the preferred proton conductivity, and well-developed hydrophilic/hydrophobic nanophase separation.

The hydrophilic−hydrophobic separation of comb-shaped copolymers can be enhanced by increasing the local sulfonic

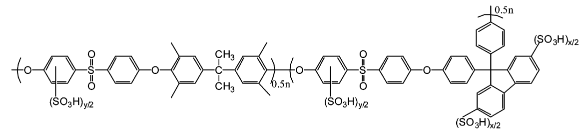

a) Poly(arylene ether sulfone) containing sulfofluorenyl groups

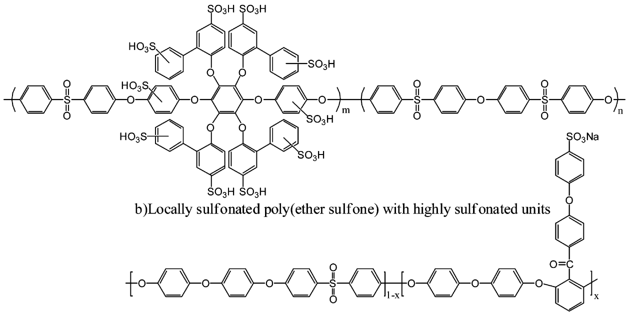

b)Locally sulfonated poly(ether sulfone) with highly sulfonated units

c)Side-Chain-Type Sulfonated Poly(aryl ether)s

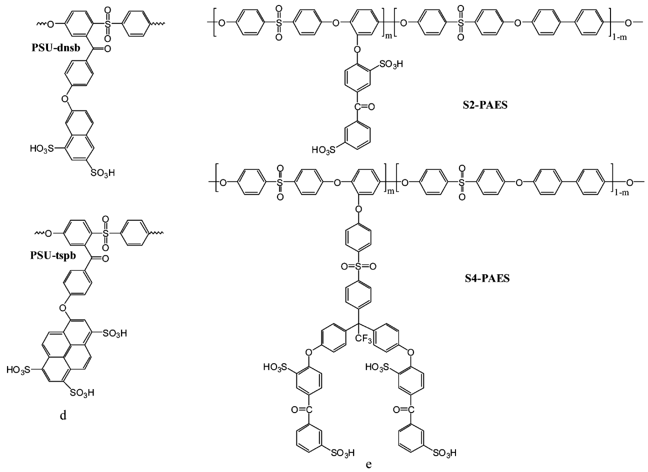

Comb-shaped poly(arylene ether) copolymers with hypersulfonated aromatic side chains

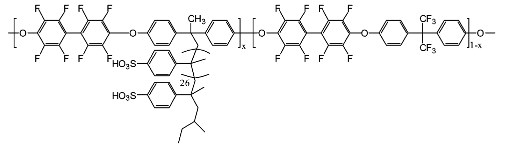

f)Highly fluorinated comb-shaped sulfonated poly(arylene ether) copolymer

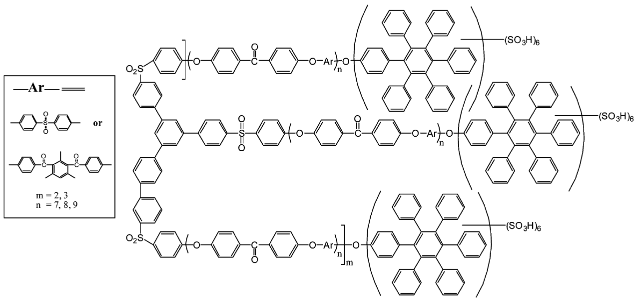

g)Branched poly(ether-ketone)s bearing sulfonic acid groups on the end groups

Figure 17. Chemical structures of poly(arylene ether)s with pendant sulfonated groups or side-chains: a,[419] b,[422] c,[423] d,[424] e,[425] f,[427] and g.[433]

acid group concentration. The comb-shaped poly(arylene ether) copolymers with hypersulfonated aromatic side chains for concentrating the sulfonic acid units locally were synthesized by Jannasch's group (Figure 17d) and Guiver's group (Figure 17e). Both of them show that high local sulfonic acid group concentration induces a distinct phase separation and, consequently, the formation of an advantageous morphology. However, higher local sulfonic acid group concentrations led to larger ionic clusters and hence to broader ion channels formed by the hydrophilic domains, all of which may promote methanol permeability. So it is the moderate, not the highest, local sulfonic acid group concentrations that produce efficient channel networks and well-balanced properties of the comb-shaped poly(arylene ether) copolymers with hypersulfonated aromatic side-chains. The membrane based on PSU-dsnb with an IEC of 1.69 mmol g^{-1} has a similar proton transfer activation energy as Nafion amd a much higher proton conductivity than that of Nafion in the temperature range 20−120 °C. The membrane based on S2-PAES with an IEC of 1.80 mmol g^{-1} shows a proton conductivity of 0.088 S cm^{-1} at 80 °C and a methanol permeability of 1.73×10^{-7} cm^2 s^{-1} at 30 °C.[424,425]

However, the comb-shaped sulfonated poly(arylene ether)s containing sulfonic acid groups on aliphatic side-chains are not always as good as their wholly aromatic analogues due to the chemical instability of aliphatic side-chains. For example, although the DMFC of highly fluorinated comb-shaped sulfonated poly(arylene ether) copolymer membrane (Figure17 f) offers a power density of 144.5 mW cm^{-2} at 80 °C when fed with a 2 M methanol solution and humidified air, the DMFC performance shows apparent loss after the 65 h life test.[427]

Only a few branched sulfonated poly(arylene ether) copolymers have been reported, and they often need blending and cross-linking with their linear analogues to improve their mechanical properties and prevent leaching caused by their low molecular weight.[432] The first example of a branched copolymer membrane without blending and cross-linking was branched wholly aromatic poly(ether ketone)s bearing clusters of sulfonic acid groups only on the end groups (Figure 17g), which is characteristic of both high local sulfonic acid group concentrations and hyperbranching. The resulting membrane shows significant phase-separated, wormlike, and highly connected morphology. Although its IEC is only similar to Nafion, the proton conductivity is still comparable to Nafion.[433]

4.1.4. Poly(arylene ether)s with Backbones Containing Heteroatoms Such as F, N, S, and P.

The aromatic polymers featuring heteroatoms in the skeleton generally show very attractive properties such as low swelling, improved thermooxidative stability, and high hydrolytic stability. The membranes from poly(arylene ether)s with backbones containing F atoms often demonstrate improved swelling behaviors and enhanced hydrophilic/hydrophobic phase separation owing to the character of the F atom.[438−441] For example, the sulfonated poly(fluorenyl ether) polymer-containing perfluorocyclobutane (PFCB) moieties (SPFE-PFCB) membrane (Figure 18a) with an IEC value of 1.86 mmol g^{-1} exhibits a water content of 25%, similar to that of Nafion115, but shows higher proton conductivity than Nafion115 over the temperature range 25−80 °C due to the strong hydrophobicity of PFCB and the bulkiness of fluorene in main chains.

The phthalazinone-based poly(arylene ether) polymers are a remarkable heterocyclic copolymer family and form a well-explored class of high performance polymers with excellent thermal, mechanical, and oxidative properties as well as good proton conductivity. In the synthesis of these polymers, the pivotal monomer is 4-(4-hydroxyphenyl)-2,3-phthalazin-1-one (DHPZ) (Figure 19a), which can readily undergo a nucleophilic substitution reaction to give polymer because the phthalazinone NH groups behave like phenolic OH groups.[443] Compared with sulfonated poly(arylene ether) copolymers with similar structure but not containing DHPZ, the sulfonated

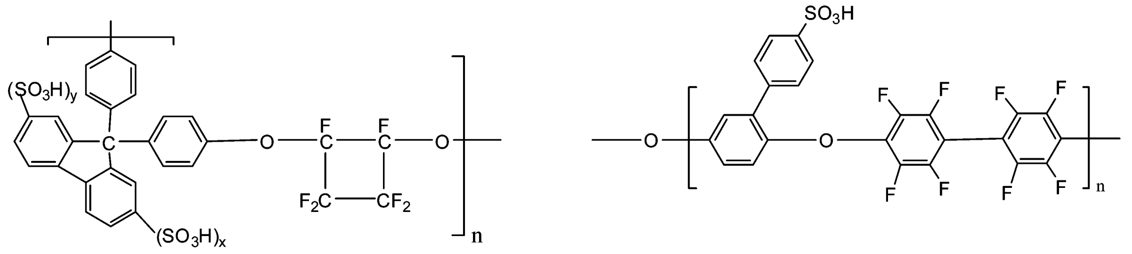

a) SPFE-PFCB b) SPAE

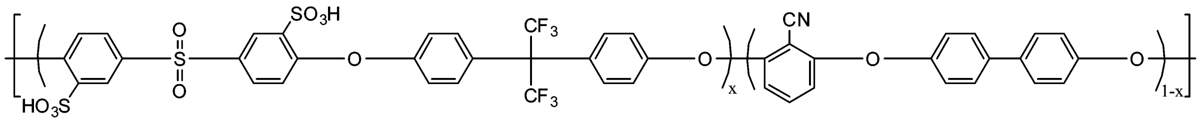

c) Partially fluorinated poly(arylene ether benzonitrile) copolymer

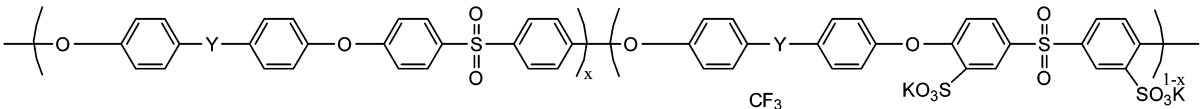

d)BPS-35 (Y= a bond) and 6FS-35 (Y= $\overset{CF_3}{\underset{CF_3}{C}}$)

Figure 18. Structures of four poly(arylene ether)s with backbones containing F atom: a,[438] b,[439] c, and [440] d.[441]

poly(arylene ether) copolymers incorporating DHPZ show relatively lower water uptake, methanol permeability, improved mechanical and thermal properties, and oxidative stability arising both from the inherent twisted noncoplanar structure of the DHPZ moiety and from the hydrogen bonding between the hydrogen atoms of the sulfonic acid and the carbonyl groups of the oxyphenyl phthalazinone unit.[444,445]

The sulfonated poly(arylene ether) copolymers containing heterocycle units such as benzoxazole, oxadiazole, oxadiazole triazole, and pyridine are yet another kind of heterocyclic polymers. The sulfonated poly(arylene ether) copolymers containing the benzoxazole moiety (SPAEBO) (Figure 19b) show a different proton-conducting trend than do the general sulfonated poly(arylene ether) copolymers at 120 °C without external humidification in that their proton conductivities decrease with DS or IEC. The SPAEBO with an IEC of 0.18 mmol g^{-1} has a proton conductivity of 1.8×10^{-2} S cm^{-1}, while the SPAEBO with an IEC of 1.59 mmol g^{-1} has a proton conductivity of only 7.6×10^{-4} S cm^{-1} at 120 °C without external humidification because higher benzoxazole content leads to a larger amount of strongly bound water. The former exhibits a surprisingly long oxidative stability (>1200 h) in Fenton's reagent at room temperature, whereas the latter only extends to 5 h.[452] The high molecular weight sulfonated poly(oxadiazole triazole) copolymers (SPOD-SPT) (Figure 19d) can be synthesized by polycondensation of sulfonated hydrazine with an aromatic dicarboxylic acid and a sulfonated or nonsulfonated daniline in poly(phosphoric acid) using short reaction times. The SPOD-SPT membranes have good mechanical properties and high thermal stability and have a high proton conductivity of up to 6×10^{-2} S cm^{-1} at 150 °C and 100% RH.[458] After the SPOD-SPT membranes are doped with 1*H*-benzimidazole-2-sulfonic acid, an amphoteric molecule, these membranes can attain conductivity values on the order of 10^{-3} S cm^{-1} under high-temperature and extremely low-humidity conditions.[459]

Kallitsis's group has synthesized a series of pyridine-based aromatic copolymers that, when doped with phosphoric acid, are used as PEMs for operation under high-temperature and very low-humidity conditions. Most of the copolymers studied exhibit good mechanical properties, excellent film-forming properties, high oxidative and thermal stabilities, and an acid-doping ability with high acid uptake.[460−463] For instance, the pyridine-based poly(ethersulfone) (Ppy-PES) (Figure 19e) membrane has a high conductivity value of 1.4×10^{-2} S cm^{-1} with a doping level of 240 wt % H_3PO_4 at 160 °C. These membrane samples retain their mechanical integrity as well as their thermal stability up to 470 °C after treatment with Fenton's reagent for 72 h at 80 °C. The H_2/O_2 PEMFC using the Ppy-PES membrane with an initial phosphoric acid doping level of 220 wt % generates a maximum performance of 214 mA cm^{-2} at a cell voltage of 0.5 V at 180 °C using dry gases under ambient pressure.[463]

The most common poly(arylene ether) polymer containing sulfur atom on the backbone is poly(phenylene sulfide) (PPS), also called poly(thiophenylene). It is a highly resistant engineering plastic and is almost totally insoluble in organic solvents below 200 °C.[464] The sulfonated PPS powders with a DS of 0.70 show 0.12 S cm^{-1} proton conductivity at 127 °C and 50% RH, but they are water-soluble and extremely brittle, which prevents them from being used as PEMs.[465]

The sulfonated poly(arylenethioethersulfone) (SPTES) (Figure 19f) polymer membranes exhibit excellent thermal stability, mechanical properties, and dimensional stability along with high oxidative stability, good water affinity, and sufficient proton conductivity. After incorporating hexafluoroisopropylidene groups into SPTES main chains, the hexafluorinated SPTES membranes still have high proton conductivity, but the water retention is inferior to that of their nonfluorinated counterparts.[466−469] However, it is difficult to synthesize high molecular weight poly(arylene ether) polymers containing sulfur because of the low reactivity of sulfur-containing monomers. To enhance the dimensional stability of such polymers, ionic or

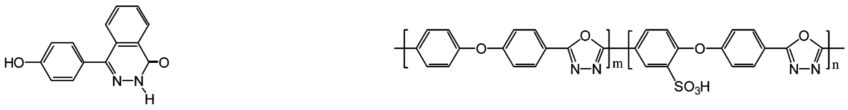

a) Chemical structure of DHPZ

c) Chemical structure of SPODDPE

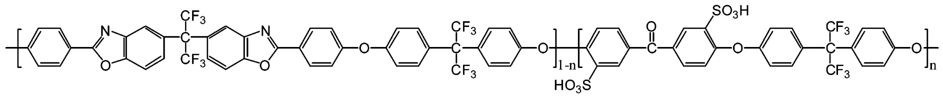

b) Chemical structure of SPAEBO

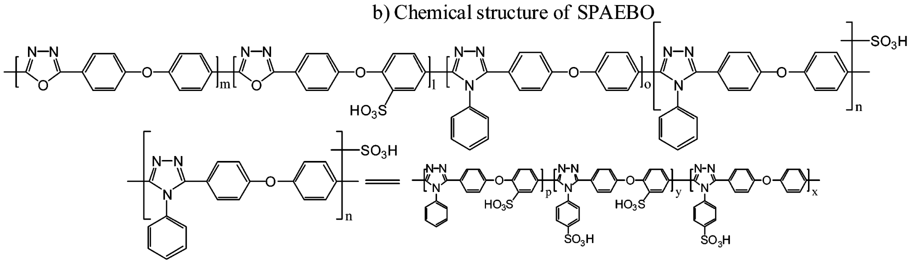

d) Chemical structure of SPOD-SPT

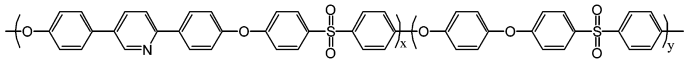

e) Chemical structure of Ppy-PES

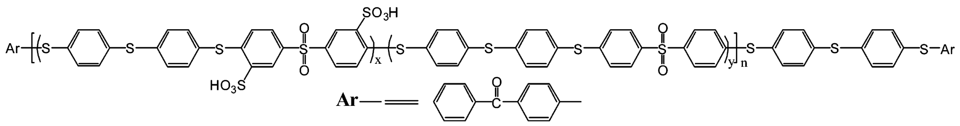

f) Chemical structure of SPTES

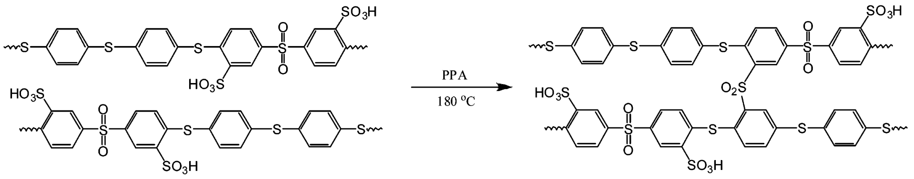

g) Schematic diagram for the crosslinking reaction of SPTES membranes

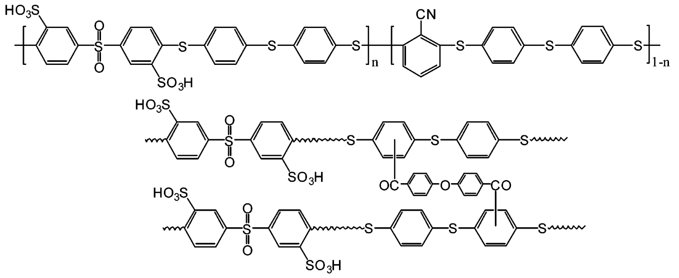

h) Chemical structure of SPPSSfN and crosslinked SPPSSfN

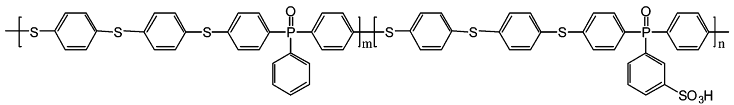

i) Chemical structure of SPATPO

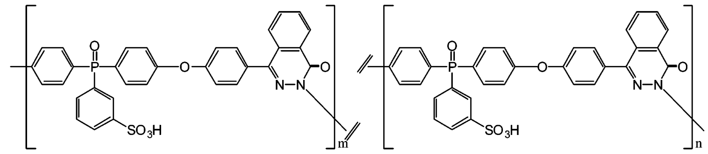

j) Chemical structure of SPPEPO

Figure 19. Chemical structures of poly(arylene ether)s with backbones containing heteroatoms: a,[443] b,[452] c,[455] d,[458] e,[463] f,[467] g,[473] h,[474] i,[476] and j.[477]

covalent cross-linking is used.[470−474] For instance, cross-linked SPTES (Figure 19g) membranes exhibit better mechanical properties, lower water uptake, and lower methanol permeability than those of the corresponding un-cross-linked SPTES membranes. The maximum output power density of an H_2/O_2 PEMFC using cross-linked SPTES membrane under a back-pressure of 0.2 MPa is 1.32 W cm^{-2} under 80 °C and 100% RH, which is slightly lower than that attained using an un-cross-linked SPTES membrane with a similar IEC, whereas the OCV decay rate in the cross-linked case is significantly slower than that in the un-cross-linked case. This indicates that the PEMFC lifetime is significantly improved by the cross-linking at the cost of negligible PEMFC performance loss. The high polyphosphoric acid (PPA) uptake of ~800 g PPA/100 g SPTES is attained during the cross-linking treatment of SPTES, which may provide an option of PEMs doping with H_3PO_4 for high-temperature PEMFCs.[473]

The cross-linking of the sulfonated poly(phenylene sulfide sulfone nitrile) (SPPSSfN) can be done by using the Friedel–Crafts acylation reaction (Figure 19h). The cross-links are formed between the carboxylic acid groups in the 4,4′-oxybis(benzoic acid) cross-linker and the nucleophilic phenyl rings in SPPSSfN rather than the $-SO_3H$ groups, which only act as a benign solid catalyst. The cross-linked SPPSSfN membranes show lower water swelling and lower methanol permeability than do un-cross-linked SPPSSfN membranes while maintaining proton conductivity, thus indicating that Friedel–Crafts cross-linking is very effective at improving dimensional stability.[474]

Phosphine oxide moieties endow materials with good water retention and adhesive ability with inorganic compounds. The poly(arylene ether phosphine oxide)s and poly(arylene thioether phosphine oxide)s show excellent mechanical properties, thermal stability, and chemical stability.[475] However, there are few reports on PEMs derived from sulfonated poly(arylene ether) copolymers containing phosphine oxides.

Ma and co-workers report high molecular weight sulfonated poly(arylene thioether phosphine oxide) (SPATPO) (Figure 19i) copolymers. They found that the SPATPO membrane with an IEC of 1.14 mmol g^{-1} exhibits a swelling ratio of 11.6% at 80 °C and a proton conductivity of 7.83×10^{-2} S cm^{-1} at 90 °C and 100% RH. But the SPATPO membranes with higher IEC often swell excessively and even dissolved in water at temperatures of >70 °C.[476] One of the ways to resolve this problem is to incorporate the DHPZ units into sulfonated poly(arylene ether) copolymers containing phosphine oxides to obtain sulfonated poly(phthalazinone ether phosphine oxide)s (SPPEPO) (Figure 19j). The experimental results indicate that SPPEPO membranes with high IEC exhibit high proton conductivity while they still maintain low swelling. It has been reported for instance that two typical SPPEPO membranes with IECs of 1.54 and 1.69 mmol g^{-1} exhibit high proton conductivities of 0.091 and 0.19 S cm^{-1} and low swelling ratios of 14.3% and 19.5% at 80 °C, respectively. This can be attributed to strong intermolecular interactions such as electrostatic forces and hydrogen bonds.[477]

4.1.5. Multiblock Copoly(arylene ether)s Synthesized by the Coupling Reaction of Hydrophilic and Hydrophobic Macromonomers. Studies on sulfonated multiblock poly(arylene ether) copolymers have indicated that multiblock copolymer systems with well-defined sulfonated regions may provide proton conductivities superior to those of the corresponding sulfonated statistical analogues, especially at low relative humidity.[478−489,491,492] They are usually synthesized by the coupling reaction of hydrophilic and hydrophobic telechelic oligomers, but highly reactive chain extenders such as decafluorobiphenyl (DFBP) and hexafluorobenzene (HFB) are needed because of the poor coupling reactivity between the two oligomers. The highly reactive nature of their fluorine-terminated telechelic oligomers permits the coupling reaction at a significantly lower temperature, which can prevent potential ether–ether exchange side-reactions.[480]

4.1.5.1. Long-Block-Induced Microstructure. Hydrophilic–hydrophobic multiblock copolymers based on poly(arylene ether)s have higher protonic conductivity, lower activation energy, and much improved self-diffusion coefficients for water as compared with the random copolymers with similar IEC values. Their proton and water transport increase significantly with increasing block length because the longer block induces a more developed phase separation. When the hydrophilic and hydrophobic block lengths are greater than or even near to 10 K g mol^{-1}, this phenomenon will be much more evident. A cocontinuous hydrophilic–hydrophobic morphology with enhanced phase separation (which can be called "*long-block-induced microstructure*") encourages the formation of free water, even at lower IEC values or under partially hydrated conditions where the morphology is more important than the acidity of the system.[483−489] Lee and co-workers find that the hydrophilic–hydrophobic multiblock copolymers based on poly(arylene ether sulfone) membranes show anisotropic swelling behaviors, whereas the random analogues are isotropic. Their in-plane swelling is lower than their through-plane swelling, especially when the block lengths exceed 10 K g mol^{-1}.[487] Nakabayashi and co-workers incorporated hexafluoroisopropylidene groups into sulfonated multiblock copoly(ether sulfone)s and found that, because of enhanced phase separation by hydrophobic domains with fluorine groups, the resultant membranes have a lower water uptake but a protonic conductivity similar to the sulfonated multiblock copoly(ether sulfone)s lacking fluorine groups.[488,489] Takimoto and co-workers investigated multiblock poly(arylene ether sulfone)s. They found that the nonconductive regions on the surface of the multiblock poly(arylene ether sulfone) (10 K–10 K g mol^{-1}) membrane is near 50% due to well-developed hydrophilic/hydrophobic microphase separation, which will affect the interfacial connection with the electrode and lead to poor PEMFC performance under low RH conditions.[490]

Yu and co-workers reported an effective synthetic method for sulfonated multiblock poly(arylene ether) copolymers that allows the hydrophobic and hydrophilic block length and the IEC to be changed simultaneously. They synthesized a series of sulfonated multiblock poly(arylene ether) copolymers (BisSF-BPSH) (Figure 20) and found that the properties of the BisSF-BPSH membranes can be tailored to some degree by altering the IEC, the hydrophilic block length, or the hydrophobic block length independently. For example, within a certain range, the proton conductivity of a BisSF-BPSH membrane at low hydration levels can be increased by three methods: increasing the IEC, increasing the hydrophilic block length, or decreasing the hydrophobic block length. Through careful balance of the three methods, the optimal trade-off between performance (proton conductivity under partially hydrated conditions) and water uptake is obtained within a BisSF-BPSH (17 K–12 K g mol^{-1}) (IEC = 1.5) copolymer membrane, and it is the only one in the series that is able to outperform Nafion112 while still maintaining a low water uptake (~40 wt %) well within the acceptable range.[491]

4.1.5.2. Similarity between the BisSF-BPSH and Pore-Filling Blending Membranes. In fact, if one considers the porosity of the reinforcing material in the pore-filling membrane[493,494] as an apparent IEC, then many similarities between the BisSF-BPSH and the pore-filling blended membrane may be found. The three parameters of BisSF-BPSH (the IEC, the

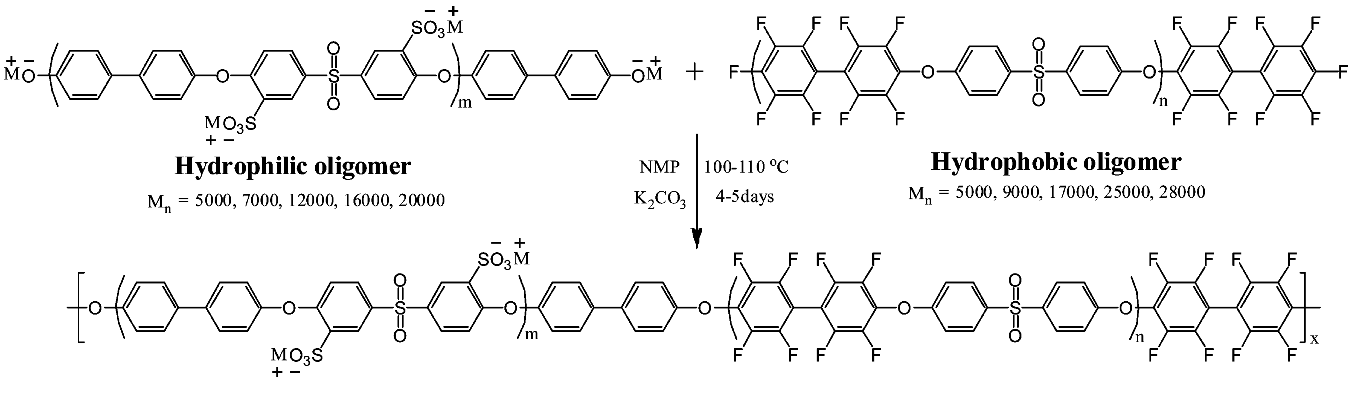

Figure 20. Synthesis of BisSF-BPSH multiblock copolymers.[491]

hydrophilic block length, and the hydrophobic block length) then correspond to the porosity, the degree of sulfonation of the sulfonated poly(ether sulfone) (SPES), and the connectivity of the porous substrate in the pore-filling membrane, respectively.

But there are still two main dissimilarities between the pore-filling membrane and BisSF-BPSH. The hydrophilic blocks and hydrophobic blocks in BisSF-BPSH are connected by chemical bonds, whereas there is only physical interfacial interaction between the reinforcing material and SPES. The BisSF-BPSH can swell freely, whereas the swelling of the pore-filling membrane is considerably suppressed by the rigid substrate, which leads to no free water in the latter. As a result, the pore-filling membrane only has a proton conductivity of 0.052 S cm^{-1} at 25 °C but has a methanol permeability 300 times lower than that of Nafion117 at 25 °C.[493,494] Although the methanol permeability of the BisSF-BPSH has not been reported, it can be surmised that those data will not be encouraging because of the clear hydrophilic/hydrophobic phase-separated structure in BisSF-BPSH.

4.2. Polyimide-Based Membranes

SPIs, especially sulfonated six-membered ring (naphthalenic) polyimides, are proposed as promising candidates for PEMs because of their excellent chemical and thermal stability, high mechanical strength, good film-forming ability, and low fuel gas (or liquid) crossover. Most of their physicochemical properties are rather different from those of Nafion.[499,500] These differences are (i) that they swell mainly along the membrane thickness due to their structural anisotropy, (ii) the incomplete separation between their hydrophobic and hydrophilic domains, (iii) their almost constant value of λ over a wide range of ion content, and (iv) a multiscale foliated structure packed along the membrane thickness. All of them yield a performance comparable to that of Nafion for PEMFC and DMFC but also give low water stability because of high sensitivity of the imide rings to hydrolysis under moist conditions and moderate temperatures (>70 °C).

Various approaches for enhancing the hydrolytic stability of sulfonated polyimides have been developed, including (i) using monomers with flexible linkages,[501] (ii) using monomers without a sulfonic acid group and an amine group both in the same ring,[502] (iii) using diamine monomers with high nucleophilicity,[503] (iv) using aliphatic diamines,[504] (v) using napthalenic dianhydrides,[505] (vi) using diamines with the sulfonic acid group in a side-chain,[506] (vii) using trifunctionalized monomers with cross-linkable groups to initiate cross-linking,[507,508] (viii) blending with aromatic engineering plastics or inorganic particles,[509−516] and (ix) forming semi-interpenetrating polymer networks with suitable materials.[517,518] This section focuses on introducing the synthesis of sulfonated polyimides using new monomers to increase their membrane stability. More comprehensive information can be found in the review about sulfonated polyimides.[500]

Because it is difficult to control the sulfonic group distribution along the SPI chains through the postsulfonation method, some SPIs using the postsulfonation method have been reported.[519−521] On the contrary, most SPIs are synthesized by the condensation of sulfonated and unsulfonated diamines with naphthalenic dianhydrides.[522−538] Typical SPIs are listed in Figure 21. From Table 5, it appears that hydrolytic stability and oxidative stability are opposing trends in SPIs, which indicates that improvement of durability for SPIs is more difficult than that for SPEs.

4.2.1. *SPIs* Based on NTDA.

All of the SPIs based on 1,4,5,8-naphthalenetetracarboxylic dianhydride (NTDA) show proton conductivities comparable to or higher than that of Nafion at high relative humidity and high temperature, as well as methanol permeability almost 10 times lower than that of Nafion. However, the hydrolytic and oxidative stability are very different. The following observations may be made:

(1) The incorporation of flexible linkages into NTDA-based SPIs (e.g., SPI-a,[522] SPI-b,[523] SPI-h[527]) can increase the hydrolytic stability, flexibility, and solubility of the final PEMs.

(2) The NTDA-based SPI-d membranes with smaller interacid separations of sulfonic acid groups show much lower water uptake and higher proton conductivities than those of SPI-c membranes with similar IECs.[524] The low water uptake confers a good hydrolytic stability on the SPI-d membranes (240−500 h at 100 °C depending on the IEC). However, their oxidation stabilities are insufficient, being only 10−17 h in Fenton's reagent at 30 °C.

(3) The NTDA-based SPIs with nonplanar structures give varying results. SPI-c membranes with a nonplanar binaphthyl result in easy relaxation of the polymer chain and produce large interchain spaces to hold water. The SPI-c membrane having an IEC of 1.50 mmol g^{-1} exhibits a swelling ratio greater than 40% at 80 °C,[524] whereas the SPI-k membrane containing DHPZ with an IEC of 1.42 mmol g^{-1} has a swelling ratio of only 7.5% at 80 °C.[531,532]

(4) The NTDA-based SPIs bearing sulfophenyl pendant groups (SPI-e,[525] SPI-f[526]) show a markedly anisotropic

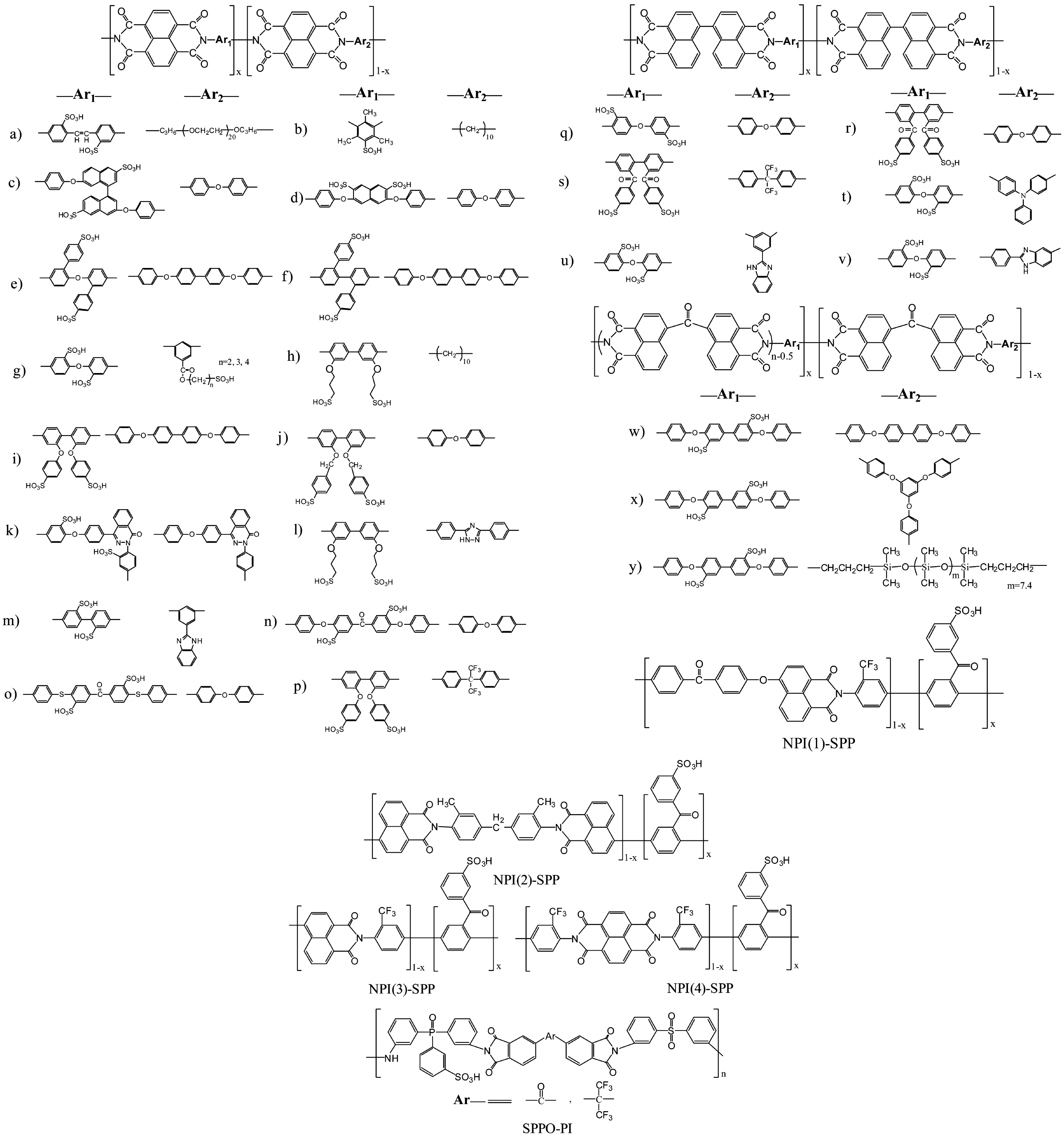

Figure 21. Chemical structures of SPIs: a,[522] b,[523] c,[524] d,[524] e,[525] f,[526] g,[527] h,[528] i,[529] j,[530] k,[532] l,[535] m,[536] n,[537] o,[537] p,[538] q,[539] r,[540] s,[540] t,[541] u,[542] v,[542] w,[543] x,[543] y,[544] NPI(1)-SPP,[545] NPI(2)-SPP,[546] NPI(3)-SPP,[547] NPI(4)-SPP,[547] SPPO-PI.[548]

character and fairly high water stability. The SPI-f membrane with an IEC of 1.58 mmol g^{-1} has a swelling in the thickness direction (34%) 10 times larger than in the in-plane direction (3%). In addition, the side-chain-type SPIs (SPI-i,[529] SPI-j[530]) also possess anisotropy and improved hydrolytic stability compared with the main-chain-type polyimides due to enhanced basicity of the amine groups as well as increased separation of the sulfonic acid group from the imide functionality. The SPI-i membrane with an IEC of 1.84 mmol g^{-1} has a proton conductivity of 0.05 S cm^{-1} under 50% RH at 120 °C. Under conditions of 90 °C, 0.3 MPa, and 30% RH, the SPI-i membrane gives a high PEMFC performance of 1.09 W cm^{-2} due to the easy back-diffusion of water.

(5) The NTDA-based SPIs with aliphatic side-chains (SPI-g,[527] SPI-h,[528] SPI-l[534,535]) often show favorable long-term durability. Both SPI-h and SPI-l membranes have a long-term durability of 5000 h in H_2/air PEMFC operation at 80 °C.

Table 5. Property Comparison of Typical SPIs

SPI	IEC (mmol/g)	water uptake (%W/W)	λ	dimensional changes		hydrolytic stability (h)	oxidative stability (h)	proton conductivity (S/cm)	methanol permeability (cm^2 s^{-1})	reference
				Δt	Δl					
SPI-b	1.57	30 (80 °C, 95% RH)	NR[b]	NR	NR	>48 (140 °C)	>1 (80 °C)	0.10 (80 °C, 95% RH)	NR	523
SPI-d	1.59	19.8	NR	0.09	0.03	320 (100 °C)	15 (30 °C)	0.138 (80 °C water)	3.8×10^{-7} (25 °C)	524
SPI-e	1.80	50 (60 °C)	15	0.13	0.06	<48 (130 °C)	NR	0.106 (60 °C water)	NR	525
SPI-f	1.58	79 (100 °C)	19	0.34	0.03	<192 (130 °C)	NR	0.121 (60 °C water)	NR	526
SPI-g	2.32	54.2	13.0	NR	NR	784 (80 °C)	36 (30 °C)	0.110 (80 °C, 90% RH)	NR	527
SPI-i	1.84	78 (30 °C)	23	0.39	0.026	500 (130 °C)	NR	0.168 (60 °C water)	NR	529
SPI-j	1.94	53	15	NR	NR	120 (80 °C)	NR	0.043 (25 °C water)	NR	530
SPI-k	1.42	39.5 (80 °C)	NR	NR	NR	34 (90 °C)	17 (25 °C)	0.038 (95 °C, 100% RH)	NR	532
SPI-m	1.94	52	15	NR	NR	NR	NR	0.040 (90 °C, 100% RH)	NR	536
SPI-n	1.75	79 (80 °C)	NR	NR	NR	390 (80 °C)	0.95 (80 °C)	0.140 (60 °C water)	3.7×10^{-7} (30 °C)	537
SPI-o	1.76	75 (80 °C)	NR	NR	NR	>1000 (80 °C)	0.60 (80 °C)	0.140 (60 °C water)	3.2×10^{-7} (30 °C)	537
SPI-p	1.42	76	28	0.48	0.019	NR	NR	0.156 (60 °C water)[a]	NR	538
SPI-q	2.21	53	13	NR	NR	>800 (100 °C)	NR	0.206 (60 °C, 100% RH)	2.25×10^{-7} (25 °C)	539
SPI-r	1.71	40.5	12.9	0.18	0.01	800 (90 °C)	35 (30 °C)	0.147 (80 °C water)	NR	540
SPI-s	1.59	37.5	12.5	0.13	0.01	130 (90 °C)	48 (30 °C)	0.139 (80 °C water)	NR	540
SPI-t	2.21	50	12.2	0.11	0.02	>1000 (90 °C)	4 (30 °C)	0.201 (80 °C water)	2.7×10^{-7} (25 °C)	541
SPI-u	2.26	55	13.5	0.18	0.06	>1000 (90 °C)	16 (30 °C)	0.166 (80 °C water)	2.4×10^{-7} (25 °C)	542
SPI-v	2.27	57	13.9	0.16	0.06	>1000 (90 °C)	16 (30 °C)	0.178 (80 °C water)	2.5×10^{-7} (25 °C)	542
SPI-w	1.71	43	14	0.11	0.069	<300 (130 °C)	NR	0.070 (60 °C water)	NR	543
SPI-x	1.79	55	16	0.12	0.038	300 (130 °C)	NR	1.240 (60 °C water)	NR	543
SPI-y	20.9	63	17	NR	NR	NR	NR	0.143 (60 °C water)	NR	544
NPI(1)-SPP	2.00	72	9.4	0.21	0.09	250 (140 °C)	10 (25 °C)	0.321 (80 °C water)	6.2×10^{-7} (25 °C)	545
NPI(2)-SPP	1.88	39	11.5	0.06	0.04	NR	41 (30 °C)	0.106 (80 °C water)	NR	546
NPI(3)-SPP	1.65	61	11.9	0.19	0.03	196 (100 °C)	>83 (25 °C)	0.260 (80 °C water)	NR	547
NPI(4)-SPP	1.89	31	5.3	0.15	0.02	<23 (100 °C)	50 (25 °C)	0.075 (80 °C water)	1.8×10^{-7} (25 °C)	547

[a] In-plane proton conductivity; its through-plane proton conductivity is only 0.033 S cm^{-1}. [b] NR = not reported

(6) Incorporation of benzimidazole heterocycles into the NTDA-based SPIs (SPI-m[536]) results in enhanced thermal and mechanical stability because of strong interactions between imidazole and sulfonic acid groups, but the proton conductivity is fairly low (~4.0×10^{-2} S cm^{-1}) even above 100 °C at 100% RH.

(7) Contrary to the case of SPEs containing a sulfur atom, the SPIs containing a sulfur atom have inferior oxidative stability, probably due to the stronger electron-donating effect of the thio-ether group.[537]

(8) The multiblock NTDA-based SPIs (SPI-p[538]) with block lengths higher than 10 K g mol^{-1} also possess a *long-block-induced microstructure* that leads to higher water uptake than that of the controlled SPI. However, the hydrophilic and hydrophobic domains of SPI-p are oriented in the in-plane direction of the membrane to form a layer-like structure, which causes anisotropic swelling and proton conductivity. These SPI-p membranes have lower PEMFC performance than the random analogues because of the lower through-plane conductivity. It seems that the multiblock SPIs with large hydrophilic and hydrophobic block lengths are unfavorable for PEMs due to the anisotropy of their proton conductivity.

4.2.2. *SPIs* based on BNTDA. 4,4′-Binaphthyl-1,1′,8,8′-tetracarboxylic dianhydride (BNTDA), with higher electron density in carbonyl carbon atoms than NTDA, is employed to prepare SPIs because the dianhydrides with higher electron density in the carbonyl carbon atoms can produce polyimides with higher hydrolytic stability.[539−542] The BNTDA-based SPIs (SPI-q,[539] SPI-r,[540] SPI-s[540]) have much better oxidative and hydrolytic stability than those based on NTDA owing to the higher electron density in the carbonyl carbon atoms of BNTDA. However, the existence of the hexafluoroisopropylidene group in the SPI-s membrane greatly impairs its hydrolytic stability.

The BNTDA-based SPI bearing basic triphenylamine groups (SPI-t) with an IEC of 2.21 mmol g^{-1} has a proton conductivity of 0.11 S cm^{-1}, a methanol permeability of 2.7×10^{-7} cm^2 s^{-1} at 20 °C, and a hydrolytic stability of >1000 h in water at 90 °C. However, it only resists Fenton's reagent for 4 h at 30 °C, indicating the very poor oxidative stability caused by the high electron density on the triphenylamine groups and the reactivity of the nitrogen atoms with highly oxidative radical species.[541]

Unlike SPI-m, the BNTDA-based SPIs containing benzimidazole groups (SPI-u and SPI-v)[542] show high proton conductivity even at 20 °C and 100% RH. The SPI-u membrane with an IEC of 2.01 mmol g^{-1} has a proton conductivity of 4.8×10^{-2} S cm^{-1} at 20 °C and 100% RH and a low methanol permeability of 1.5×10^{-7} cm^2 s^{-1}, because the formation of an acid−base complex reduces the vacant space that absorbs free water molecules and thus induces a much denser structure that acts as a methanol barrier.

All of the SPI-u and SPI-v membranes have a hydrolytic stability of >1000 h in 90 °C water, but only those membranes with an IEC lower than 2.0 mmol g^{-1} can endure 18 h without dissolving in Fenton's reagent at 30 °C.

4.2.3. *SPIs* Based on Other Dianhydrides.

There are a few SPIs with different structures than those mentioned above.[543−549] The flexible 4,4′-ketone dinaphthalene 1,1′,8,8′-tetracarboxylic dianhydride (KDNTDA)-based SPIs (SPI-w) have good solubility in common aprotic solvents, but they show slightly lower water stability than do the NTDA-based ones. This is probably due to the better solubility in hot water of the KDNTDA-based sulfonated oligomer or the hydrolysis product. When 1,3,5-tris(4-aminophenoxy)benzene (TAPB) is incorporated, the branched/cross-linked KDNTDA-based SPIs (SPI-x) are obtained. The SPI-x membrane with an IEC of 1.85 mmol g^{-1} has greater water stability and still maintains good mechanical properties and proton conductivity even after aging in water at 130 °C for 300 h.[543]

The multiblock KDNTDA-based SPIs bearing dimethyl siloxane oligomers (SPI-y) display reasonably acceptable proton conductivity, thermal stability, anisotropic swelling, and mechanical properties. The SPI-y membrane with an IEC of 2.09 mmol g^{-1} exhibits a rather humidity-dependent proton conductivity of 4.3×10^{-2} S cm^{-1} at 60 °C and 70% RH. However, the ratio of SiRDA monomer in SPI-y to the feed is only ∼10% due to low reactive activity between the hydrophobic poly(siloxane imide) block and the hydrophilic SPI block.[544]

The SPIs with asymmetrical chain structure (NPI(1)-SPP, NPI(2)-SPP, NPI(3)-SPP) exhibit enhanced free volume and decreased interchain interaction because of both the loosened chain packing and the markedly increased interchain space, which are derived from their idiographic chain structure. As a result, all of them have higher water uptake and better hydrolytic stability than the SPIs with symmetrical chain structure (NPI(4)-SPP) because of the decreased positive charge densities in the asymmetrical imide rings and the protection of the hydrophobic groups at the ortho-position of the imido bond.[545−547] Although SPEs containing phosphine oxides also have unique properties, the SPIs (SPPO-PI) derived from sulfonated bis(3-aminophenyl)phenylphosphine oxide may not provide satisfactory hydrolytic stability because of the five-membered imide rings.[548]

What is worthy of note is that the novel sulfonated graft copolyimides in which the sulfonated polyimide is graft-polymerized to the fluorinated polyimide as the main-chain polymer present significantly higher proton conductivity, even exceeding that of Nafion. The SPI membrane with an IEC of 2.41 mmol g^{-1} exhibits a proton conductivity of 0.69 S cm^{-1} at 90 °C and 98% RH, an oxidative stability of 4.5 h (completely dissolved in 80 °C Fenton's reagent), and a hydrolysis stability of 1300 h in 80 °C water.[550]

4.3. Hydrocarbon Polymer with Aliphatic Main-Chain-Based Membranes

Many researchers are interested in hydrocarbon polymers with an aliphatic main chain for PEMs. However, this kind of PEM is mainly used for low-temperature PEMFC or DMFC due to the inferior oxidative stability of these aliphatic main-chain hydrocarbon polymers.[551−641] The frequently used aliphatic main-chain hydrocarbon polymers include varieties of styrene-based block copolymers, CS, poly(vinyl alcohol) (PVA), and so on. To enhance mechanical strength, methanol barrier, or proton conductivity, these polymers often require doping with inorganic proton-conducting moieties, blending with polymer pairs, or forming into IPNs. Most of them do not give encouraging results, but there are still some particularly attractive routes worthy of being noted.

There are two strategies that have been employed to enhance their oxidative stability. One strategy is cross-linking to form a compact structure to decrease the probability of the OH• radical diffusing into the membranes.[554] The other strategy is incorporating an HO• trapping material such as fullerene into the membrane (Figure 22).[560]

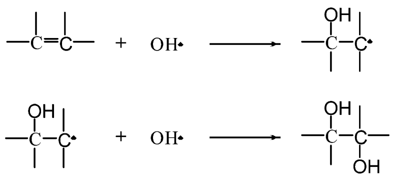

Figure 22. Mechanism of the fullerene trapping HO• species.[560]

PEMs (Figure 23) prepared by the synchronous cross-linking imidized method possess good mechanical strength, high thermal stability, and excellent flexibility. The final membrane with an IEC of 1.25 mmol g^{-1} has a proton conductivity of 0.21 S cm^{-1} at 30 °C and 0.49 S cm^{-1} at 95 °C, and it survives 7 h in Fenton's reagent at 30 °C before the membrane becomes a little brittle.[552,553] However, a large improvement in the oxidative stability of hydrocarbon polymers with an aliphatic main chain has been achieved by Fu and co-workers.[564,565] They prepared the composite membranes with semi-IPN via styrene-impregnated polymerization within a nonporous dense PVC supporting film followed by sulfonation. The developed membranes cross-linked with DVB display a durability of 4.0 days in 3 wt % aqueous H_2O_2 solution at 60 °C. The preliminary data for PEMFC fed with humidified H_2 and O_2 showed a maximum power density of ∼740 mW cm^{-2} under atmospheric pressure and 60 °C, which is comparable to commercial Nafion. When inorganic silica is covalently bound in these composite membranes, the mechanical strength and oxidative stability of the resultant membranes can be further enhanced, while their proton conductivity is simultaneously reduced.

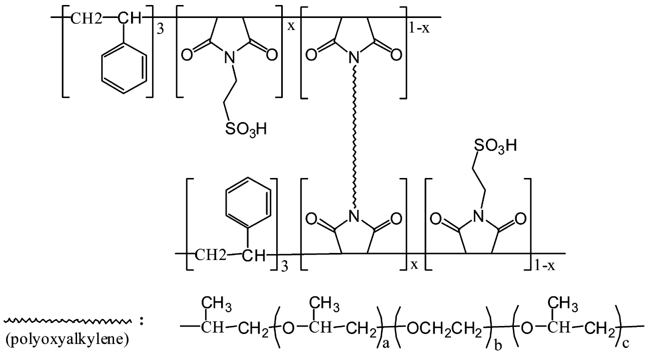

Figure 23. Schematic representation for PEMs based on SMA cross-linked by polyoxyalkylenediamine (PEGDA).[553]

The hybrid membranes composed of inorganic Si−O−Si linkages and organic polymer chains covalently immobilized with phosphonic acid (Figure 24a) have good thermal stability up to 200 °C. The proton conductivity of an optimum hybrid membrane achieves 4.0×10^{-2} S cm^{-1} under 100% RH at 130 °C.[561,562]

Saxena and co-workers prepared highly conductive and stable organic–inorganic nanocomposite PEMs with controlled spacing between the inorganic segment and covalently bound sulfonic acid functional groups (Figure 24b) through a more ingenious method. The resulting PEMs exhibit obvious improvement over the Nafion membrane as evidenced by the higher ratio of proton conductivity to methanol permeability (β-value), which is caused by the lower methanol permeability.[563]

Park and co-workers studied the influence of block lengths on the properties of PEMs prepared from PSS-*b*-PMB copolymer. Because of the flexibility of their aliphatic main chains, the *long-block-induced microstructures* can be established in the PEMs with relatively low-block molecular weight (>1.8 K–1.4 K g mol^{-1}). In PSS-*b*-PMB PEMs with block lengths no larger than 5.1 K–4.6 K g mol^{-1}, an unusual behavior can be observed: their moisture content increases as the temperature of the surrounding air is increased at constant RH. These PEMs have hydrophilic PSS phases with widths ranging from 2 to 5 nm, which results in capillary condensation. The PSS-*b*-PMB membrane containing hydrophilic domains with a width of 2.5 nm (IEC = 2.168 mmol g^{-1}) exhibits the highest proton conductivity at 50% RH, with a value of ~0.045 S cm^{-1} at 90 °C. It is also found that the sulfonation levels of the PSS-*b*-PMB copolymers play an important role in determining domain orientation. These findings may give some guidance in the construction of more efficient high-temperature PEMs.[570,571]

The CS, a natural and low-cost biopolymer, is a cationic polyelectrolyte containing functional amino and hydroxyl groups on the polymer chains. Considering β-values, few composite membranes based on CS show remarkable advantages over Nafion.

The leakage problem of HPAs such as PWA, phosphomolybdic acid (PMA), or silicotungstic acid (SiWA) can be overcome by blending them with CS because insoluble complexes can be formed between HPAs and CS through strong electrostatic interaction. The best PMA/CS membrane reported has a low methanol permeability (2.7×10^{-7} cm^2 s^{-1}) and comparatively high proton conductivity (0.015 S cm^{-1} at 25 °C).[610,611]

Wang and co-workers sulfonated zeolite β-particles ~800 nm in size using three different approaches and incorporated them into CS to prepare composite membranes. The experimental results indicate that the introduction of sulfonic groups can suppress the methanol permeability further as a result of the enhanced interfacial interaction between zeolite β and CS matrix. The highest β-value of these composite membranes is 4.6 times higher than that of Nafion117 when a 12 M concentration of methanol is used.[616]

The PVA also is a fairly attractive polymer rich in hydroxyl groups for PEMs because it can function as an excellent methanol barrier due to the dense molecular packing structure caused by inter- and intramolecular hydrogen bonding. However, there are not any negatively charged ions on PVA, so the proton-conducting groups or conductors generally need to be incorporated. Most PVA-based membranes show notably lower methanol permeability values and also comparatively lower proton conductivity values than those of Nafion. Similarly, few PVA-based membranes show significant advantages over Nafion.

In the organic/inorganic hybrid membranes that are prepared through solution blending of PVA and sulfonated polyhedral oligosilsesquioxane (sPOSS) followed by cross-linking with ethylenediaminetetraacetic dianhydride (EDTAD), it has been shown that the proton conductivity increases and methanol permeability decreases with increasing sPOSS content in the hybrid membranes. The hybrid membrane with 50 wt % sPOSS gives a proton conductivity as high as 0.042 S cm^{-1} at 25 °C while providing a methanol permeability ~1 order of magnitude lower than that of Nafion.[625] Kim and co-workers prepared cross-linked PVA membranes using poly(styrene sulfonic acid-*co*-maleic acid) (PSSA-MA) as a cross-linking agent as well as a donor of the hydrophilic groups, and the surfaces of these membranes are subjected to a fluorination treatment to reduce water content and maintain proton conductivity. Direct fluorination dramatically improves surface properties, and the proton conductivity increases with increasing fluorination time for all cross-linked membranes. For example, the proton conductivity of nonfluorinated PVA/PSSA-MA 5 wt %

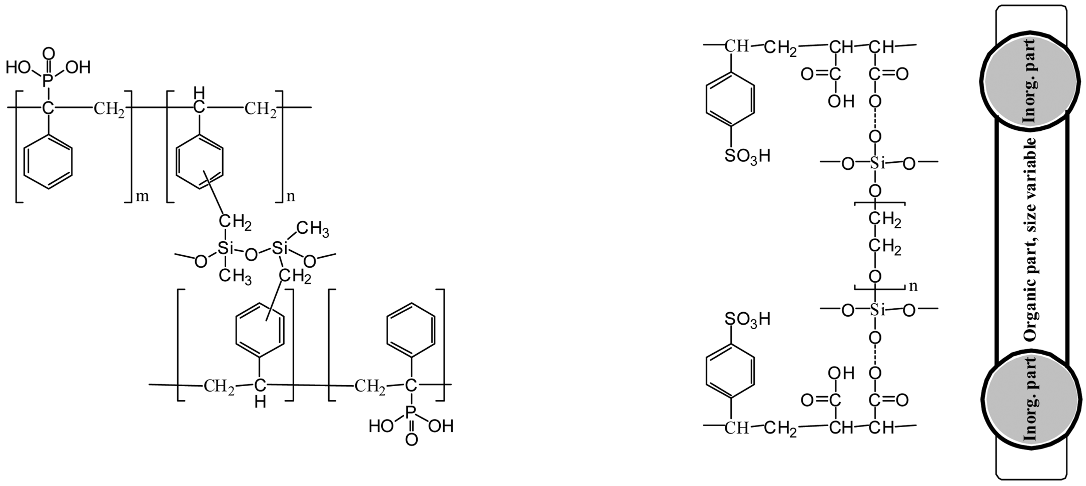

a) Chemical structure of inorganic-organic hybrid membrane based on Si-O networks with phosphonic acid groups

b) Chemical structure and schematic representation of inorganic-organic hybrid membrane with controlled spacing between inorganic segment and covalently bound sulfonic acid groups

Figure 24. Structures of two inorganic–organic hybrid membranes: a;[562] b, Reprinted with permission from ref 563. Copyright 2007 American Chemical Society.

membrane increases from 0.0386 to 0.053 S cm^{-1} at room temperature after 60 min fluorination while its methanol permeability decreases from 8.45 × 10^{-7} to 5.0 × 10^{-7} cm^2 s^{-1} at the same time, thus demonstrating desirable properties for DMFC.[639]

4.4. Glass Membranes

The glass membranes display a high proton conductivity as well as excellent mechanical, chemical, electrochemical, and thermal stabilities comparable to those of Nafion and provide a superior methanol barrier and a lower cost. They primarily serve as PEMs under low RH operational conditions. This section primarily describes glass membranes, ceramic membranes, and organic–inorganic hybrid membranes based on a silicate matrix.[642−668] Uma and co-workers prepared a series of glass membranes, including PMA–P_2O_5–SiO_2, PMA/PWA–P_2O_5–SiO_2, PWA/TiO_2–P_2O_5–SiO_2, TiO_2/ZrO_2–P_2O_5–SiO_2, PMA/ZrO_2–P_2O_5–SiO_2, and PWA/ZrO_2–P_2O_5–SiO_2 glass membranes.[642−648] Their investigations indicate that the proton conductivity in the glass membranes mainly occurs through the hydrogen bonding of water and hydroxyl groups on the network structure. The proton conductivity is considerably dependent on the temperature, humidity conditions, and pore characteristics such as the pore size and the functional groups on the pore surfaces (i.e., SiOH, POH, and P═O), as well as on the chemical composition. However, it depends only weakly on the thickness. On the other hand, the PEMFC performance is notedly influenced by the thickness of the glass membranes. The performance characteristics of glass membranes with various compositions are listed in Table 6.

Mesoporous acid-free silica xerogels with average pore size of 3.7 nm can be used to prepare 0.5 μm thin supported films. Their proton conductivity is highly sensitive to RH, and the highest value of proton conductivity, 2.0 × 10^{-2} S cm^{-1}, is achieved at 80 °C and 81% RH.[652]

Some of the organic–inorganic hybrid membranes based on silicate matrix have excellent performance under high temperature and low RH. After mesoporous silica materials with highly ordered high surfaces are functionalized by imidazole groups or sulfonic acid groups, they may serve as promising water-retaining additives to PEMs for applications at low RH operating conditions. The hybrid membrane derived from SO_3H-functionalized mesoporous silica particles and a polysiloxane matrix with sulfonic acid and benzimidazole groups exhibits higher proton conductivity than that of Nafion by a factor of 10 at temperatures > 180 °C and RH < 10%.[654−656] When the cofunctionalized perfluorosulfonic acid–aluminosilica films, which are functionalized free-standing mesostructured silica thin films with three-dimensionally interconnected pore networks, are back-filled with 8 wt % triflic acid, the final PEMs can give a proton conductivity ~1.50 × 10^{-2} S cm^{-1} at 50% RH and maintain this value up to 160 °C.[659] Similarly, the proton-conducting solid electrolyte membranes based on polyvinyl phosphonic acid (PVPA) and 3-glycidoxypropyltrimethoxysilane (GPTMS) (Figure 25) have a proton conductivity of 1.3 × 10^{-2} S cm^{-1} at 125 °C and 30% RH, which is similar to that of Nafion at the same temperature under 100% RH,[663] whereas the inorganic–organic hybrid membranes based on dimethylethoxyvinylsilane (DMEVS), vinylphosphonic acid (VPA), and GPTMS display a proton conductivity of 6.3 × 10^{-2} S cm^{-1} at 130 °C and 100% RH.[664]

The remaining organic–inorganic hybrid membranes based on a silicate matrix can serve as an effective resistance to methanol permeability. The three-dimensionally ordered macroporous (3DOM) silica composite membranes filled with a binary polymer (PAMPS-SPEES), which possess a core–shell-like structure, a 3DOM silica surface coated by SPEES, and the remaining vacancy occupied by PAMPS, display methanol permeability decreasing from 1.9 × 10^{-6} to 3.2 × 10^{-7} cm^2 s^{-1} at 30 °C. The proton conductivity is mainly dependent on the SPEES phase coating on the 3DOM pore surface. The β value of PAMPS-SPEES-3DOM composite membrane is >10 times higher than that of Nafion.[660]

But the greatest infusive progress in this field was reported by Horan and co-workers.[668] They fabricated a highly proton-conductive membrane via copolymerization of divinylsilyl-11-silicotungstic acid (vinyl-functionalized SiWA) with butyl acrylate (BA) and hexanediol diacrylate (HDDA). The resulting hybrid membrane exhibits at 100% RH superior proton conductivity as compared to Nafion. Its H_2/air fuel cell displays an OCV of 0.86 V and a power density of 180 mW cm^{-2} at 0.3 V under 70 °C and 75% RH, indicating significant potential for application in PEMFC under low RH and elevated temperature conditions.

5. POLYBENZIMIDAZOLE/H_3PO_4 MEMBRANES

It is well-known that the high-temperature PEMFCs provide several potential benefits such as improved electrode kinetics,

Table 6. Performance Characteristics of Glass Membranes with Various Compositions

glass membrane	compositions (mol %)	average pore size (nm)	proton conductivity (S/cm)	OCV (V)	Power density[a] (mW/cm^2)	reference
PMA–P_2O_5–SiO_2	4–4–92	NR[b]	1.0 × 10^{-3} (30 °C, 30% RH)	~1	23.9 (30 °C, 30% RH)	642
PMA/PWA–P_2O_5–SiO_2	1/2–2–95	3.7–5.4	1.34 × 10^{-1} (90 °C, 70% RH)	~0.93	35.0 (30 °C, 30% RH)	643, 644
PWA/TiO_2–P_2O_5–SiO_2	5/1–5–85	~2.5–3	7.2 × 10^{-2} (85 °C, 80% RH)	0.95	46.3 (28 °C)	645
TiO_2/ZrO_2–P_2O_5–SiO_2	4/5–5–86	~2.2	5.8 × 10^{-3} (80 °C, 50% RH)	NR	NR	646
PMA/ZrO_2–P_2O_5–SiO_2	2/4–4–90	~3	~10^{-3} (30 °C, 80% RH)	~1	32.0 (29 °C, 30% RH)	647
PWA/ZrO_2–P_2O_5–SiO_2	6/2–5–87	~3	NR	~0.92	43.0 (27 °C, 30% RH)	648

[a] All H_2/O_2 fuel cells with glass membranes are conducted at 1 atmospheric pressure. [b] NR = not reported.

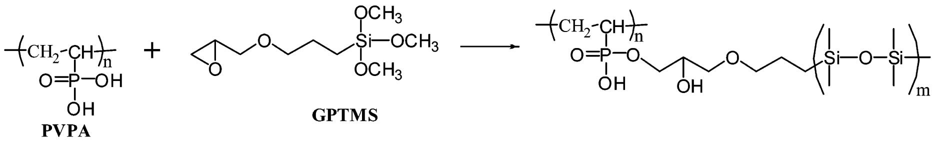

Figure 25. Schematic reaction process for fabricating PVPA-based hybrid membranes.[563]

high tolerance to fuel impurities (e.g., CO), enhanced efficiency of the waste heat utilization, and simplified thermal and water management systems. The PBI is a basic polymer with excellent thermal and chemical stability. When it is dipped in aqueous phosphoric acid to form an acid−base complex, the PBI/H_3PO_4 complex shows high proton conductivity at high temperatures even in the anhydrous state, low gas permeability, and nearly zero water drag coefficient. It has been realized that this system is a promising candidate for high-temperature (from 100 to 200 °C, especially from 150 to 200 °C) PEMFCs.

Because of its commercial availability, the most systematically studied PBI is the poly[2,2′-(*m*-phenylene)-5,5′-bibenzimidazole] (mPBI) (Figure 26a), but its processability is limited by its very rigid molecular structure, which gives very poor solubility in common organic solvents. When it is doped with H_3PO_4, the composite system will further encounter several disadvantages, including leaching out of H_3PO_4, poisoning of cathode Pt electrocatalyst by H_3PO_4, self-dehydration of H_3PO_4 above 140 °C, low loading level of H_3PO_4, and deterioration of mechanical stability by H_3PO_4 particularly at high H_3PO_4 concentrations and high temperatures, because only the dry-doped mPBI membranes with low acid uptake (<6 H_3PO_4 molecules per mPBI repeating unit, molecules/RU) are tough films, or else they become flexible in nature.[669] Despite the fact that pure phosphoric acid may have a proton conductivity of 7.7×10^{-2} S cm^{-1} at 42 °C, high temperature is often needed to maintain sufficient mPBI/H_3PO_4 composite membrane proton conductivity caused by the low mobility of phosphate species and the low H_3PO_4-doping levels.

Solving these problems has been a challenge. Two detailed overviews of the progress and present state of the PBI/PA complex for high-temperature PEMFC have been published.[670,671] The major focus of this section is on the approaches used to increase the conductivity of the PBI/H_3PO_4 complex and improve their mechanical properties, including optimization of preparing and operating parameters,[672−682] functionalization of mPBI,[683] inorganic additives,[684−688] polymer blends,[689−693] and doping with different electrolytes[694−698] and the synthesis of PBIs with different structures.[699−721] The structure and performance of the acid-doped PBIs are listed in Table 7.

5.1. Modifications to mPBI

5.1.1. Optimizations of Preparation and Operation of Acid-Doped mPBI System. On the basis of the effects of the optimization of preparation and operation parameters, it can be concluded that there are two types of polymer sites that complex with the doping acid: one with a higher affinity and the other with a lower affinity.[672] Cell temperature is an important parameter that influences the cell performance significantly; increasing temperature can lead to rapidly improved electrolyte conductivity and electrode kinetics, but it impairs cell performance in the long term by reducing the hydration level of the membrane or by self-dehydration of the phosphoric acid.[673−675]

It is necessary to control precisely the amounts of H_3PO_4 dopant in the mPBI membrane and the catalyst layer. Excess H_3PO_4 often results in blocking the oxygen supply into the catalyst layer and solid material build-up in the flow field plate and the MEA. On the other hand, insufficient H_3PO_4 usually leads to the incomplete contact area between the catalyst and the mPBI/H_3PO_4 ionomer.[676−679] Kongstein and co-workers optimized gas diffusion electrodes (GDEs) and used them in the H_2/O_2 PEMFC with mPBI/H_3PO_4, to give a H_2/O_2 PEMFC with an OCV of 0.9 V and a maximum power density of 830 mW cm^{-2} at 0.4 V under atmospheric pressure and 175 °C.[680] Lobato and co-workers investigated the influence of several parameters on the polycondensation synthesis of the high molecular weight mPBI from 3,3′-diaminobenzidine (DAB) and isophthalic acid (IPA) using PPA as the polycondensing agent. They concluded that the dosage of PPA and the reaction temperature significantly affect the molecular weight of the resulting mPBI and that a reaction time of 9 h appears to be long enough to produce a high-quality mPBI at no more than 275 °C. Compared to those from low molecular weight mPBIs, membranes cast from these high molecular weight mPBIs have enhanced mechanical resistance, a reduced degradation rate in Fenton's reagent at 68 °C, and a high thermal stability even after hydrogen peroxide treatment. These high molecular weight mPBI membranes still maintain acceptable mechanical properties even when impregnated with massive amounts of acid (doping level of 14.5 molecules/RU), which implies a significant increase in the proton conductivity and a much enhanced cell performance. For example, the mPBI membranes with acid-doping levels of 4.7, 6.7, and 14.5 molecules/RU display proton conductivities of 0.018, 0.022, and 0.079 S cm^{-1}, respectively, at 150 °C.[681] In addition, the high-temperature vapor-fed DMFC with mPBI/H_3PO_4 as the electrolyte has also been studied. It was found that the methanol concentration requires optimization, because small amounts of methanol limits mass transfer, but large amounts of methanol promote crossover and limit availability of water for methanol oxidation. The DMFC fed by 33.3 wt % methanol concentration and pure O_2 without back-pressure displays an OCV of 0.7 V and a maximum power density of 138.5 mW cm^{-2} at 200 °C. Furthermore, a preliminary durability test shows quite stable performance over 120 h.[682]

5.1.2. Modified mPBI/H_3PO_4 System. Only some modified mPBI's containing H_3PO_4 exhibit properties superior to those of pristine mPBI/H_3PO_4. The incorporation of inorganic additives such as $Cs_{2.5}H_{0.5}PMo_{12}O_{40}$ (CsPOM) and functionalized SiO_2 particles into mPBi membranes can result in increased acid-retention capability and consequently enhanced proton conductivity of modified mPBI/H_3PO_4 membranes. For example, the proton conductivity of the CsPOM/mPBI composite membrane doped with H_3PO_4 achieves at least 0.15 S cm^{-1} at 160 °C and 8.4% RH. Its H_2/O_2 PEMFC exhibits a maximum power density near 700 mW cm^{-2} at 150 °C under atmospheric pressure, which is close to 300 mW cm^{-2} larger than that of the mPBI/H_3PO_4 membrane.[684]

The blending membranes based on partially fluorinated SPE with high DS and mPBI reveal excellent oxidative stability, which is comparable to that of Nafion in 68 °C Fenton's reagent. When they are doped with H_3PO_4 up to 10−13 molecules/RU, the resultant ternary blend membranes still show small swelling and excellent mechanical strength. At an acid doping level of 11 H_3PO_4 molecules/RU, a proton conductivity of 0.12 S cm^{-1} can be obtained at 175 °C and 10% RH. More than 40 MEAs with an active area of 256 cm^2 have been prepared for a 2 kW$_{el}$ stack and display good performance and reproducibility.[691,692]

The PTFE/mPBI composite membrane doped with H_3PO_4 has larger proton conductivity than that of mPBI doped with phosphoric acid. The PTFE/mPBI membrane with a

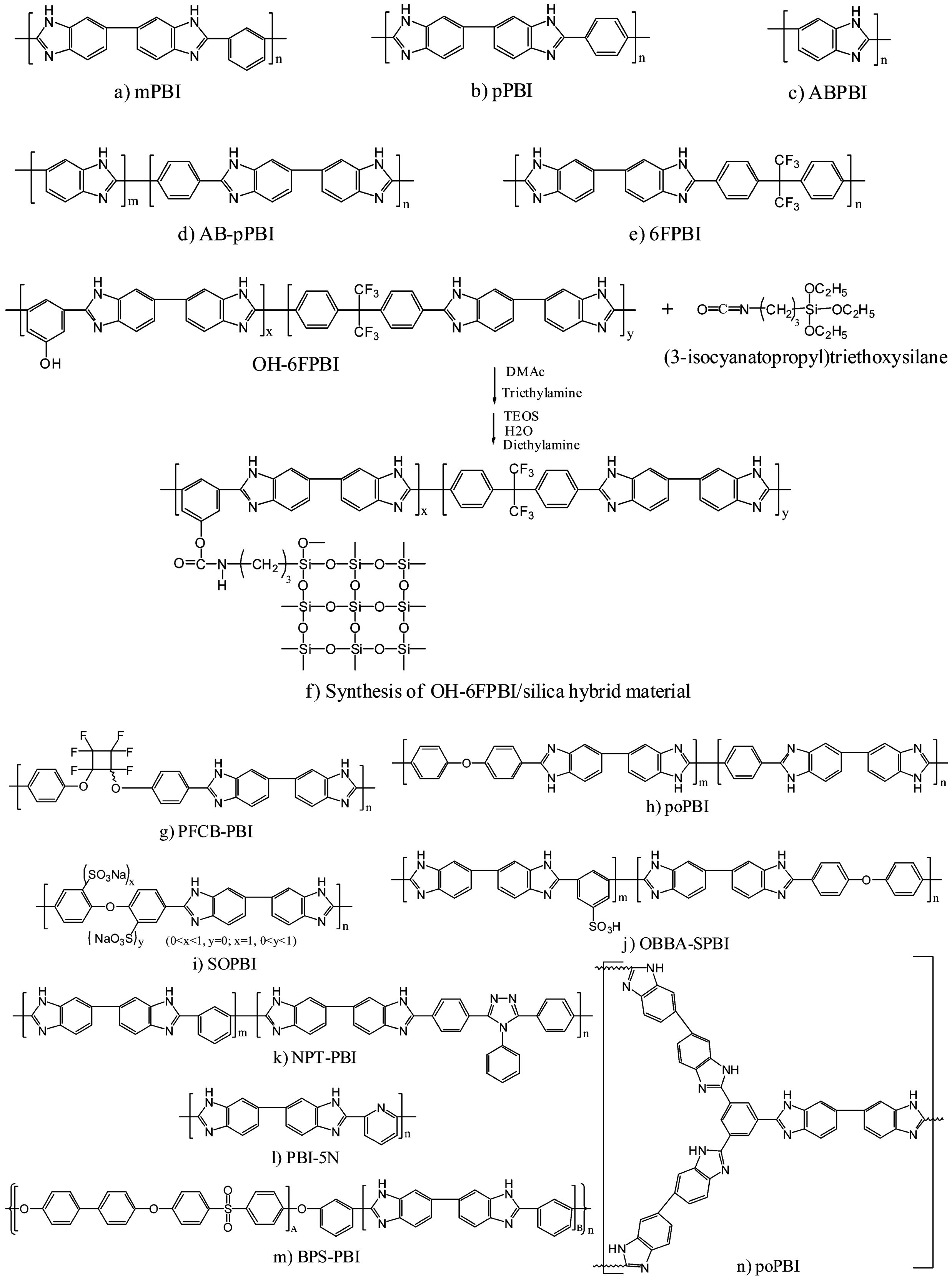

Figure 26. Chemical structures of PBIs: a,[699] b,[699] c,[702] d,[706] e,[707] f,[710] g,[711] h,[712] i,[713] j,[715] k,[716] l,[717] m,[718] and n.[719]

300% H_3PO_4 doping level achieves a conductivity higher than 0.3 S cm^{-1} at 8.4% RH and 180 °C, and the PEMFC using it with dry H_2/O_2 at 1 bar overpressure gives a peak power density of 1.2 W cm^{-2} at 170 °C.[693]

5.2. pPBI

To achieve more favorable performance, PBIs with different chemical structures than mPBI have been designed and implemented. Compared with the meta-structured mPBI,

Table 7. Structure and Performances of Acid-Doped PBIs

PBI polymers	modified methods	acid doping (molecules/RU)	main conclusions and comments	reference
mPBI with high molecular weight	polycondensation of DAB and IPA in PPA	14.5	enhanced mechanical resistance and suppressed degradation rate in 68 °C Fenton's reagent; proton conductivity up to 0.079 S cm^{-1} at 150 °C	681
mPBI (Figure 26a)	reinforced by microporous PTFE	NR[a]	thickness of 20−30 μm; the cell voltage decays after 240 h due to the delamination	690
mPBI	doped with $Cs_{2.5}H_{0.5}PMo_{12}O_{40}$	NR	proton conductivity higher than 0.15 S cm^{-1} at 160 °C and 8.4% RH; power density near 700 mW cm^{-2} at 150 °C under atmospheric pressure (H_2/O_2 PEMFC)	684
mPBI	incorporating functionalized SiO_2 particles	NR	increased acid retention capability; improved performance at 120 °C and 50% RH	685−687
mPBI	blending with partially fluorinated SPE	11	excellent oxidative stability comparable to that of Nafion in 68 °C Fenton's reagent; proton conductivity of 0.12 S cm^{-1} at 175 °C and 10% RH	691, 692
pPBI (Figure 26b)	PPA process	27.7	amorphous structure, enhanced acid-doping level, increased water uptake, proton conductivity of 0.24 S cm^{-1} at 160 °C, durability of at least 2500 h, voltage degradation rate of only 4.9 μV h^{-1}, and very low H_3PO_4 loss (H_2/air PEMFC)	699−701
ABPBI (Figure 26c)	low-temperature casting procedure	NR	higher acid-doping level comparing to ABPBI and PBI membranes prepared by casting at high temperature	702
ABPBI	impregnating catalyst layers with H_3PO_4	NR	voltage degradation rate of about −25 μV h^{-1} at 160 °C under stationary conditions (H_2/air PEMFC), while significantly increased voltage degradation rate under dynamic load changes or during start−stop cycling	703, 704
ABPBI	PPA process	2.5	increased acid-absorbing capability; proton conductivity of 0.14 S cm^{-1} at 180 °C and 1% RH	705
ABPBI	incorporation of ZPP	NR	improved thermal and dimensional stabilities without sacrificing proton conductivity; maintaining shapes after 3 days in 85 wt % phosphoric acid solution; proton conductivity of >0.12 S cm^{-1} at 180 °C and 1% RH	705
AB-pPBI (Figure 26d)	solution-casting method of methanesulfonic acid (MSA) solution of AB-pPBI	NR	better dimensional stability and larger acid-absorbing ability than ABPBI membrane; proton conductivity of 0.15 S cm^{-1} at 180 °C under anhydrous conditions	706
6FPBI (Figure 26e)	PPA process	30−40	high phosphoric acid-doping level and excellent oxidative stability in Fenton's reagent; proton conductivity of 0.09 S cm^{-1} at 180 °C under anhydrous conditions; CO tolerance up to 0.2% at 160 °C	707
PFCB-PBI (Figure 26g)	modified PPA process	>50	very high phosphoric acid-doping level; sufficient strength for MEAs; proton conductivity of 0.12 S cm^{-1} is achieved at 140 °C without external humidification; a power density of 150 mW cm^{-2} at 140 °C and atmospheric pressure (H_2/air PEMFC), but the PFCB-PBI membranes redissolve in phosphoric acid beyond 140 °C	711
poPBI (Figure 26h)	PPA process	6.6	good thermal and mechanical stability; decreased crystallinity; a proton conductivity of 0.098 S cm^{-1} (comparable to that of the conventional mPBI membrane at 180 °C under anhydrous conditions)	712
sulfonated poly[2,2′-(*p*-oxidiphenylene)-5,5′-bibenzimidazole] (SOPBI) (Figure 26i)	solution-casting method of DMSO	extremely low[b]	cross-linked SOPBI having improved water stability and radical oxidative stability but inadequate proton conductivity for PEMFC under high temperature and anhydrous conditions	713, 714
4,4′-oxybis(benzoic acid) (OBBA)-SPBI (Figure 26j)	PPA process	NR	proton conductivity higher than 0.1 S cm^{-1} at >120 °C and low RH	715
NPT-PBI (Figure 26k)	traditional solution casting	NR	prone to dissolve in 12 M H_3PO_4 at 100 °C; proton conductivity at the order of 10^{-3} S cm^{-1} under anhydrous conditions and 120 °C due to low acid-doping level	716
PBI-5N (Figure 26l)	incorporating SiO_2-based filler	undergoing washing procedure	permanent proton conductivity higher than 10^{-3} S cm^{-1} at 120 °C and 50% RH	717
multiblock BPS-PBI (Figure 26m)	solution-casting method of DMAc	11.5	selectively absorbing H_3PO_4 into PBI phase; reduced swelling behavior; proton conductivity of 0.047 S cm^{-1} at 200 °C without external humidification	718
mesoporous (~10 nm) PBI (Figure 26n)	solvent-mediated hard-templating procedure	NR	proton conductivity of this system with excess H_3PO_4 is 1−2 orders of magnitude higher than that of the corresponding nonporous PBI with excess H_3PO_4	719

[a] NR = not reported. [b] Acid-doped SOPBI membranes are rinsed with deionized water after the thermal cross-linking treatment.

poly[2,2′-(*p*-phenylene)-5,5′-bibenzimidazole] (pPBI) (Figure 26b) has superior mechanical properties, and it can sustain its mechanical strength with a high acid-doping level. Just like mPBI, pPBI is not suitable for industrial-scale production because of its low processability caused by poor solubility. Kim and co-workers fabricated pPBI membranes by a direct-casting method using the hot pPBI polymerization solution of PPA and subsequently in situ hydrolysis of PPA to H_3PO_4 (named the PPA process) or by a solution-casting method using MSA as a casting solvent. The pPBI membranes display higher acid-doping levels, larger water uptake, and remarkably higher tensile strength values than mPBI membranes. The pPBI membranes prepared by the PPA process also have an almost amorphous structure and much higher acid-doping levels and larger water uptake values than pPBI membranes prepared by the solution-casting method. The pPBI membrane from the PPA process with a doping level of 8.78 molecules/RU exhibits a proton conductivity of 0.15 S cm^{-1} at 180 °C and 1% RH.[699] The acid-doping level of pPBI membranes from the PPA process can achieve 30−40 molecules/RU, while the content of pPBI is only 3−6 wt %. The pPBI membrane with a doping level of 27.7 molecules/RU made by this process gives a high proton conductivity of 0.24 S cm^{-1} at 160 °C mainly due to the high acid content in the gel membrane. The H_2/air PEMFC based on this membrane shows excellent performance (power density of higher than >400 mW cm^{-2} at 0.4 V under atmospheric pressure and 160 °C) and minimal CO poisoning effects. Long-term durability testing of this membrane indicated that the voltage degradation rate over 2500 h during steady-state fuel cell operation at 160 °C is only 4.9 μV h^{-1} and the H_3PO_4 loss is a fairly small amount relative to abundance of H_3PO_4 in membranes. From the H_3PO_4 loss in the membrane aspect, long-term operation (>10 000 h) is expected for steady-state fuel cell operation using this membrane in the range of 80−160 °C.[700,701]

5.3. ABPBI

Poly(2,5-benzimidazole) (ABPBI) (Figure 26c), another member of the polybenzimidazoles, uses a single 3,4-diaminobenzoic acid monomer for the polycondensation. Different casting procedures of ABPBIs can induce distinct morphology. The ABPBI membranes produced by a low-temperature casting procedure using formic acid as casting solvent (type I) show polymer chain aggregation yielding fibers ∼25 nm in diameter, whereas the ABPBI membranes produced by the classical high-temperature casting from MSA (type II) reveal more important polymer-chain aggregation resulting in fibers ∼200 nm in diameter. As a consequence, ABPBI membranes of type I yield higher acid-doping levels compared with ABPBI and mPBI membranes of type II due to a larger number of exposed acid sorption sites caused by a less compact supramolecular packing.[702] However, the increased acid-absorbing capability causes ABPBI membranes to have more significant dimensional swelling than mPBI membranes when using a high concentration of H_3PO_4, which makes the reproducible production of MEAs for cells with a large active area difficult. Wannek and co-workers developed an easy and reproducible fabrication method for MEAs using ABPBI membrane with large active areas. They impregnated electrocatalyst layers instead of predoped membranes with H_3PO_4. A power density of ∼300 mW cm^{-2} was achieved at full load under ambient pressure and 160 °C with hydrogen and air as reactants. Under stationary conditions, the voltage degradation rate is about −25 μV h^{-1} at 200 mA cm^{-2}, which is deduced from a 1000 h durability test. Under dynamic load changes or during start−stop cycling, the degradation rate is significantly increased because of a large loss of catalytically active sites, which can be corroborated by a significant increase in the catalyst particle size.[703,704]

ABPBI membranes using the PPA process and zirconium pyrophosphate (ZPP)/ABPBI composite membranes have been prepared to enhance the dimensional stability of ABPBI membranes. The ABPBI membranes were prepared by controlling the doping level of phosphoric acid to obtain a certain level of proton conductivity because of their increased acid-absorbing capability compared to type II ABPBI membranes. As a result, the ABPBI membrane with a phosphoric acid doping level of only 2.5 molecules/RU displays a very high proton conductivity of 0.14 S cm^{-1} at 180 °C and 1% RH. On the other hand, the ZPP/ABPBI membranes immersed in 85 wt % phosphoric acid solution for 3 days still maintain their shape, indicating good dimensional stability, whereas the ABPBI membranes dissolved completely when they were immersed in 85 wt % phosphoric acid solution for 3 days.[705] The copolymers of ABPBI and pPBI (AB-pPBI) (Figure 26d) can also enhance the stability of ABPBI and improve the processability of rigid pPBI through taking advantage of the properties of both constituents. The acid-doped copolymer membranes display better dimensional stability and mechanical properties than the acid-doped ABPBI membrane, as well as a larger acid-absorbing ability and higher proton conductivity values as compared with commercial mPBI membranes. The AB-pPBI containing 80 mol % of ABPBI unit membrane displays a tensile strength 3 times larger than that of the mPBI membrane at the same acid content (59 wt %) and also achieves a very high proton conductivity of 0.15 S cm^{-1} at 180 °C under anhydrous conditions.[706]

5.4. Explorations of Other PBIs

5.4.1. PBI Containing Hexafluoroisopropylidene Groups.

The incorporation of the hexafluoroisopropylidene group into polymers such as SPE and SPI has been widely used to improve the membrane performance. Likewise, the PBI containing hexafluoroisopropylidene group (6FPBI) (Figure 26e) has been properly explored. The thermally and chemically stable 6FPBI in high molecular weight polymers exhibits excellent resistance to hydroxyl/peroxyl radical attack in Fenton's reagent at low and high temperatures.

These 6FPBI membranes with high H_3PO_4 doping levels (up to 30−40 molecules/RU) exhibit tensile strengths greater than 0.8 MPa and elongations at break ∼100% as well as proton conductivity of 0.09 S cm^{-1} at 180 °C under anhydrous conditions. The power density of their H_2/O_2 fuel cells reaches ∼430 mW cm^{-2} at 1 A cm^{-2} at 160 °C and atmospheric pressure. The CO tolerance test indicates that, at an operation temperature of 160 °C, the presence of CO at 0.2% has a relatively minor effect on the fuel cell performance.[707] Several methods have been adopted by Chuang and co-workers to further reduce the methanol permeability of the 6FPBI system.[708−710] The most effective method is to synthesize a 6FPBI copolymer containing hydroxyl groups that provide the bonding sites for the bonding agent (OH-6FPBI). The OH-6FPBI/silica nanocomposite membranes (Figure 26f) display good compatibility between the OH-6FPBI polymer and the inorganic silica phase, which leads to enhanced mechanical properties and reduces the methanol permeability. Although the conductivity is slightly decreased by the silica, the overall performance of the nanocomposite membranes is still obviously improved by the addition of silica.[710]

5.4.2. PBI Containing Perfluorocyclobutyl Group. High molecular weight perfluorocyclobutyl-containing PBI (PFCB-PBI) (Figure 26g) membranes, which are prepared by a modified PPA process and have a very high phosphoric acid-doping level (>50 molecules/RU), display sufficient strength to fabricate into MEAs. The maximum power densities of fuel cells with phosphoric acid-doped PFCB-PBI membranes are 210 mW cm^{-2} (H_2/O_2) and 150 mW cm^{-2} (H_2/air) at 140 °C and atmospheric pressure. However, the redissolution of the PFCB-PBI membranes in phosphoric acid occurs when the temperature is beyond 140 °C, which limits the operation of fuel cells based on phosphoric acid doped PFCB–PBI membranes containing high levels of phosphoric acid.[711]

5.4.3. Poly(aryl ether benzimidazole) Copolymers. The incorporation of flexible aryl ether linkages into PBI can improve the solubility of the copolymer, increase the chain *d*-spacings of the polymer backbones, and decrease the crystallinity of the copolymers. Membranes of the poly(aryl ether benzimidazole) copolymers bearing different aryl ether linkage contents (poPBI) (Figure 26h) display reasonably high thermal and mechanical stability as well as high proton conductivity. For instance, the copolymer membrane with 30 mol % ether linkage exhibits a tensile strength of 43 MPa (at 26 °C and 40% RH) at an acid-doping level of 7.5 molecules/RU and a proton conductivity of 0.098 S cm^{-1} (at 180 °C and anhydrous conditions) at an acid-doping level of 6.6 molecules/RU, which is comparable to that of the conventional mPBI membrane at the same doping level.[712]

5.4.4. PBIs with Sulfonic Acid Groups. Theoretically, the addition of H_3PO_4 in PBI membranes is avoidable by incorporating conducting groups such as sulfonic acid groups into the backbone of PBI through chemical linkage. Practically, because the acid–base interaction between the benzimidazole and sulfonic acid groups results in insufficient proton carriers for proton conduction at high temperature and under anhydrous conditions, H_3PO_4 is still needed.

Bai and co-workers synthesized sulfonated PBI copolymers from DAB, OBBA, and 5-sulfoisophthalic acid (SIPA) (OBBA-SPBI) (Figure 26j). The pure OBBA-SPBI copolymer membrane is fabricated by the traditional solution-casting techniquem and the OBBA-SPBI/H_3PO_4 composite membrane is prepared through the PPA process. The membranes prepared by both methods possess desirable mechanical, chemical, thermal, and hydrolytic stability. However, the pure copolymer membrane exhibits very poor proton conductivity due to the acid–base interaction between the benzimidazole and the sulfonic acid groups. On the other hand, the OBBA-SPBI/H_3PO_4 composite membrane from the PPA process shows extremely high proton conductivity (>0.1 S cm^{-1}) at high temperatures (>120 °C) and low RH, even under anhydrous conditions.[715]

5.4.5. Pyridine-Based PBIs. The incorporation of the extra nitrogen in the PBI backbone, e.g., the poly-2,2′-(2,6-pyridine)-5,5′-bibenzimidazole (PBI-5N, Figure 26l), significantly improves the acid retention and thus enhances the permanent conductivity. A small amount of SiO_2-based fillers such as imidazole-functionalized SiO_2 or mesoporous silica can greatly increase the permanent proton conductivity of PBI-5N/SiO_2 composite membranes. Permanent conductivity values higher than 10^{-3} S cm^{-1} have been obtained at 120 °C and 50% RH after the washing procedure, which causes leaching of the acid fractions that are not hydrogen-bonded to the nitrogen atoms.[717] Similar results are also found for the mPBI/SiO_2-based filler system.[685]

5.4.6. Multiblock PBI Copolymers. As mentioned above, multiblock copolymers display unique structures and properties. Multiblock PBI copolymers based on poly(arylene ether sulfone) and PBI with different block lengths (BPS-PBI) (Figure 26m) have been prepared by Lee and co-workers.[718] The doping level strongly depends on the concentration of H_3PO_4, and the H_3PO_4 is selectively absorbed into the PBI phase, which leads to significantly reduced swelling behavior compared with a conventional mPBI/H_3PO_4 membrane. Among the BPS-PBI membranes, the highest proton conductivity (0.047 S cm^{-1} at 200 °C without external humidification) was attained by BPS-BPI (15 K–15 K g mol^{-1}) membrane with a doping level of 11.5 molecules/RU. The proton conductivity increases significantly beyond a particular doping level (~4 molecules/RU) for all the BPS-PBI membranes, which is attributed to the appearance of "free" phosphoric acid. As the block lengths increase from 5 to 10 K g mol^{-1}, a morphological change occurs and the *long-block-induced microstructures* with well-connected phase-separated morphology emerge. Consequently, the proton conductivities of these BPS-BPI membranes increase with increasing block length, especially at low doping levels (6–7 molecules/RU), because the well-connected phase-separated morphology is favorable for lowering the morphological barrier to proton transport.

5.4.7. Mesoporous PBI Filled with H_3PO_4. Weber and co-workers prepared mesoporous (~10 nm) PBI (mp-PBI) (Figure 26n) networks by a solvent-mediated hard-templating procedure and impregnated H_3PO_4 into them. The impregnation of H_3PO_4 into mp-PBI proceeds in two steps: a fast step during which the mesopores are filled with molten H_3PO_4 and a second slower step, which leads to the incorporation of H_3PO_4 into the pores of the wall. The driving force of the first step is capillarity, and that for the second step is salt formation (an acid/base reaction). The mp-PBIs filled with an excess of H_3PO_4 show very good conductivities due to the existence of a two-phase structure made of PBI and phosphoric acid domains. The conductivity of the nanostructured material, mp-PBI with excess H_3PO_4, is 1–2 orders of magnitude higher than that of the corresponding nonporous PBI with excess H_3PO_4.[719] These results, that the PBI/H_3PO_4 membranes with a well-defined biphasic structure have better proton conductivity than those with a less clearly defined biphasic structure, are to some extent in accordance with the multiblock BPS-PBI/H_3PO_4 membranes, thus validating certain similarities between multiblock copolymer membranes and pore-filling membranes.

6. ALKALINE IONOMER MEMBRANES

Alkaline fuel cells (AFCs) have an advantage over proton-exchange membrane fuel cells in both cathode kinetics and ohmic polarization. The inherently faster kinetics of the oxygen reduction reaction in an alkaline fuel cell allows the use of Pt-free electrocatalysts that, while contributing directly to lower short-term costs, also have environmental benefits.[722,723] However, despite their early success in certain applications, alkaline fuel cells have an intrinsic difficulty with carbonation that is prohibitive for broad commercialization. This section describes the technology of anion-exchange membrane fuel cells. Using an anion-exchange membrane instead of a liquid caustic alkali electrolyte in an alkaline fuel cell avoids the problems of leakage, carbonation, precipitation of carbonate salts, and preventing the gas electrode flooding, thus increasing the volumetric energy density.

Alkaline ionomer membranes (also called anion-exchange membranes (AEMs) or anion-conducting PEMs) are a class of solid-state polymer electrolyte fixed with basic functional groups. The fuel cells using alkaline ionomer membranes, a kind of PEMFC, can be called anion-exchange membrane fuel cells (AEMFCs) or alkaline membrane fuel cells (AMFCs). These have several important advantages: (i) a facile electrokinetics in high-pH environment for methanol oxidation, oxygen reduction, and carbon monoxide oxidation, (ii) extended selective range of Pt-free electrocatalysts, e.g., Ni, Pd, Ag, or alloys, (iii) reverse methanol crossover direction to hydroxide (OH^-) ion migration, (iv) potentially simplified water management, (v) improved radical oxidation stability of hydrocarbon membranes in alkaline environments, (vi) superior corrosion resistance of metal components in alkaline environments, (vii) simple fabrication of the membranes with good mechanical strength, (viii) wide choice of fuels, and so on.[724−732]

Nevertheless, the application of AEMFCs faces many challenges before they can compete with acidic PEMFC. First, AEMFCs have an inherently high thermodynamic voltage loss of >300 mV due to the pH difference, which lowers their OCV.[724] Although the pH difference can dwindle with increasing temperature, it is never decreased greatly. Second, the basic functional groups of most AEMs are quaternary ammonium groups, but they are unstable at temperatures above 60 °C because they are apt to be replaced by OH^- ions via a direct nucleophilic displacement or a Hofmann elimination reaction when β-hydrogens are present. Good solvation of the quaternary ammonium head-groups and OH^- ions is favorable for the overall chemical stability of alkaline membranes.[733] Third, the ionic conductivity of alkaline PEMs is lower than that of acidic PEMs because the transfer number of OH−, which is only 0.25 times the transfer number of H+, is inherently much lower than that of H+.[734] Lastly, AEMFCs lack universally soluble ionomers that can be used in MEA as a binder to build an efficient three-phase boundary, just like the functions of Nafion ionomers in MEA used for acidic PEMFC.[735] Because of the sluggish development of AEMs, the investigation of AEMFCs still remains at its initial stage. Recent progress in AEMs and binding materials for MEAs of AEMFC and PEMFCs with combined configuration will be well reviewed. The progress in the AEMFC can be found in two published reviews.[736,737]

6.1. Status Quo of AEMs

Even though they may have a hydroxide ion conductivity of 0.53 S cm^{-1} under ambient temperature and a power density of 100 mW cm^{-2} (H_2/O_2) at room temperature,[738−746] this section will not describe composite membranes doped with liquid alkaline electrolyte, e.g., KOH, because of their difficulties with leaching out and carbonate-precipitate issues. Only limited AEMs for AEMFCs were reported, including the organic−inorganic hybrid membranes through a sol−gel reaction based on alkoxysilane,[747−749] modified aliphatic polymer membranes incorporating basic functional groups,[750−761] and quaternized aromatic polymer membranes.[762−773] The structures and performance of AEMs are shown in Table 8.

6.1.1. AEMs Based on Modified Aliphatic Polymer Membranes.

The organic−inorganic hybrid AEMs give only inadequate hydroxide ion conductivity (10^{-4}−10^{-3} S cm^{-1}) because of the inherent low hydroxide ion transport ability and

Table 8. Status Quo of AEMs

membranes	preparing methods	main conclusions and comments	reference
organic−inorganic hybrid AEMs	sol−gel reaction based on alkoxysilane	inadequate hydroxide ion conductivity of only 10^{-4}−10^{-3} S cm^{-1}	747−749
quaternized PVA (Figure 27a)	cross-linked by GA or reacting with TEOS or blending with quaternized CS	improved thermal stability and reduced methanol permeability; hydroxide ion conductivity of 1.4×10^{-2} S cm^{-1} at 60 °C	750−753
IPN based on PVA and poly(acrylic acid)	PVA and acrylic acid monomer mixture solutions irradiated by UV	hydroxide ion conductivity of 0.312 S cm^{-1} at room temperature, but KOH solution is needed	754
poly(epichlorydrin allyl glycidyl ether) copolymer with cyclic diamines	chloride substitution on the $-CH_2Cl$ function of the epichlorhydrin units	insensitive to Hoffman elimination; thermal stability up to 220 °C; hydroxide ion conductivity of 1.3×10^{-2} S cm^{-1} at 60 °C and 98% RH without any KOH	755
polymerized 4-vinylpyridine-based thin membrane	plasma treatment	hydroxide ion conductivity only 5×10^{-4} S cm^{-1}	756
aminated chlorinated polypropylene by polyethyleneimine	amination	ionic conductivities from 0.89×10^{-2} to 1.36×10^{-2} S cm^{-1} depending on the IEC; facile swollen polymer structure	757
ETFE with quaternary ammonium groups	E-beam irradiation	increased water crossover from the anode to the cathode; power density of 230 mW cm^{-2} at 50 °C (H_2/O_2 AEMFC)	759
quaternized polysulfones	chloromethylation/quaternization	power density of H_2/air AEMFC using 2.0 mg cm^{-2} Ag/C at the cathode, which is comparable to the one with 0.5 mg cm^{-2} Pt/C	762
quaternized cardo polyetherketone (Figure 27c)	chloromethylation/quaternization	methanol permeability less than 10^{-9} cm^2 s^{-1} at 30 °C, but low hydroxide ion conductivity (1.6×10^{-3} to 5.1×10^{-3} S cm^{-1}) at 20−60 °C	763
quaternized poly(ether imide) (Figure 27d)	chloromethylation/quaternization	hydroxide ion conductivity ranging from 9.21×10^{-4} to 4.20×10^{-3} S cm^{-1} at 24 °C	764
chloroacetylated PPO/bromomethylated PPO membranes (Figure 27g)	blending/heat-treating	intercross-linking structure; enhanced mechanical properties and thermal stability; low methanol permeability (1.35×10^{-7} to 1.46×10^{-7} cm^2 s^{-1}) and comparatively high hydroxyl conductivity (2.2×10^{-2} to 3.2×10^{-2} S cm^{-1} at 25 °C)	767, 768

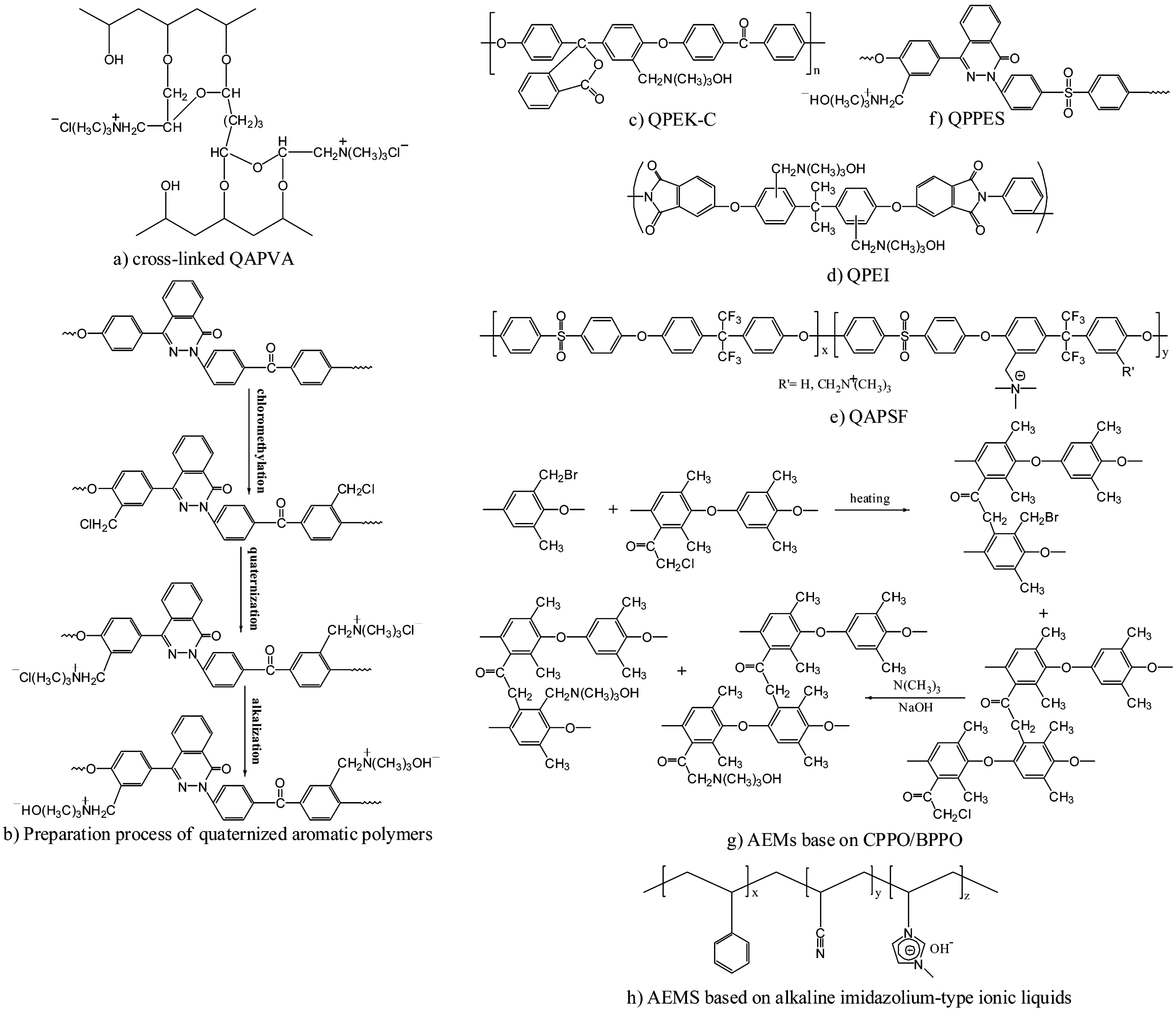

a) cross-linked QAPVA

b) Preparation process of quaternized aromatic polymers

c) QPEK-C

d) QPEI

e) QAPSF

f) QPPES

g) AEMs base on CPPO/BPPO

h) AEMS based on alkaline imidazolium-type ionic liquids

Figure 27. Chemical structures of AEMs: a,[750] b,[727] c,[763] d,[764] e,[765] f,[766] g,[767] and h.[773]

the poor conductivity of silica components.[747−749] On the contrary, some modified aliphatic polymer membranes with basic functional groups incorporated show relatively high hydroxide ion conductivity. Xiong and co-workers prepared a series of quaternized PVA (QAPVA) membranes (Figure 27a) and then employed glutaraldehyde (GA) or TEOS to form modified QAPVA membranes. The introduction of silica improves the thermal stability and decreases the methanol permeability of the final QAPVA membranes. The highest hydroxide ion conductivity of these QAPVA membranes can achieve 1.4 × 10^{-2} S cm^{-1} at 60 °C. The cross-linked composite membranes consisting of QAPVA and quaternized CS have also been studied. These composite membranes show properties similar to QAPVA/silica hybrid membranes and have greater improvement when compared to plain cross-linked quaternized CS membranes.[750−753]

Stoica and co-workers have studied the incorporation of two cyclic diamines, 1,4-diazabicyclo-[2.2.2]-octane (DABCO) and 1-azabicyclo-[2.2.2]-octane (Quinuclidine), into poly(epichlorydrin allyl glycidyl ether) copolymer to form anion-conducting membranes. These membranes are insensitive to Hoffman elimination and show good thermal stability up to 220 °C. The membrane with an IEC of 1.3 mmol g^{-1} without KOH displays a hydroxide ion conductivity of 1.3 × 10^{-2} S cm^{-1} at 60 °C and 98% RH, indicating a promising prospect for low-temperature alkaline DMFC applications. Moreover, the reinforcement of these membranes using polyamide supports considerably improves the mechanical properties without compromising ionic conductivity.[755]

Water is an important reactant at the cathode for the formation of OH^- ions from gaseous O_2, so the decrease in AEM thickness can result in an increase in water crossover from the anode to the cathode and improve the performance of AEMFCs. The performance of H_2/O_2 AEMFCs using the thinnest ETFE membrane with quaternary ammonium groups (17 μm) can attain a power density of up to 230 mW cm^{-2} at 50 °C.[759]

6.1.2. AEMs Based on Quaternized Aromatic Polymer Membranes. The quaternized aromatic polymer membranes are usually prepared via chloromethylation, quaternization, and alkalization. The general process is outlined in Figure 27b.[727] Park and co-workers prepared chloromethylated polysulfones and aminated them with a diamine or a mixture of monoamine and diamine. They show that the use of a diamine with a longer alkyl chain in the mixture can enhance the hydroxide ion conductivity and thermal properties of AEMs. The H_2/air AEMFC performance using 0.5 mg cm^{-2} Pt/C at both the anode and cathode is comparable to one with 0.5 mg cm^{-2} Pt/C at the anode and 2.0 mg cm^{-2} Ag/C at the cathode. It is evident that AEMFCs allow nonprecious catalysts at the cathode.[762] Quaternized cardo polyetherketone (QPEK-C) (Figure 27c), quaternized poly(ether imide) (QPEI) (Figure 27d), quaternized poly(arylene ether sulfone) ionomers containing fluorenyl groups, and quaternized polyphthalazione ether sulfone) (QPPES) (Figure 27f) membranes have also been explored, but no exciting results have been obtained.[763−766]

Wu and co-workers have developed a series of AEMs obtainable by a convenient and effective method and based on chloroacetylated PPO with bromomethylated PPO (Figure 27g). An intercross-linking structure is formed in the final AEMs, and most of them have IEC values exceeding 1.5 mmol g^{-1}. Their toughness, mechanical properties, and thermal stabilities are remarkably enhanced by the cross-linked structures. Furthermore, low methanol permeability (1.35 × 10^{-7} to 1.46 × 10^{-7} cm^2 s^{-1}) and comparatively high hydroxyl conductivity (2.2 × 10^{-2} to 3.2 × 10^{-2} S cm^{-1} at 25 °C) are achieved. These results indicate a good prospect for use of these AEMs in low-temperature alkaline DMFC applications.[767,768]

Pan and co-workers developed a self-cross-linked quaternary ammonia polysulfone AEM by substituting a part of the quaternary ammonium group with a tertiary amino group. The resultant AEM displays excellent dimensional stability and a hydroxyl conductivity of 4.3 × 10^{-2} S cm^{-1} at 90 °C. More importantly, it shows no sign of degradation after immersion in 90 °C water for 500 h.[770] Lin and co-workers prepared AEMs based on alkaline imidazolium-type ionic liquids (Figure 27h) that maintain hydroxide conductivity above 10^{-2} S cm^{-1} at 30 °C, even after immersion in 1 M KOH solution at 60 °C for 400 h, and thus also showing excellent chemical stability.[773]

It can be deduced from these published papers that very few AEMs display hydroxide ion conductivities exceeding 10^{-2} S cm^{-1} at room temperature, in contrast to PEMs. Besides the relatively weak basicity of quaternary ammonium functional groups and the inherent low mobility of hydroxyl anions, the morphology and water-binding properties of AEMs also play a considerably important role in this result. The AEMs have a greater self-diffusion coefficient for water and a lower water binding, but a lower ionic conductivity than acidic PEMs with similar IEC because the AEMs lack a percolated ionic morphology formed by phase-separated domains. This lack arises from the generally used postamination process that prevents formation of ionic clusters.[774,775]

6.2. Binding Materials for MEAs of AEMFC

Some attractive efforts have been made in binding materials used for MEAs of AEMs. Valade and co-workers partially replace the anions of a water-soluble commercially available poly(diallyldimethylammonium chloride) [poly(DADMAC)] by fluorinated bistrifluoromethanesulfonimide (TFSI$^-$) anions followed by OH$^-$ exchange for the remaining Cl$^-$ anions in poly(DADMAC). The resulting materials (Figure 28a) with IEC up to 0.7 mmol g^{-1} are soluble in DMSO but insoluble in water. When used in a MEA as a binder, encouraging improvements in the performance of the AEMFC (with a 50% increase of the open circuit voltage, a 580% in current density, and a 540% in accessible power) are obtained. However, the material only displays a hydroxyl conductivity of 10^{-3} S cm^{-1}, which will limit steady operation of the AEMFC under high current density.[776]

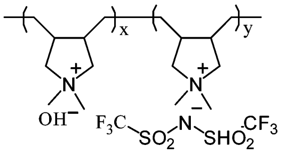

a) Ionomers based on fluorinated poly(DADMAC)

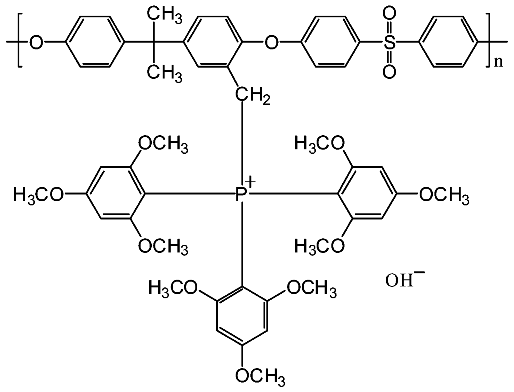

b) TPQPOH

Figure 28. Chemical structures of two ionomers used for binders: a[776] and b.[735]

Gu and co-workers presented an exciting result about a hydroxide-conductive ionomer that can be used as a binder in MEAs of AEMFCs. They synthesized a quaternary phosphonium based ionomer, tris(2,4,6-trimethoxyphenyl) polysulfone methylene quaternary phosphonium hydroxide (TPQPOH, Figure 28b), which is soluble in low-boiling-point water-soluble solvents and possesses high hydroxide ion conductivity. The TPQPOH ionomer with an IEC of 1.09 mmol g^{-1} exhibits a remarkable hydroxide ion conductivity of 2.7 × 10^{-2} S cm^{-1}. Moreover, no decrease of ionic conductivity is observed for TPQPOH after immersion in either deionized water or 1 M KOH solution for 30 days, indicating good long-term stability arising from participation of the 2,4,6-trimethoxyphenyl groups in conjugation. They are also strong electron donors, which, along with the conjugation, enhances the stability of the quaternary phosphonium group. Besides, the high steric bulk of tris(2,4,6-trimethoxyphenyl) phosphine also protects the core phosphorus atom and the α-carbon atom against hydroxide attack. The peak power density of the H_2/O_2 (back-pressure of 2.50 MPa) AEMFC using a commercial AEM and TPQPOH ionomer as a binder is 3.5 times higher than the one without TPQPOH ionomer at 50 °C (138 vs 40 mW cm^{-2}), indicating the more efficient three-phase boundary in the MEA with TPQPOH.[735] When a 50 μm TPQPOH membrane and TPQPOH ionomer are used, the AEMFC achieves the peak power density of 258 mW cm^{-2} at 70 °C under the same conditions, showing good potential of TPQPOH for applications in AEMFCs.[777]

Finally, the concept of a hybrid PEMFC that binds an alkaline PEM and an acidic PEM in series must be mentioned. This kind of hybrid PEMFC can work like a self-hydrating PEMFC due to proton-hydroxide recombination at the junction of two membranes. Thus, they may offer obvious advantages compared with the conventional humidified acidic PEM fuel cells because nonplatinum catalysts can be considered, and self-humidification can allow operation under low RH or dry conditions.[778] When methanol is used as fuel, the hybrid PEM can effectively suppress methanol permeability without a large reduction of conductivity because the proton or hydroxide ion must only move half of the hybrid PEM thickness to recombine, while the methanol has to transfer across the full thickness of the hybrid PEM. Although the current performance of the hybrid PEMFC is still inferior to that of conventional self-humidified acidic PEM fuel cells due to the immature AEM, they will show more merits with the advance of AEM technology.

7. SUMMARY AND OUTLOOK

The PEMs are an important part of fuel cell systems, and the success of PEMs is able to pave the road toward commercialization of PEMFCs. From this review, it can be deduced that the dramatic advance leading to PEMFCs being cheaper than fossil fuels used by internal combustion engines (ICEs) has not yet been reported in spite of intense research efforts toward development of less-expensive and more-efficient PEMs. The membranes described in this article each show their own respective unique characteristics, but each one is still far from perfect. Table 9 briefly compares the advantages, disadvantages, and applications of these five types of PEMs.

In the foreseeable future, it will be difficult to completely replace PFSI membranes, especially at temperatures less than 80 °C, because of their excellent oxidative stability and superior proton conductivity. The PFSI membranes reinforced by filling pores offer a cost-effective option under this condition. Radiation-grafted membranes can be prepared in large scale via established industrial processes, but their durability is still unacceptable. Hydrocarbon membranes are the main candidates for the replacement of the expensive PFSI membranes. Aromatic and heteroaromatic hydrocarbon polymer membranes with high IEC do exhibit excellent conductivities in the fully hydrated state, especially for applications above 80 °C, but they are often subject to excessive swelling and are very brittle in the dry state. However, the poly(arylene ether) membrane with a durability of 10 000 h suggests a promising perspective for alternatives to PFSI membranes. As for the hydrocarbon polymer membranes with aliphatic main chains, they are only profitable supplements to PEMs for applications below 80 °C. The phosphoric acid-doped PBI membrane-based fuel cells are not good for a pure hydrogen feed, and they provide performance inferior to that of Nafion-based fuel cells but provide performance superior to that of Nafion-based fuel cells above a certain CO level in the gas feed. The AEMs are still not competitive with acidic PEMs in the present stage or in the near future, even at low temperatures (i.e., <60 °C), but the promising binding material casts a new light on the development of AEMFCs. It is necessary to collect information on the lifetime and degradation of the AEMs and modified PEMs under realistic operating conditions.

As far as the future directions for PEM research and developments in fuel cell applications are concerned, the competitive cost of the nonfluorinated acidic ionomer membranes makes them one of the most important directions for development. One of the possible approaches for the "future" PEMs is to enhance well-defined phase separation by properly increasing the length of blocks or side-chains (e.g., multiblock copolymers or comb-shaped copolymers). To improve swelling and durability, it is necessary to

Table 9. Comparison of the Advantages, Disadvantages, and Applications of Five Types of PEM

PEMs	advantages	disadvantages	applications
perfluorosulfonic acid ionomer membranes	excellent chemical and electrochemical stability, superior proton conductivity	intolerant to CO in impure H_2; expensive; high methanol crossover; prone to dehydrate above 80 °C	low-temperature PEMFC (<80 °C); partial modified PFSI membranes up to 120 °C
partially fluorinated acid ionomer membranes	inexpensive commercial base films, reduced film-forming step, abundant experimental accumulations from other fields, base matrix with good anti-free radical oxidation, low methanol crossover	unacceptable low durability; intolerant to CO in impure H_2	low-temperature PEMFC and DMFC
nonfluorinated acid ionomer membrane	proton conductivity comparable to Nafion at high water uptake, low methanol crossover, low cost	excessive swelling at high water uptake above 80 °C; inadequate durability; intolerant to CO in impure H_2 or poisonous byproduct in DMFC	potential alternatives to PFSI membranes in PEMFC and DMFC
PBI/H_3PO_4 membranes	high tolerance to fuel impurities, enhanced efficiency of the waste heat utilization, simplified thermal and water management systems, operating temperature up to 200 °C	leaching out of H_3PO_4; corrosion of mechanical stability by H_3PO_4 at high H_3PO_4 concentrations and high temperatures	high-temperature PEMFC (120−200 °C) using impure H_2
alkaline ionomer membranes	facile electrokinetics in high-pH environment for methanol oxidation, oxygen reduction, and carbon monoxide oxidation, extended selective range of metal catalysts, improved radical oxidation stability of hydrocarbon membranes	inherently high thermodynamic voltage loss; unstable quaternary ammonium groups at temperature above 60 °C; low ionic conductivity; lack of universal binder for MEA; low efficiency	low-temperature PEMFC (<60 °C)

attach cross-linkable groups to the "future" PEMs and/or to reinforce them at the same time.

It is impractical to expect that a single type of membrane can meet the requirements of all of the automotive, stationary, and portable fuel cell applications. In such a highly interdisciplinary field, what is needed are collaborations of experts from various fields including polymer chemists, physicists, electrochemists, and process engineers. As a consequence, the educational community may afford the opportunity for developing more effective and economical PEMs based on well-studied materials. It is expected that the useful data and knowledge concerning PEMS will become much more extensive. If the present fervor for PEM research continues, a bright prospect for PEMs lies ahead.

AUTHOR INFORMATION

Corresponding Author

*Phone (office): +86-20-84036736. Fax: +86-20-84113369. E-mail: stsspk@mail.sysu.edu.cn.

Biographies

Hongwei Zhang earned his B.S. degree in Chemical Engineering from Anhui University of Science and Technology in 2002, and received his Ph.D. in Chemistry at the Zhejiang University in China under the direction of Prof. Youyi Xu in 2006. Currently, he is a research fellow of the Advanced Energy Materials Research Laboratory at the Sun Yat-sen University after two years postdoctoral research in the South China University of Technology. His fields of research include the polymer electrolyte membranes derived from aromatic hydrocarbon polymers and polyphosphazenes for fuel cell applications. E-mail: hanqiujiang@163.com.

Pei Kang Shen obtained his B.Sc. degree in Electrochemistry at Xiamen University in 1982, and he continuously carried out his research and teaching at the same university for seven years before he became a visiting researcher in the United Kingdom. He received his Ph.D. in Chemistry at Essex University in 1992. From then on he has been working at Essex University, Hong Kong University, the City University of Hong Kong, and the South China University of Technology. Since 2001, he has been the Director and Professor of the Advanced Energy Materials Research Laboratory at the Sun Yat-sen University (Guangzhou, P. R. China). He is the author of over 200 publications in qualified journals or specialized books, of 30 patents, and of more than 100 meeting presentations. His research interests include fuel cells and batteries, electrochemistry of nanomaterials and of nanocomposite functional materials, and electrochemical engineering.

ACKNOWLEDGMENTS

This work was supported by the National Natural Science Foundation of China (21073241, U1034003), the China National 863 Program (2009AA034400), the State Key Laboratory of Optoelectronic Materials and Technologies (2010-ZY-4-4, 2010-ZY-4-7), and the China Postdoctoral Science Foundation (Grant No. 20100480789). We thank Ms. Wuqingfeng Ye for the painting of the cover art.

LIST OF SYMBOLS AND ABBREVIATIONS

1VIm	1-vinylimidazole
3-APTES	3-aminopropyl triethoxysilane
3DOM	three-dimensionally ordered macroporous
4VP	4-vinylpyridine
ABPBI	poly(2,5-benzimidazole)
AEM	anion-exchange membranes
AEMFC	anion-exchange membrane fuel cell
AESA-Na	2-aminoethanesulfonic acid sodium salt
AMFC	alkaline membrane fuel cell
AMS	α-methylstyrene
APTMS	3-aminopropyltrimethoxysilane
ATRP	atom transfer radical polymerization
β	ratio of proton conductivity to methanol permeability
BA	butyl acrylate
BMMT	biofunctionalized montmorillonite
BNTDA	4,4′-binaphthyl-1,1′,8,8′-tetracarboxylic dianhydride
BPO	benzoyl peroxide
bpy	2,2′-bipyridyl
BrTFF	2-bromotetrafluoroethyl trifluorovinyl ether
cPTFE	cross-linked poly(tetrafluoroethylene)
CS	chitosan
$Cs_{2.5}H_{0.5}PWO_{40}$	Cs-substituted tungstophosphoric acid salt
cSMM	charged surface-modifying macromolecule
DAB	3,3′-diaminobenzidine
DFBP	decafluorobiphenyl
DHPZ	4-(4-hydroxyphenyl)-2,3-phthalazin-1-one
DMEVS	dimethylethoxyvinylsilane
DMF	*N*,*N*-dimethyl formamide
DMFC	direct methanol fuel cell
DMSO	dimethyl sulfoxide
DS	degree of sulfonation

DVB	divinylbenzene
EB	electron beam
EDTAD	ethylenediaminetetraacetic dianhydride
ePTFE	expanded poly(tetrafluoroethylene)
ErTfO	erbium triflate salts
ETFE	poly(ethylene-*co*-tetrafluoroethylene)
ETSS	ethyl styrenesulfonate
EW	equivalent weight
FEP	poly(tetrafluoroethylene-*co*-hexafluoropropylene)
GA	glutaraldehyde
GDE	gas diffusion electrode
GPTMS	3-glycidoxypropyltrimethoxysilane
HDDA	hexanediol diacrylate
HFB	hexafluorobenzene
HPA	heteropoly acid
IDA	4,5-imidazole dicarboxylic acid
IEC	ion-exchange capacity
IPA	isophthalic acid
IPN	interpenetrating polymer network
iPrOH	isopropanol
KDNTDA	4,4′-ketone dinaphthalene 1,1′,8,8′-tetracarboxylic dianhydride
λ	total number of water molecules per sulfonate group
LbL	layer-by-layer
MAN	methacrylonitrile
MDA	4,4′-methylenedianiline
MEA	membrane electrode assembly
MEHCl	2-mercaptoethylamine hydrochloride
MeSt	methylstyrene
MMT	montmorillonite
mPBI	poly[2,2′-(*m*-phenylene)-5,5′-bibenzimidazole]
MPMDMS	(3-mercaptopropyl)methyldimethoxysilane
MPTMS	(3-mercaptopropyl)trimethoxysilane
MSA	methanesulfonic acid
MWCNT	multiwalled carbon nanotube
NMR	nuclear magnetic resonance
NPT	*N*-phenyl 1,2,4-triazole
NTDA	1,4,5,8-naphthalenetetracarboxylic dianhydride
NVF	*N*-vinylformamide
OBBA	4,4′-oxybis(benzoic acid)
OCV	open-circuit voltage
ODA	4,4′-diaminodiphenyl ether
ODADS	4,4′-diaminodiphenyl ether-2,2′-disulfonic acid
ORMOSIL	organically modified silicate
PAH	poly(allylamine hydrochloride)
PAMPS	poly(2-acrylamido-2-methyl-1-propanesulfonic acid
PANI	polyaniline
PBI	polybenzimidazole
PBI-OO	poly[(1-(4,4′-diphenylether)-5-oxybenzimidazole)benzimidazole]
Pd	palladium
PDMS	poly(dimethyl siloxane)
PEDOT	poly(3,4-ethylenedioxythiophene)
PEG	poly(ethylene glycol)
PEGDA	polyoxyalkylenediamine
PEI	poly(ether imide)
PEEK	poly(ether ether ketone)
PEM	polymer electrolyte membrane
PEMFC	polymer electrolyte membrane fuel cell
PEO	poly(ethylene oxide)
PFA	poly(tetrafluoroethylene-*co*-perfluorinated alkyl vinyl ethers)
PFSI	perfluorosulfonic acid ionomer
PHEA	poly(hydroxy ethyl acrylate)
PhVPA	phenylvinylphosphonic acid
PI	polyimide
PMA	phosphomolybdic acid
PPA	polyphosphoric acid
pPBI	poly[2,2′-(*p*-phenylene)-5,5′-bibenzimidazole]
PPMA	phosphorus pentoxide and methanesulfonic acid
PPO	poly(2,6-dimethyl-1,4-phenylene oxide)
PPS	poly(phenylene sulfide)
PPSQ	poly(phenylmethyl silsesquioxane)
PPV	poly(*p*-phenylene vinylene)
P(S-*co*-SSA)-*b*-PMMA	poly(styrene-*co*-styrene sulfonic acid)-*b*-poly(methyl methacrylate)
PSSA	polystyrene sulfonic acid
PSSA-MA	poly(styrene sulfonic acid-*co*-maleic acid)
PSS-*b*-PMB	polystyrenesulfonate-*block*-polymethylbutylene
PTFE	poly(tetrafluoroethylene)
PTFE-*g*-PSSA	poly(tetrafluoroethylene)-*graft*-polystyrene sulfonic acid
PVA	poly(vinyl alcohol)
PVC	polyvinyl chloride
PVDF	poly(vinylidene fluoride)
P(VDF-*co*-CTFE)	poly(vinylidene fluoride-*co*-chlorotrifluoroethylene)
P(VDF-*co*-HFP)	poly(vinylidene fluoride-*co*-hexafluoropropylene)
PVF	poly(vinyl fluoride)
PVI	poly(1-vinylimidazole)
PVOS	poly(vinyl-pendant octasiloxane)
PVPA	polyvinyl phosphonic acid
PWA	phosphotungstic acid
QPEK-C	quaternized cardo polyetherketone
RH	relative humidity
RTILs	room-temperature ionic liquids
Sc-CO$_2$	supercritical carbon dioxide
SEM	scanning electron microscopy
SiO-NH$_2$	3-aminopropyl functionalized silica
SiO$_2$	silicon dioxide
SiO$_2$−SZ	SiO$_2$ supported sulfated zirconia particles
SIPA	5-sulfoisophthalic acid
SiWA	silicotungstic acid
SMA	poly(styrene-*co*-maleic anhydride)
SOPBI	sulfonated poly[2,2′-(*p*-oxidiphenylene)-5,5′-bibenzimidazole]
SPAEK	sulfonated poly(aryl ether ketone)
SPAEKKS	sulfonated poly(arylene ether ketone ketone sulfone)
SPBIBI	poly[bis(benzimidazobenzisoquinolinones)]
SPEEK	sulfonated poly(ether ether ketone)

SPEES	sulfonated poly(1,4-phenylene ether ether sulfone)
SPES	sulfonated poly(ether sulfone)
SPhODA	2,2′-bis(4-sulfophenyl)-4,4′-oxidianiline
SPI	sulfonated polyimide
sPOSS	sulfonated polyhedral oligosilsesquioxane
sPPSQ	sulfonated poly(phenylmethyl silsesquioxane)
SPS	sulfonated polystyrene
$Sr(OH)_2$	strontium hydroxide
SSS	sodium styrene sulfonate
SSt	sulfonated styrene
STEM	scanning transmission electron microscopic
StSi	*p*-styryltrimethoxysilane
TAPB	1,3,5-tris(4-aminophenoxy)benzene
tBuSt	*t*-butylstyrene
TCE	tetrachloroethane
TEOS	tetraethyl orthosilicate
TFMSA	trifluoromethanesulfonic acid
THF	tetrahydrofuran
TiO_2	titanium dioxide
T_{m}	melting temperature
TMSPMA	3-(trimethoxysilyl) propyl methacrylate
TPQPOH	tris(2,4,6-trimethoxyphenyl) polysulfone methylene quaternary phosphonium hydroxide
UHMWPE	ultrahigh molecular weight polyethylene
UV	ultraviolet
VI	*N*-vinylimidazole
VPA	vinylphosphonic acid
WO_3	tungsten trioxide
ZPP	zirconium pyrophosphate
ZrP	zirconium hydrogenphosphate
ZrPSPP	zirconium phosphate sulfophenylenphosphonate

REFERENCES

(1) Wycisk, R.; Pintauro, P. N. *Fuel Cells II* **2008**, *216*, 157.

(2) Allcock, H. R. *Curr. Opin. Solid State Mater. Sci.* **2006**, *10*, 231.

(3) Hickner, M. A.; Ghassemi, H.; Kim, Y. S.; Einsla, B. R.; McGrath, J. E. *Chem. Rev.* **2004**, *104*, 4587.

(4) Paddison, S. J.; Promislow, K. S. *Device and Materials Modeling in PEM Fuel Cells*; Springer Berlin: Heidelberg, Germany, 2009; p 19.

(5) Spohr, E. *Ionic Soft Matter: Modern Trends in Theory and Applications*; Springer Netherlands: Netherlands, 2005; p 361.

(6) Büchi, F. N.; Inaba, M.; Schmidt, T. J. *Polymer Electrolyte Fuel Cell Durability*; Springer New York: New York, 2009; p 57.

(7) Mauritz, K. A.; Moore, R. B. *Chem. Rev.* **2004**, *104*, 4535.

(8) Kreuer, K. D.; Paddison, S. J.; Spohr, E.; Schuster, M. *Chem. Rev.* **2004**, *104*, 4637.

(9) Eikerling, M.; Kornyshev, A. A.; Spohr, E. *Fuel Cells I* **2008**, *215*, 15.

(10) Paul, R.; Paddison, S. J. *Solid State Ionics* **2004**, *168*, 245.

(11) Scott, K.; Shukla, A. K. *Rev. Environ. Sci. Biotechnol.* **2004**, *3*, 273.

(12) Berezina, N. P.; Kononenko, N. A.; Dyomina, O. A.; Gnusin, N. P. *Adv. Colloid Interface Sci.* **2008**, *139*, 3.

(13) Yang, Y.; Holdcroft, S. *Fuel Cells* **2005**, *5*, 171.

(14) Hickner, M. A.; Pivovar, B. S. *Fuel Cells* **2005**, *5*, 213.

(15) Zhang, H. W.; Zhou, Z. T. *Prog. Chem.* **2008**, *20*, 602.

(16) Ioselevich, A. S.; Kornyshev, A. A.; Steinke, J. H. G. *J. Phys. Chem. B* **2004**, *108*, 11953.

(17) Devanathan, R. *Energy Environ. Sci.* **2008**, *1*, 101.

(18) Eikerling, M.; Kornyshev, A. A.; Stimming, U. *J. Phys. Chem. B* **1997**, *101*, 10807.

(19) Yang, Y. S.; Siu, A.; Peckham, T. J.; Holdcroft, S. *Fuel Cells I* **2008**, *215*, 55.

(20) Seger, B.; Vinodgopal, K.; Kamat, P. V. *Langmuir* **2007**, *23*, 5471.

(21) Gebel, G. *Polymer* **2000**, *41*, 5829.

(22) Haubold, H. G.; Vad, T.; Jungbluth, H.; Hiller, P. *Electrochim. Acta* **2001**, *46*, 1559.

(23) Eikerling, M.; Kornyshev, A. A. *J. Electroanal. Chem.* **2001**, *502*, 1.

(24) Eikerling, M.; Kornyshev, A. A.; Kuznetsov, A. M.; Ulstrup, J.; Walbran, S. *J. Phys. Chem. B* **2001**, *105*, 3646.

(25) Spohr, E.; Commer, P.; Kornyshev, A. A. *J. Phys. Chem. B* **2002**, *106*, 10560.

(26) Eikerling, M.; Paddison, S. J.; Pratt, L. R.; Zawodzinski, T. A. *Chem. Phys. Lett.* **2003**, *368*, 108.

(27) Weber, A. Z.; Newman, J. *Chem. Rev.* **2004**, *104*, 4679.

(28) Devanathan, R.; Venkatnathan, A.; Dupuis, M. *J. Phys. Chem. B* **2007**, *111*, 13006.

(29) Devanathan, R.; Venkatnathan, A.; Dupuis, M. *J. Phys. Chem. B* **2007**, *111*, 8069.

(30) Venkatnathan, A.; Devanathan, R.; Dupuis, M. *J. Phys. Chem. B* **2007**, *111*, 7234.

(31) Cui, S. T.; Liu, J. W.; Selvan, M. E.; Keffer, D. J.; Edwards, B. J.; Steele, W. V. *J. Phys. Chem. B* **2007**, *111*, 2208.

(32) Marechal, M.; Souquet, J. L.; Guindet, J.; Sanchez, J. Y. *Electrochem. Commun.* **2007**, *9*, 1023.

(33) Elfring, G. J.; Struchtrup, H. *J. Membr. Sci.* **2007**, *297*, 190.

(34) Moilanen, D. E.; Piletic, I. R.; Fayer, M. D. *J. Phys. Chem. C* **2007**, *111*, 8884.

(35) Kreuer, K. D.; Schuster, M.; Obliers, B.; Diat, O.; Traub, U.; Fuchs, A.; Klock, U.; Paddison, S. J.; Maier, J. *J. Power Sources* **2008**, *178*, 499.

(36) Costamagna, P.; Grosso, S.; Di Felice, R. *J. Power Sources* **2008**, *178*, 537.

(37) Moilanen, D. E.; Spry, D. B.; Fayer, M. D. *Langmuir* **2008**, *24*, 3690.

(38) Hristov, I. H.; Paddison, S. J.; Paul, R. *J. Phys. Chem. B* **2008**, *112*, 2937.

(39) Chaabane, L.; Bulvestre, G.; Larchet, C.; Nikonenko, V.; Deslouis, C.; Takenouti, H. *J. Membr. Sci.* **2008**, *323*, 167.

(40) Kim, E.; Weck, P. F.; Balakrishnan, N.; Bae, C. *J. Phys. Chem. B* **2008**, *112*, 3283.

(41) Wu, D. S.; Paddison, S. J.; Elliott, J. A. *Macromolecules* **2009**, *42*, 3358.

(42) Peckham, T. J.; Schmeissert, J.; Holdcroft, S. *J. Phys. Chem. B* **2008**, *112*, 2848.

(43) Pineri, M.; Gebel, G.; Davies, R. J.; Diat, O. *J. Power Sources* **2007**, *172*, 587.

(44) Hou, J. B.; Yu, H. M.; Wang, L. A.; Xing, D. M.; Hou, Z. J.; Ming, P. W.; Shao, Z. G.; Yi, B. L. *J. Power Sources* **2008**, *180*, 232.

(45) Hensley, J. E.; Way, J. D. *J. Power Sources* **2007**, *172*, 57.

(46) Hensley, J. E.; Way, J. D. *Chem. Mater.* **2007**, *19*, 4576.

(47) Wang, J. T.; Xiao, L. L.; Zhao, Y. N.; Wu, H.; Jiang, Z. Y.; Hou, W. Q. *J. Power Sources* **2009**, *192*, 336.

(48) Polak, P. L.; Mousinho, A. P.; Ordonez, N.; da Silva Zambom, L.; Mansano, R. D. *Appl. Surf. Sci.* **2007**, *254*, 173.

(49) Lue, S. J. J.; Hsiaw, S. Y.; Wei, T. C. *J. Membr. Sci.* **2007**, *305*, 226.

(50) Choi, W. C.; Kim, J. D.; Woo, S. I. *J. Power Sources* **2001**, *96*, 411.

(51) Sun, H.; Sun, G. Q.; Wang, S. L.; Liu, J. G.; Zhao, Z. S.; Wang, G. X.; Xu, H. Y.; Hou, S. F.; Xin, Q. *J. Membr. Sci.* **2005**, *259*, 27.

(52) Han, S.; Lee, J. W.; Kwak, C.; Chai, G. S.; Son, I. H.; Jang, M. Y.; An, S. G.; Cho, S. Y.; Kim, J. Y.; Kim, H. W.; Serov, A. A.; Yoo, Y.; Nam, K. H. *J. Power Sources* **2007**, *167*, 74.

(53) Ma, Z. Q.; Cheng, P.; Zhao, T. S. *J. Membr. Sci.* **2003**, *215*, 327.

(54) Prabhuram, J.; Zhao, T. S.; Liang, Z. X.; Yang, H.; Wong, C. W. *J. Electrochem. Soc.* **2005**, *152*, A1390.

(55) Zhang, D. F. *Appl. Surf. Sci.* **2009**, *255*, 4119.

(56) Tian, A. H.; Kim, J. Y.; Shi, J. Y.; Kim, K.; Lee, K. *J. Power Sources* **2007**, *167*, 302.

(57) Kim, Y. J.; Choi, W. C.; Woo, S. I.; Hong, W. H. *Electrochim. Acta* **2004**, *49*, 3227.

(58) Lin, J.; Wu, P. H.; Wycisk, R.; Trivisonno, A.; Pintauro, P. N. *J. Power Sources* **2008**, *183*, 491.

(59) Lin, H. L.; Yu, T. L.; Han, F. H. *J. Polym. Res.* **2006**, *13*, 379.

(60) Nagata, S.; Konishi, Y.; Tsuchiya, B.; Toh, K.; Yamamoto, S.; Takahiro, K.; Shikama, T. *Nucl. Instrum. Methods, Sect. B* **2007**, *257*, 519.

(61) Hensley, J. E.; Way, J. D.; Dec, S. F.; Abney, K. D. *J. Membr. Sci.* **2007**, *298*, 190.

(62) Ramya, K.; Dhathathreyan, K. S. *J. Membr. Sci.* **2008**, *311*, 121.

(63) Luan, Y. H.; Zhang, H.; Zhang, Y. M.; Li, L.; Li, H.; Liu, Y. G. *J. Membr. Sci.* **2008**, *319*, 91.

(64) Su, L. J.; Li, L.; Li, H.; Zhang, Y. M.; Yu, W.; Zhou, C. X. *J. Membr. Sci.* **2009**, *335*, 118.

(65) Xu, H. F.; Wang, X.; Shao, Z. G.; Hsing, I. M. *J. Appl. Electrochem.* **2002**, *32*, 1337.

(66) Tang, H.; Jiang, S. P. *J. Phys. Chem. C* **2008**, *112*, 19748.

(67) Kamavaram, V.; Veedu, V.; Kannan, A. M. *J. Power Sources* **2009**, *188*, 51.

(68) Yoshitake, M.; Watakabe, A. *Fuel Cells I* **2008**, *215*, 127.

(69) Tang, Y. L.; Kusoglu, A.; Karlsson, A. M.; Santare, M. H.; Cleghorn, S.; Johnson, W. B. *J. Power Sources* **2008**, *175*, 817.

(70) Rodgers, M. P.; Berring, J.; Holdcroft, S.; Shi, Z. Q. *J. Membr. Sci.* **2008**, *321*, 100.

(71) Tang, H. L.; Wang, X. E.; Pan, M.; Wang, F. *J. Membr. Sci.* **2007**, *306*, 298.

(72) Tang, H. L.; Pan, M.; Wang, F.; Shen, P. K.; Jiang, S. P. *J. Phys. Chem. B* **2007**, *111*, 8684.

(73) Yildirim, M. H.; Stamatialis, D.; Wessling, M. *J. Membr. Sci.* **2008**, *321*, 364.

(74) Choi, S. W.; Fu, Y. Z.; Ahn, Y. R.; Jo, S. M.; Manthiram, A. *J. Power Sources* **2008**, *180*, 167.

(75) Zhu, J.; Tang, H. L.; Pan, M. *J. Membr. Sci.* **2008**, *312*, 41.

(76) Jung, G. B.; Weng, F. B.; Su, A.; Wang, J. S.; Yu, T. L.; Lin, H. L.; Yang, T. F.; Chan, S. H. *Int. J. Hydrogen Energy* **2008**, *33*, 2413.

(77) Weng, F. B.; Wang, J. S.; Yu, T. L. *J. Chin. Inst. Chem. Eng* **2008**, *39*, 429.

(78) Chen, L. C.; Yu, T. L.; Lin, H. L.; Yeh, S. H. *J. Membr. Sci.* **2008**, *307*, 10.

(79) Lin, H. L.; Chang, T. J. *J. Membr. Sci.* **2008**, *325*, 880.

(80) Lin, H. L.; Yeh, S. H.; Yu, T. L.; Chen, L. C. *J. Polym. Res.* **2009**, *16*, 519.

(81) Ainla, A.; Brandell, D. *Solid State Ionics* **2007**, *178*, 581.

(82) Huang, Q. M.; Zhang, Q. L.; Huang, H. L.; Li, W. S.; Huang, Y. J.; Luo, J. L. *J. Power Sources* **2008**, *184*, 338.

(83) Berezina, N. P.; Kononenko, N. A.; Sytcheva, A. A. R.; Loza, N. V.; Shkirskaya, S. A.; Hegman, N.; Pungor, A. *Electrochim. Acta* **2009**, *54*, 2342.

(84) Wang, C. H.; Chen, C. C.; Hsu, H. C.; Du, H. Y.; Chen, C. R.; Hwang, J. Y.; Chen, L. C.; Shih, H. C.; Stejskal, J.; Chen, K. H. *J. Power Sources* **2009**, *190*, 279.

(85) Yang, J. Y.; Shen, P. K.; Varcoe, J.; Wei, Z. D. *J. Power Sources* **2009**, *189*, 1016.

(86) Chen, C. Y.; Garnica-Rodriguez, J. I.; Duke, M. C.; Dalla Costa, R. F.; Dicks, A. L.; da Costa, J. C. D. *J. Power Sources* **2007**, *166*, 324.

(87) Bae, B. C.; Ha, H. Y.; Kim, D. *J. Electrochem. Soc.* **2005**, *152*, A1366.

(88) Choa, H. D.; Won, J.; Ha, H. Y. *Renewable Energy* **2008**, *33*, 248.

(89) Kim, H.; Kang, M. S.; Lee, D. H.; Won, J.; Kim, J.; Kang, Y. S. *J. Membr. Sci.* **2007**, *304*, 60.

(90) Cui, Z. M.; Li, N. W.; Zhou, X. C.; Liu, C. P.; Liao, J. H.; Zhang, S. B.; Xing, W. *J. Power Sources* **2007**, *173*, 162.

(91) Jeon, J. D.; Kwak, S. Y. *J. Power Sources* **2008**, *185*, 49.

(92) Jeon, J. D.; Kwak, S. Y. *J. Phys. Chem. B* **2007**, *111*, 9437.

(93) Wu, Z. M.; Sun, G. Q.; Jin, W.; Wang, Q.; Hou, H. Y.; Chan, K. Y.; Xin, Q. *J. Power Sources* **2007**, *167*, 309.

(94) Kundu, P. P.; Kim, B. T.; Ahn, J. E.; Han, H. S.; Shul, Y. G. *J. Power Sources* **2007**, *171*, 86.

(95) Li, L.; Zhang, Y. M. *J. Power Sources* **2008**, *175*, 256.

(96) Li, L.; Drillet, J. F.; Dittmeyer, R.; Juttner, K. *J. Solid State Electrochem.* **2006**, *10*, 708.

(97) Lin, Y. F.; Hsiao, Y. H.; Yen, C. Y.; Chiang, C. L.; Lee, C. H.; Huang, C. C.; Ma, C. C. M. *J. Power Sources* **2007**, *172*, 570.

(98) Sato, Y.; Fujii, K.; Mitani, N.; Matsuura, A.; Kakigi, T.; Muto, F.; Li, J.; Oshima, A.; Washio, M. *Nucl. Instrum. Methods, Sect. B* **2007**, *265*, 213.

(99) Park, H.; Kim, Y.; Choi, Y. S.; Hong, W. H.; Jung, D. *J. Power Sources* **2008**, *178*, 610.

(100) Tian, A. H.; Kim, J. Y.; Shi, J. Y.; Kim, K. *J. Power Sources* **2008**, *183*, 1.

(101) Kim, I. T.; Choi, J.; Kim, S. C. *J. Membr. Sci.* **2007**, *300*, 28.

(102) Tsai, J. C.; Cheng, H. P.; Kuo, J. F.; Huang, Y. H.; Chen, C. Y. *J. Power Sources* **2009**, *189*, 958.

(103) Tsai, J. C.; Kuo, J. F.; Chen, C. Y. *J. Power Sources* **2009**, *194*, 226.

(104) Kumar, G. G.; Lee, D. N.; Kim, P.; Nahm, K. S.; Elizabeth, R. N. *Eur. Polym. J.* **2008**, *44*, 2225.

(105) Zhai, Y. F.; Zhang, H. M.; Zhang, Y.; Xing, D. M. *J. Power Sources* **2007**, *169*, 259.

(106) Deligoz, H.; Yilmazturk, S.; Karaca, T.; Ozdemir, H.; Koc, S. N.; Oksuzomer, F.; Durmus, A.; Gurkaynak, M. A. *J. Membr. Sci.* **2009**, *326*, 643.

(107) Di Noto, V.; Gliubizzi, R.; Negro, E.; Vittadello, M.; Pace, G. *Electrochim. Acta* **2007**, *53*, 1618.

(108) Noto, V.; Lavina, S.; Negro, E.; Vittadello, M.; Conti, F.; Piga, M.; Pace, G. *J. Power Sources* **2009**, *187*, 57.

(109) Yang, J. Y.; Li, Y. L.; Huang, Y. Q.; Liang, J. Y.; Shen, P. K. *J. Power Sources* **2008**, *177*, 56.

(110) Zeng, R.; Wang, Y.; Wang, S. L.; Shen, P. K. *Electrochim. Acta* **2007**, *52*, 3895.

(111) Vengatesan, S.; Kim, H. J.; Lee, S. Y.; Cho, E.; Ha, H. Y.; Oh, I. H.; Lim, T. H. *J. Power Sources* **2007**, *167*, 325.

(112) Park, C. H.; Kim, H. K.; Lee, C. H.; Park, H. B.; Lee, Y. M. *J. Power Sources* **2009**, *194*, 646.

(113) Jin, Y. G.; Qiao, S. Z.; Zhang, L.; Xu, Z. P.; Smart, S.; da Costa, J. C. D.; Lu, G. Q. *J. Power Sources* **2008**, *185*, 664.

(114) Mistry, M. K.; Choudhury, N. R.; Dutta, N. K.; Knott, R.; Shi, Z. Q.; Holdcroft, S. *Chem. Mater.* **2008**, *20*, 6857.

(115) Hudiono, Y.; Choi, S.; Shu, S.; Koros, W. J.; Tsapatsis, M.; Nair, S. *Microporous Mesoporous Mater.* **2009**, *118*, 427.

(116) Yuan, J. J.; Zhou, G. B.; Pu, H. T. *J. Membr. Sci.* **2008**, *325*, 742.

(117) Tang, H.; Wan, Z.; Pan, M.; Jiang, S. P. *Electrochem. Commun.* **2007**, *9*, 2003.

(118) Pan, J. J.; Zhang, H. I.; Pan, M. *J. Colloid Interface Sci.* **2008**, *326*, 55.

(119) Lin, Y. H.; Li, H. D.; Liu, C. P.; Xing, W.; Ji, X. L. *J. Power Sources* **2008**, *185*, 904.

(120) Rodgers, M. P.; Shi, Z. Q.; Holdcroft, S. *J. Membr. Sci.* **2008**, *325*, 346.

(121) Dura, J. A.; Murthi, V. S.; Hartman, M.; Satija, S. K.; Majkrzak, C. F. *Macromolecules* **2009**, *42*, 4769.

(122) Chen, W. F.; Kuo, P. L. *Macromolecules* **2007**, *40*, 1987.

(123) Li, T.; Yang, Y. *J. Power Sources* **2009**, *187*, 332.

(124) Zhang, X. H.; Tay, S. W.; Hong, L.; Liu, Z. L. *J. Membr. Sci.* **2008**, *320*, 310.

(125) Mura, F.; Silva, R. F.; Pozio, A. *Electrochim. Acta* **2007**, *52*, 5824.

(126) Kang, M. S.; Lee, M. J. *Electrochem. Commun.* **2009**, *11*, 457.

(127) Santiago, E. I.; Isidoro, R. A.; Dresch, M. A.; Matos, B. R.; Linardi, M.; Fonseca, F. C. *Electrochim. Acta* **2009**, *54*, 4111.

(128) Barbora, L.; Acharya, S.; Verma, A. *Macromol. Symp.* **2009**, *277*, 177.

(129) Matos, B. R.; Arico, E. M.; Linardi, M.; Ferlauto, A. S.; Santiago, E. I.; Fonseca, F. C. *J. Therm. Anal. Calorim.* **2009**, *97*, 591.
(130) Chen, S. Y.; Han, C. C.; Tsai, C. H.; Huang, J.; Chen-Yang, Y. W. *J. Power Sources* **2007**, *171*, 363.
(131) Li, X.; Roberts, E. P. L; Holmes, S. M.; Zholobenko, V. *Solid State Ionics* **2007**, *178*, 1248.
(132) Yildirim, M. H.; Curos, A. R.; Motuzas, J.; Julbe, A.; Stamatialis, D. F.; Wessling, M. *J. Membr. Sci.* **2009**, *338*, 75.
(133) Kang, S.; Peck, D. H.; Park, Y. C.; Jung, D. H.; Jang, J. H.; Lee, H. R. *J. Phys. Chem. Solids* **2008**, *69*, 1280.
(134) Burgaz, E.; Lian, H. Q.; Alonso, R. H.; Estevez, L.; Kelarakis, A.; Giannelis, E. P. *Polymer* **2009**, *50*, 2384.
(135) Alonso, R. H.; Estevez, L.; Lian, H. Q.; Kelarakis, A.; Giannelis, E. P. *Polymer* **2009**, *50*, 2402.
(136) He, X. C.; Tang, H. L.; Pan, M. *J. Appl. Polym. Sci.* **2008**, *108*, 529.
(137) Pan, J. J.; Zhang, H. N.; Chen, W.; Pan, M. *Int. J. Hydrogen Energy* **2010**, *35*, 2796.
(138) Tasaki, K.; Gasa, J.; Wang, H. B.; DeSousa, R. *Polymer* **2007**, *48*, 4438.
(139) Yan, L. M.; Zhu, S. H.; Ji, X. B.; Lu, W. C. *J. Phys. Chem. B* **2007**, *111*, 6357.
(140) Mecheri, B.; D'Epifanio, A.; Traversa, E.; Licoccia, S. *J. Power Sources* **2007**, *169*, 247.
(141) Alberti, G.; Casciola, M.; Pica, M.; Di Cesare, G. *Adv. Membr. Technol.* **2003**, *984*, 208.
(142) Sen, U.; Celik, S. U.; Ata, A.; Bozkurt, A. *Int. J. Hydrogen Energy* **2008**, *33*, 2808.
(143) Alberti, G.; Casciola, M.; Capitani, D.; Donnadio, A.; Narducci, R.; Pica, M.; Sganappa, M. *Electrochim. Acta* **2007**, *52*, 8125.
(144) Hwang, M.; Ha, H. Y.; Kim, D. *J. Membr. Sci.* **2008**, *325*, 647.
(145) Truffier-Boutry, D.; De Geyer, A.; Guetaz, L.; Diat, O.; Gebel, G. *Macromolecules* **2007**, *40*, 8259.
(146) Casciola, M.; Capitani, D.; Comite, A.; Donnadio, A.; Frittella, V.; Pica, M.; Sganappa, M.; Varzi, A. *Fuel Cells* **2008**, *8*, 217.
(147) Casciola, M.; Capitani, D.; Donnadio, A.; Frittella, V.; Pica, M.; Sganappa, M. *Fuel Cells* **2009**, *9*, 381.
(148) Hou, H. Y.; Sun, G. Q.; Wu, Z. M.; Jin, W.; Xin, Q. *Int. J. Hydrogen Energy* **2008**, *33*, 3402.
(149) Barbora, L.; Acharya, S.; Singh, R.; Scott, K.; Verma, A. *J. Membr. Sci.* **2009**, *326*, 721.
(150) Sahu, A. K.; Pitchumani, S.; Sridhar, P.; Shukla, A. K. *Fuel Cells* **2009**, *9*, 139.
(151) Navarra, M. A.; Abbati, C.; Croce, F.; Scrosati, B. *Fuel Cells* **2009**, *9*, 222.
(152) Montoneri, E.; Boffa, V.; Bottigliengo, S.; Casciola, M.; Sganappa, M.; Marigo, A.; Speranza, G.; Minati, L.; Torrengo, S.; Alberti, G.; Bertinetti, L. *Solid State Ionics* **2010**, *181*, 578.
(153) Jung, E. H.; Jung, U. H.; Yang, T. H.; Peak, D. H.; Jung, D. H.; Kim, S. H. *Int. J. Hydrogen Energy* **2007**, *32*, 903.
(154) Son, D. H.; Sharma, R. K.; Shul, Y. G.; Kim, H. *J. Power Sources* **2007**, *165*, 733.
(155) Wang, L.; Yi, B. L.; Zhang, H. M.; Xing, D. M. *Electrochim. Acta* **2007**, *52*, 5479.
(156) Wu, Z. M.; Sun, G. Q.; Jin, W.; Hou, H. Y.; Wang, S. L.; Xin, Q. *J. Membr. Sci.* **2008**, *313*, 336.
(157) Navarra, M. A.; Abbati, C.; Scrosati, B. *J. Power Sources* **2008**, *183*, 109.
(158) Bi, C.; Zhang, H. M.; Zhang, Y.; Zhu, X. B.; Ma, Y. W.; Dai, H.; Xiao, S. H. *J. Power Sources* **2008**, *184*, 197.
(159) Park, K. T.; Jung, U. H.; Choi, D. W.; Chun, K.; Lee, H. M.; Kim, S. H. *J. Power Sources* **2008**, *177*, 247.
(160) Sacca, A.; Carbone, A.; Pedicini, R.; Marrony, M.; Barrera, R.; Elomaa, M.; Passalacqua, E. *Fuel Cells* **2008**, *8*, 225.
(161) Di Noto, V.; Piga, M.; Piga, L.; Polizzi, S.; Negro, E. *J. Power Sources* **2008**, *178*, 561.
(162) Di Noto, V.; Piga, M.; Lavina, S.; Negro, E.; Yoshida, K.; Ito, R.; Furukawa, T. *Electrochim. Acta* **2010**, *55*, 1431.
(163) Thomassin, J. M.; Kollar, J.; Caldarella, G.; Germain, A.; Jerome, R.; Detrembleur, C. *J. Membr. Sci.* **2007**, *303*, 252.
(164) Wang, L.; Xing, D. M.; Zhang, H. M.; Yu, H. M.; Liu, Y. H.; Yi, B. L. *J. Power Sources* **2008**, *176*, 270.
(165) Kannan, R.; Parthasarathy, M.; Maraveedu, S. U.; Kurungot, S.; Pillai, V. K. *Langmuir* **2009**, *25*, 8299.
(166) Kim, T. K.; Kang, M.; Choi, Y. S.; Kim, H. K.; Lee, W.; Chang, H.; Seung, D. *J. Power Sources* **2007**, *165*, 1.
(167) Lee, W.; Kim, H.; Kim, T. K.; Chang, H. *J. Membr. Sci.* **2007**, *292*, 29.
(168) Lin, Y. F.; Yen, C. Y.; Hung, C. H.; Hsiao, Y. H.; Ma, C. C. M. *J. Power Sources* **2007**, *168*, 162.
(169) Hasani-Sadrabadi, M. M.; Dashtimoghadam, E.; Majedi, F. S.; Kabiri, K. *J. Power Sources* **2009**, *190*, 318.
(170) Holmberg, B. A.; Wang, X.; Yan, Y. S. *J. Membr. Sci.* **2008**, *320*, 86.
(171) Tominaga, Y.; Hong, I. C.; Asai, S.; Sumita, M. *J. Power Sources* **2007**, *171*, 530.
(172) Lin, Y. F.; Yen, C. Y.; Ma, C. C. M.; Liao, S. H.; Lee, C. H.; Hsiao, Y. H.; Lin, H. P. *J. Power Sources* **2007**, *171*, 388.
(173) Pereira, F.; Valle, K.; Belleville, P.; Morin, A.; Lambert, S.; Sanchez, C. *Chem. Mater.* **2008**, *20*, 1710.
(174) Park, J. W.; Kim, Y. C.; Jeong, Y. J.; Kim, S. D.; Ha, H. Y.; Kim, W. J. *Microporous Mesoporous Mater.* **2008**, *114*, 238.
(175) Tay, S. W.; Zhang, X.; Liu, Z.; Hong, L.; Chan, S. H. *J. Membr. Sci.* **2008**, *321*, 139.
(176) Wang, K. P.; McDermid, S.; Li, J.; Kremliakova, N.; Kozak, P.; Song, C. J.; Tang, Y. H.; Zhang, J. L.; Zhang, J. J. *J. Power Sources* **2008**, *184*, 99.
(177) Kang, J. S.; Ghil, L. J.; Kim, Y. S.; Kim, Y. T.; Rhee, H. W. *Colloids Surf., A* **2008**, *313*, 207.
(178) Nam, S. E.; Kim, S. O.; Kang, Y.; Lee, J. W.; Lee, K. H. *J. Membr. Sci.* **2008**, *322*, 466.
(179) Lavorgna, M.; Mascia, L.; Mensitieri, G.; Gilbert, M.; Scherillo, G.; Palomba, B. *J. Membr. Sci.* **2007**, *294*, 159.
(180) Yen, C. Y.; Lee, C. H.; Lin, Y. F.; Lin, H. L.; Hsiao, Y. H.; Liao, S. H.; Chuang, C. Y.; Ma, C. C. M. *J. Power Sources* **2007**, *173*, 36.
(181) Ladewig, B. P.; Knott, R. B.; Martin, D. J.; da Costa, J. C. D.; Lu, G. Q. *Electrochem. Commun.* **2007**, *9*, 781.
(182) Ladewig, B. P.; Knott, R. B.; Hill, A. J.; Riches, J. D.; White, J. W.; Martin, D. J.; da Costa, J. C. D.; Lu, G. Q. *Chem. Mater.* **2007**, *19*, 2372.
(183) Su, L. J.; Li, L.; Li, H.; Tang, J. K.; Zhang, Y. M.; Yu, W.; Zhou, C. X. *J. Power Sources* **2009**, *194*, 220.
(184) Su, L. J.; Pei, S. P.; Li, L.; Li, H.; Zhang, Y. M.; Yu, W.; Zhou, C. X. *Int. J. Hydrogen Energy* **2009**, *34*, 6892.
(185) Wu, J.; Cui, Z. M.; Zhao, C. J.; Li, H. T.; Zhang, Y.; Fu, T. Z.; Na, H.; Xing, W. *Int. J. Hydrogen Energy* **2009**, *34*, 6740.
(186) Zhang, Y.; Zhang, H. M.; Zhu, X. B.; Gang, L.; Bi, C.; Liang, Y. M. *J. Power Sources* **2007**, *165*, 786.
(187) Endoh, E.; Hommura, S. *Polymer Electrolyte Fuel Cell Durability*; Springer New York: New York, 2009; p 119.
(188) Jones, D. J.; Roziere, J. *Fuel Cells I* **2008**, *215*, 219.
(189) Ye, G.; Hayden, C. A.; Goward, G. R. *Macromolecules* **2007**, *40*, 1529.
(190) Gursel, S. A.; Gubler, L.; Gupta, B.; Scherer, G. G. *Fuel Cells I* **2008**, *215*, 157.
(191) Slade, R. C. T.; Varcoe, J. R. *Solid State Ionics* **2005**, *176*, 585.
(192) Chen, J. H.; Asano, M.; Maekawa, Y.; Yoshida, M. *J. Membr. Sci.* **2006**, *277*, 249.
(193) Asano, M.; Chen, J.; Maekawa, Y.; Sakamura, T.; Kubota, H.; Yoshida, M. *J. Polym. Sci., Part A: Polym. Chem.* **2007**, *45*, 2624.
(194) Sawada, S.; Yamaki, T.; Nishimura, H.; Asano, M.; Suzuki, A.; Terai, T.; Maekawa, Y. *Solid State Ionics* **2008**, *179*, 1611.
(195) Sawada, S. I.; Yamaki, T.; Kawahito, S.; Asano, M.; Suzuki, A.; Terai, T.; Maekawa, Y. *Polym. Degrad. Stab.* **2009**, *94*, 344.

(196) Muto, F.; Oshima, A.; Kakigi, T.; Mitani, N.; Matsuura, A.; Fujii, K.; Sato, Y.; Li, J. Y.; Washio, M. *Nucl. Instrum. Methods, Sect. B* **2007**, *265*, 162.

(197) Kim, B. N.; Lee, D. H.; Lee, S. W.; Han, D. H. *Korean J. Chem. Eng.* **2008**, *25*, 1212.

(198) Kim, B. N.; Lee, D. H.; Han, D. H. *Polym. Degrad. Stab.* **2008**, *93*, 1214.

(199) Gubler, L.; Kuhn, H.; Schmidt, T.; Scherer, G.; Brack, H.-P.; Simbeck, K. *Fuel Cells* **2004**, 196.

(200) Gubler, L.; Slaski, M.; Wallasch, F.; Wokaun, A.; Scherer, G. G. *J. Membr. Sci.* **2009**, *339*, 68.

(201) Kimura, Y.; Chen, J.; Asano, M.; Maekawa, Y.; Katakai, R.; Yoshida, M. *Nucl. Instrum. Methods, Sect. B* **2007**, *263*, 463.

(202) Farquet, P.; Padeste, C.; Borner, M.; Ben Youcef, H.; Gursel, S. A.; Scherer, G. G.; Solaka, H. H.; Sailec, V.; Wokaun, A. *J. Membr. Sci.* **2008**, *325*, 658.

(203) Nasef, M. M.; Saidi, H. *J. Polym. Res.* **2005**, *12*, 305.

(204) Gupta, B.; Muzyyan, N.; Saxena, S.; Grover, N.; Alam, S. *Radiat. Phys. Chem.* **2008**, *77*, 42.

(205) Matsuura, A.; Kakigi, T.; Sato, Y.; Fujii, K.; Mitani, N.; Li, J. Y.; Oshima, A.; Washio, M. *Macromol. Symp.* **2007**, *249*, 221.

(206) Schnyder, B.; Ragert, T. *J. Appl. Polym. Sci.* **2007**, *104*, 1973.

(207) Kimura, Y.; Asano, M.; Chen, J. H.; Maekawa, Y.; Katakai, R.; Yoshida, M. *Radiat. Phys. Chem.* **2008**, *77*, 864.

(208) Larsen, M. J.; Ma, Y.; Qian, H.; Toftlund, H.; Lund, P. B.; Skou, E. M. *Solid State Ionics* **2010**, *181*, 201.

(209) Ben Youcef, H.; Gursel, S. A.; Wokaun, A.; Scherer, G. G. *J. Membr. Sci.* **2008**, *311*, 208.

(210) Gursel, S. A.; Schneider, J.; Ben Youcef, H.; Wokaun, A.; Scherer, G. G. *J. Appl. Polym. Sci.* **2008**, *108*, 3577.

(211) Chen, J. H.; Asano, M.; Yamaki, T.; Yoshida, M. *J. Mater. Sci.* **2006**, *41*, 1289.

(212) Larsen, M. J.; Ma, Y.; Lund, P. B.; Skou, E. M. *Appl. Phys. A: Mater. Sci. Process.* **2009**, *96*, 569.

(213) Ben youcef, H.; Gubler, L.; Gursel, S. A.; Henkensmeier, D.; Wokaun, A.; Scherer, G. G. *Electrochem. Commun.* **2009**, *11*, 941.

(214) Zhai, M. L.; Chen, J. H.; Hasegawa, S.; Li, D. R.; Oku, H.; Maekawa, Y. *Eur. Polym. J.* **2009**, *45*, 1668.

(215) Zhai, M. L.; Hasegawa, S.; Chen, J. H.; Maekawa, Y. *J. Fluorine Chem.* **2008**, *129*, 1146.

(216) Zhai, M. L.; Chen, J. H.; Hasegawa, S.; Maekawa, Y. *Polymer* **2009**, *50*, 1159.

(217) Chen, J. H.; Asano, M.; Maekawa, Y.; Yoshida, M. *J. Membr. Sci.* **2007**, *296*, 77.

(218) Chen, J. H.; Asano, M.; Maekawa, Y.; Yoshida, M. *J. Polym. Sci., Part A: Polym. Chem.* **2008**, *46*, 5559.

(219) Sogaard, S. R.; Huan, Q.; Lund, P.; Donnadio, A.; Casciola, M.; Skou, E. M. *Solid State Ionics* **2007**, *178*, 493.

(220) Schmidt, C.; Schmidt-Naake, G. *Macromol. Symp.* **2007**, *259*, 181.

(221) Schmidt, C.; Schmidt-Naake, G. *Macromol. Mater. Eng.* **2007**, *292*, 1164.

(222) Nasef, M. M.; Saidi, H.; Dahlan, K. Z. M. *J. Membr. Sci.* **2009**, *339*, 115.

(223) Nasef, M. M.; Saidi, H.; Dahlan, K. Z. M. *Nucl. Instrum. Methods, Sect. B* **2007**, *265*, 168.

(224) Chen, Y. B.; Kim, H. *J. Power Sources* **2009**, *190*, 311.

(225) Kim, Y. W.; Choi, J. K.; Park, J. T.; Kim, J. H. *J. Membr. Sci.* **2008**, *313*, 315.

(226) Choi, J. K.; Kim, Y. W.; Koh, J. H.; Kim, J. H. *Polym. Adv. Technol* **2008**, *19*, 915.

(227) Kim, Y. W.; Lee, D. K.; Lee, K. J.; Kim, J. H. *Eur. Polym. J.* **2008**, *44*, 932.

(228) Patel, R.; Park, J. T.; Lee, W. S.; Kim, J. H.; Min, B. R. *Polym. Adv. Technol.* **2009**, *20*, 1146.

(229) Roh, D. K.; Park, J. T.; Koh, J. H.; Koh, J. K.; Kim, J. H. *Ionics* **2009**, *15*, 439.

(230) Kim, Y. W.; Park, J. T.; Koh, J. H.; Roh, D. K.; Kim, J. H. *J. Membr. Sci.* **2008**, *325*, 319.

(231) Tsang, E. M. W.; Zhang, Z.; Shi, Z.; Soboleva, T.; Holdcroft, S. *J. Am. Chem. Soc.* **2007**, *129*, 15106.

(232) Taguet, A.; Ameduri, B.; Boutevin, B. *J. Polym. Sci., Part A: Polym. Chem.* **2009**, *47*, 121.

(233) Hassoun, J.; Croce, F.; Tizzani, C.; Scrosati, B. *Electrochem. Commun.* **2007**, *9*, 2045.

(234) Quartarone, E.; Carollo, A.; TomaSi, C.; Belotti, F.; Grandi, S.; Mustarelli, P.; Magistris, A. *J. Power Sources* **2007**, *168*, 126.

(235) Kumar, G. G.; Kim, P.; Nahm, K. S.; Elizabeth, R. N. *J. Membr. Sci.* **2007**, *303*, 126.

(236) Mustarelli, P.; Carollo, A.; Grandi, S.; Quartarone, E.; Tomasi, C.; Leonardi, S.; Magistris, A. *Fuel Cells* **2007**, *7*, 441.

(237) Sekhon, S. S.; Lalia, B. S.; Kim, C. S.; Lee, W. Y. *Macromol. Symp.* **2007**, *249*, 216.

(238) Lalia, B. S.; Yamada, K.; Hundal, M. S.; Park, J. S.; Park, G. G.; Lee, W. Y.; Kim, C. S.; Sekhon, S. S. *Appl. Phys. A: Mater. Sci. Process.* **2009**, *96*, 661.

(239) Izak, P.; Hovorka, S.; Bartovsky, T.; Bartovska, L.; Crespo, J. G. *J. Membr. Sci.* **2007**, *296*, 131.

(240) Singh, B.; Hundal, M. S.; Park, G. G.; Park, J. S.; Lee, W. Y.; Kim, C. S.; Yamada, K.; Sekhon, S. S. *Solid State Ionics* **2007**, *178*, 1404.

(241) Lee, J. S.; Nohira, T.; Hagiwara, R. *J. Power Sources* **2007**, *171*, 535.

(242) Fernicola, A.; Panero, S.; Scrosati, B.; Tamada, M.; Ohno, H. *ChemPhysChem* **2007**, *8*, 1103.

(243) Martinelli, A.; Matic, A.; Jacobsson, P.; Borjesson, L.; Fernicola, A.; Panero, S.; Scrosati, B.; Ohno, H. *J. Phys. Chem. B* **2007**, *111*, 12462.

(244) Fernicola, A.; Panero, S.; Scrosati, B. *J. Power Sources* **2008**, *178*, 591.

(245) Che, Q. T.; Sun, B. Y.; He, R. H. *Electrochim. Acta* **2008**, *53*, 4428.

(246) Sancho, T.; Soler, J.; Pina, M. P. *J. Power Sources* **2007**, *169*, 92.

(247) Sancho, T.; Lemus, J.; Urbiztondo, M.; Soler, J.; Pina, M. P. *Microporous Mesoporous Mater.* **2008**, *115*, 206.

(248) Martinelli, A.; Matic, A.; Jacobsson, P.; Borjesson, L.; Navarra, M. A.; Munao, D.; Panero, S.; Scrosati, B. *Solid State Ionics* **2007**, *178*, 527.

(249) Malers, J. L.; Sweikart, M. A.; Horan, J. L.; Turner, J. A.; Herring, A. M. *J. Power Sources* **2007**, *172*, 83.

(250) Liu, D.; Yates, M. Z. *J. Membr. Sci.* **2009**, *326*, 539.

(251) Niepceron, F.; Lafitte, B.; Galiano, H.; Bigarre, J.; Nicol, E.; Tassin, J. F. *J. Membr. Sci.* **2009**, *338*, 100.

(252) Reichman, S.; Burstein, L.; Peled, E. *J. Power Sources* **2008**, *179*, 520.

(253) Piboonsatsanasakul, P.; Wootthikanokkhan, J.; Thanawan, S. *J. Appl. Polym. Sci.* **2008**, *107*, 1325.

(254) Jung, H. Y.; Park, J. K. *Electrochim. Acta* **2007**, *52*, 7464.

(255) Choi, W. H.; Jo, W. H. *J. Power Sources* **2009**, *188*, 127.

(256) Byun, J.; Sauk, J.; Kim, H. *Int. J. Hydrogen Energy* **2009**, *34*, 6437.

(257) Greaves, T. L.; Drummond, C. J. *Chem. Rev.* **2008**, *108*, 206.

(258) Wang, L.; Yi, B. L.; Zhang, H. M.; Liu, Y. H.; Xing, D. M.; Shao, Z. G.; Cai, Y. H. *J. Power Sources* **2007**, *167*, 47.

(259) Choi, D. H.; Lee, J.; Kwon, O.; Kim, J. Y.; Kim, K. *J. Power Sources* **2008**, *178*, 677.

(260) Rusanov, A. L.; Likhatchev, D.; Kostoglodov, P. V.; Mullen, K.; Klapper, M. *Inorg. Polym. Nanocomposites Membr.* **2005**, *179*, 83.

(261) Maier, G.; Meier-Haack, J. *Fuel Cells II* **2008**, *216*, 1.

(262) Rusanov, A. L.; Kostoglodov, P. V.; Abadie, M. J. M.; Voytekunas, V. Y.; Likhachev, D. Y. *Fuel Cells II* **2008**, *216*, 125.

(263) Jaafar, J.; Ismail, A. F.; Mustafa, A. *Mater. Sci. Eng., A* **2007**, *460*, 475.

(264) Park, J. S.; Krishnan, P.; Park, S. H.; Park, G. G.; Yang, T. H.; Lee, W. Y.; Kim, C. S. *J. Power Sources* **2008**, *178*, 642.

(265) Luu, D. X.; Cho, E. B.; Han, O. H.; Kim, D. *J. Phys. Chem. B* **2009**, *113*, 10072.
(266) Lee, J. K.; Li, W.; Manthiram, A. *J. Power Sources* **2008**, *180*, 56.
(267) Ye, G.; Mills, C. M.; Goward, G. R. *J. Membr. Sci.* **2008**, *319*, 238.
(268) Baias, M.; Demco, D. E.; Colicchio, I.; Blumich, B.; Moller, M. *Chem. Phys. Lett.* **2008**, *456*, 227.
(269) Takimoto, N.; Wu, L.; Ohira, A.; Takeoka, Y.; Rikukawa, M. *Polymer* **2009**, *50*, 534.
(270) Sambandam, S.; Ramani, V. *Electrochim. Acta* **2008**, *53*, 6328.
(271) Lin, C. K.; Kuo, J. F.; Chen, C. Y. *J. Power Sources* **2009**, *187*, 341.
(272) Conceicao, T. F.; Bertolino, J. R.; Barra, G. M. O.; Pires, A. T. N. *Mater. Sci. Eng., C* **2009**, *29*, 575.
(273) Do, K. N. T.; Kim, D. *J. Appl. Polym. Sci.* **2008**, *110*, 1763.
(274) Do, K. N. T.; Kim, D. *J. Power Sources* **2008**, *185*, 63.
(275) Roelofs, K. S.; Kampa, A.; Hirth, T.; Schiestel, T. *J. Appl. Polym. Sci.* **2009**, *111*, 2998.
(276) Brijmohan, S. B.; Shaw, M. T. *J. Membr. Sci.* **2007**, *303*, 64.
(277) Marrony, M.; Barrera, R.; Quenet, S.; Ginocchio, S.; Montelatici, L.; Aslanides, A. *J. Power Sources* **2008**, *182*, 469.
(278) Prado, L. A. S. D.; Ponce, M. L.; Goerigk, G.; Funari, S. S.; Garamus, V. M.; Willumeit, R.; Schulte, K.; Nunes, S. P. *J. Non-Cryst. Solids* **2009**, *355*, 6.
(279) Krishnan, P.; Park, J. S.; Kim, C. S. *Eur. Polym. J.* **2007**, *43*, 4019.
(280) Zhang, H. W.; Fan, X. H.; Zhang, J.; Zhou, Z. T. *Solid State Ionics* **2008**, *179*, 1409.
(281) Zhang, G. W.; Zhou, Z. T. *J. Membr. Sci.* **2005**, *261*, 107.
(282) Zhang, Y.; Zhang, H. M.; Zhai, Y. F.; Zhu, X. B.; Bi, C. *J. Power Sources* **2007**, *168*, 323.
(283) Zhang, Y.; Zhang, H. M.; Bi, C.; Zhu, X. B. *Electrochim. Acta* **2008**, *53*, 4096.
(284) Carbone, A.; Pedicini, R.; Sacca, A.; Gatto, I.; Passalacqua, E. *J. Power Sources* **2008**, *178*, 661.
(285) Bello, M.; Zaidi, S. M. J.; Rahman, S. U. *J. Membr. Sci.* **2008**, *322*, 218.
(286) Mecheri, B.; D'Epifanio, A.; Traversa, E.; Licoccia, S. *J. Power Sources* **2008**, *178*, 554.
(287) Tripathi, B. P.; Kumar, M.; Shahi, V. K. *J. Membr. Sci.* **2009**, *327*, 145.
(288) Gao, Q. J.; Wang, Y. X.; Xu, L.; Wei, G. Q.; Wang, Z. T. *Chin. J. Chem. Eng* **2009**, *17*, 207.
(289) Pezzin, S. H.; Stock, N.; Shishatskiy, S.; Nunes, S. P. *J. Membr. Sci.* **2008**, *325*, 559.
(290) Othman, M. H. D.; Ismail, A. F.; Mustafa, A. *J. Membr. Sci.* **2007**, *299*, 156.
(291) Park, S. H.; Park, J. S.; Yim, S. D.; Park, S. H.; Lee, Y. M.; Kim, C. S. *J. Power Sources* **2008**, *181*, 259.
(292) Li, W.; Bellay, A.; Fu, Y. Z.; Manthiram, A. *J. Power Sources* **2008**, *180*, 719.
(293) Totsatitpaisan, P.; Nunes, S. P.; Tashiro, K.; Chirachanchai, S. *Solid State Ionics* **2009**, *180*, 738.
(294) Tripathi, B. P.; Shahi, V. K. *J. Colloid Interface Sci.* **2007**, *316*, 612.
(295) Kalappa, P.; Lee, J. H. *Polym. Int.* **2007**, *56*, 371.
(296) Norddin, M. N. A. M.; Ismail, A. F.; Rana, D.; Matsuura, T.; Mustafa, A.; Tabe-Mohammadi, A. *J. Membr. Sci.* **2008**, *323*, 404.
(297) Norddin, M. N. A. M.; Ismail, A. F.; Rana, D.; Matsuura, T.; Tabe, S. *J. Membr. Sci.* **2009**, *328*, 148.
(298) Sambandam, S.; Ramani, V. *J. Power Sources* **2007**, *170*, 259.
(299) Deb, P. C.; Rajput, L. D.; Hande, V. R.; Sasane, S.; Kumar, A. *Polym. Adv. Technol* **2007**, *18*, 419.
(300) Jang, I. Y.; Kweon, O. H.; Kim, K. E.; Hwang, G. J.; Moon, S. B.; Kang, A. S. *J. Power Sources* **2008**, *181*, 127.
(301) Wang, J. W.; Yue, Z. R.; Economy, J. *J. Membr. Sci.* **2007**, *291*, 210.
(302) Di Vona, M. L.; Ahmed, Z.; Bellitto, S.; Lenci, A.; Traversa, E.; Licoccia, S. *J. Membr. Sci.* **2007**, *296*, 156.
(303) Licoccia, S.; Di Vona, M. L.; D'Epifanio, A.; Ahmed, Z.; Bellitto, S.; Marani, D.; Mecheri, B.; de Bonis, C.; Trombetta, M.; Traversa, E. *J. Power Sources* **2007**, *167*, 79.
(304) Di Vona, M. L.; Marani, D.; D'Ottavi, C.; Trombetta, M.; Traversa, E.; Beurroies, I.; Knauth, P.; Licoccia, S. *Chem. Mater.* **2006**, *18*, 69.
(305) Di Vona, M. L.; Marani, D.; D'Epifanio, A.; Licoccia, S.; Beurroies, I.; Denoyel, R.; Knauth, P. *J. Membr. Sci.* **2007**, *304*, 76.
(306) Di Vona, M. L.; Licoccia, S.; Knauth, P. *Solid State Ionics* **2008**, *179*, 1161.
(307) Di Vona, M. L.; Sgreccia, E.; Licoccia, S.; Khadhraoui, M.; Denoyel, R.; Knauth, P. *Chem. Mater.* **2008**, *20*, 4327.
(308) Di Vona, M. L.; Luchetti, L.; Spera, G. P.; Sgreccia, E.; Knauth, P. *C. R. Chim.* **2008**, *11*, 1074.
(309) de Bonis, C.; D'Epifanio, A.; Di Vona, M. L.; D'Ottavi, C.; Mecheri, B.; Traversa, E.; Trombetta, M.; Licoccia, S. *Fuel Cells* **2009**, *9*, 387.
(310) Sgreccia, E.; Khadhraoui, M.; de Bonis, C.; Licoccia, S.; Di Vona, M. L.; Knauth, P. *J. Power Sources* **2008**, *178*, 667.
(311) Chen, J. H.; Maekawa, Y.; Asano, M.; Yoshida, M. *Polymer* **2007**, *48*, 6002.
(312) Hasegawa, S.; Suzuki, Y.; Maekawa, Y. *Radiat. Phys. Chem.* **2008**, *77*, 617.
(313) Chen, J.; Asano, M.; Maekawa, Y.; Yoshida, M. *J. Membr. Sci.* **2008**, *319*, 1.
(314) Chen, J. H.; Zhai, M. L.; Asano, M.; Huang, L.; Maekawa, Y. *J. Mater. Sci.* **2009**, *44*, 3674.
(315) Yang, T. *Int. J. Hydrogen Energy* **2008**, *33*, 6772.
(316) Yang, T. *J. Membr. Sci.* **2009**, *342*, 221.
(317) Carbone, A.; Sacca, A.; Gatto, I.; Pedicini, R.; Passalacqua, E. *Int. J. Hydrogen Energy* **2008**, *33*, 3153.
(318) Sengul, E.; Erdener, H.; Akay, R. G.; Yucel, H.; Bac, N.; Eroglu, I. *Int. J. Hydrogen Energy* **2009**, *34*, 4645.
(319) Kim, T. W.; Sahimi, M.; Tsotsis, T. T. *Ind. Eng. Chem. Res.* **2009**, *48*, 9504.
(320) Pasupathi, S.; Ji, S.; Bladergroen, B. J.; Linkov, V. *Int. J. Hydrogen Energy* **2008**, *33*, 3132.
(321) Liu, D.; Yates, M. Z. *J. Membr. Sci.* **2008**, *322*, 256.
(322) Bi, C.; Zhang, H. M.; Zhang, Y.; Xiao, S. H. *J. Power Sources* **2009**, *194*, 838.
(323) Gosalawit, R.; Chirachanchai, S.; Shishatskiy, S.; Nunes, S. P. *J. Membr. Sci.* **2008**, *323*, 337.
(324) Colicchio, I.; Wen, F.; Keul, H.; Simon, U.; Moeller, M. *J. Membr. Sci.* **2009**, *326*, 45.
(325) Ismail, A. F.; Othman, N. H.; Mustafa, A. *J. Membr. Sci.* **2009**, *329*, 18.
(326) Hande, V. R.; Rao, S.; Rath, S. K.; Thakur, A.; Patri, M. *J. Membr. Sci.* **2008**, *322*, 67.
(327) Xue, Y. H.; Fu, R. Q.; Wu, C. M.; Lee, J. Y.; Xu, T. W. *J. Membr. Sci.* **2010**, *350*, 148.
(328) Sisbandini, C.; Every, H. A.; Viale, S.; Mendes, E.; Picken, S. J. *J. Polym. Sci., Part B: Polym. Phys.* **2007**, *45*, 666.
(329) Zhong, S. L.; Cui, X. J.; Cai, H. L.; Fu, T. Z.; Shao, K.; Na, H. *J. Power Sources* **2007**, *168*, 154.
(330) Zhao, C. J.; Wang, Z.; Bi, D. W.; Lin, H. D.; Shao, K.; Fu, T. Z.; Zhong, S. L.; Na, H. *Polymer* **2007**, *48*, 3090.
(331) Cai, H. L.; Shao, K.; Zhong, S. L.; Zhao, C. J.; Zhang, G.; Li, X. F.; Na, H. *J. Membr. Sci.* **2007**, *297*, 162.
(332) Fu, T. Z.; Zhao, C. J.; Zhong, S. L.; Zhang, G.; Shao, K.; Zhang, H. Q.; Wang, J.; Na, H. *J. Power Sources* **2007**, *165*, 708.
(333) Zhang, H. Q.; Li, X. F.; Zhao, C. J.; Fu, T. Z.; Shi, Y. H.; Na, H. *J. Membr. Sci.* **2008**, *308*, 66.
(334) Choi, J.; Lee, K. M.; Wycisk, R.; Pintauro, P. N.; Mather, P. T. *Macromolecules* **2008**, *41*, 4569.
(335) Pisani, L. *J. Power Sources* **2009**, *194*, 451.
(336) Fu, Y. Z.; Li, W.; Manthiram, A. *J. Membr. Sci.* **2008**, *310*, 262.
(337) Parvole, J.; Jannasch, P. *Macromolecules* **2008**, *41*, 3893.
(338) Zhong, S. L.; Cui, X. J.; Cai, H. L.; Fu, T. Z.; Na, H. *J. Polym. Sci., Part B: Polym. Phys.* **2007**, *45*, 2871.

(339) Zhao, C.; Li, X.; Lin, H.; Shao, K.; Na, H. *J. Appl. Polym. Sci.* **2008**, *108*, 671.

(340) Zhong, S. L.; Cui, X. J.; Fu, T. Z.; Na, H. *J. Power Sources* **2008**, *180*, 23.

(341) Zhang, G.; Fu, T. Z.; Shao, K.; Li, X. F.; Zhao, C. J.; Na, H.; Zhang, H. *J. Power Sources* **2009**, *189*, 875.

(342) Fu, T. Z.; Wang, J.; Ni, J.; Cui, Z. M.; Zhong, S. L.; Zhao, C. J.; Na, H.; Xing, W. *Solid State Ionics* **2008**, *179*, 2265.

(343) Dou, Z. Y.; Zhong, S. G.; Zhao, C. J.; Li, X. F.; Fu, T. Z.; Na, H. *J. Appl. Polym. Sci.* **2008**, *109*, 1057.

(344) Fu, T. Z.; Cui, Z. M.; Zhong, S. L.; Shi, Y. H.; Zhao, C. J.; Zhang, G.; Shao, K.; Na, H.; Xing, W. *J. Power Sources* **2008**, *185*, 32.

(345) Fu, T. Z.; Zhong, S. L.; Cui, Z. M.; Zhao, C. J.; Shi, Y. H.; Yu, W. Z.; Na, H.; Xing, W. *J. Appl. Polym. Sci.* **2009**, *111*, 1335.

(346) Dai, H.; Guan, R.; Li, C. H.; Liu, J. H. *Solid State Ionics* **2007**, *178*, 339.

(347) Ekstrom, H.; Lafitte, B.; Ihonen, J.; Markusson, H.; Jacobsson, P.; Lundblad, A.; Jannasch, P.; Lindbergh, G. *Solid State Ionics* **2007**, *178*, 959.

(348) Xing, D. M.; Zhang, H. M.; Wang, L.; Zhai, Y. F.; Yi, B. L. *J. Membr. Sci.* **2007**, *296*, 9.

(349) Torras, C.; Zhang, X.; Garcia-Valls, R.; Benavente, J. *J. Membr. Sci.* **2007**, *297*, 130.

(350) Kim, D. H.; Choi, J.; Hong, Y. T.; Kim, S. C. *J. Membr. Sci.* **2007**, *299*, 19.

(351) Lee, C. H.; Min, K. A.; Park, H. B.; Hong, Y. T.; Jung, B. O.; Lee, Y. M. *J. Membr. Sci.* **2007**, *303*, 258.

(352) Joo, S. H.; Pak, C.; Kim, E. A.; Lee, Y. H.; Chang, H.; Seung, D.; Choi, Y. S.; Park, J. B.; Kim, T. K. *J. Power Sources* **2008**, *180*, 63.

(353) Lufrano, F.; Baglio, V.; Staiti, P.; Arico, A. S.; Antonucci, V. *J. Power Sources* **2008**, *179*, 34.

(354) Pedicini, R.; Carbone, A.; Sacca, A.; Gatto, I.; Di Marco, G.; Passalacqua, E. *Polym. Test.* **2008**, *27*, 248.

(355) Liang, C.; Nagami, C.; Maruyama, T.; Sotani, T.; Matsuyama, H. *J. Appl. Polym. Sci.* **2008**, *109*, 3739.

(356) Choi, Y. S.; Kim, T. K.; Kim, E. A.; Joo, S. H.; Pak, C.; Lee, Y. H.; Chang, H.; Seung, D. *Adv. Mater.* **2008**, *20*, 2341.

(357) Zhao, C. J.; Lin, H. D.; Cui, Z. M.; Li, X. F.; Na, H.; Xing, W. *J. Power Sources* **2009**, *194*, 168.

(358) Su, Y. H.; Liu, Y. L.; Wang, D. M.; Lai, J. Y.; Guiver, M. D.; Liu, B. J. *J. Power Sources* **2009**, *194*, 206.

(359) Roy, A.; Hickner, M. A.; Lane, O.; McGrath, J. E. *J. Power Sources* **2009**, *191*, 550.

(360) de Carvalho, L. M.; Tan, A. R.; Gomes, A. D. *J. Appl. Polym. Sci.* **2008**, *110*, 1690.

(361) Wang, Z.; Ni, H. Z.; Zhao, C. J.; Zhang, M. Y.; Na, H. *J. Appl. Polym. Sci.* **2009**, *112*, 858.

(362) Devrim, Y.; Erkan, S.; Bac, N.; Eroglu, I. *Int. J. Hydrogen Energy* **2009**, *34*, 3467.

(363) Zhang, N.; Li, J. J.; Wang, X. Y.; Xia, Z.; Liu, H. L. *J. Appl. Polym. Sci.* **2009**, *114*, 304.

(364) Hartmann-Thompson, C.; Merrington, A.; Carver, P. I.; Keeley, D. L.; Rousseau, J. L.; Hucul, D.; Bruza, K. J.; Thomas, L. S.; Keinath, S. E.; Nowak, R. M.; Katona, D. M.; Santurri, P. R. *J. Appl. Polym. Sci.* **2008**, *110*, 958.

(365) Wang, L.; Yi, B. L.; Zhang, H. M.; Xing, D. M. *Polym. Adv. Technol.* **2008**, *19*, 1809.

(366) Smitha, B.; Devi, D. A.; Sridhar, S. *Int. J. Hydrogen Energy* **2008**, *33*, 4138.

(367) Gasa, J. V.; Weiss, R. A.; Shaw, M. T. *J. Membr. Sci.* **2008**, *320*, 215.

(368) Krishnan, N. N.; Kim, H. J.; Jang, J. H.; Lee, S. Y.; Cho, E.; Oh, I. H.; Hong, S. A.; Lim, T. H. *J. Appl. Polym. Sci.* **2009**, *113*, 2499.

(369) Lawrence, J.; Yamaguchi, T. *J. Membr. Sci.* **2008**, *325*, 633.

(370) Gosalawit, R.; Chirachanchai, S.; Basile, A.; Iulianelli, A. *Desalination* **2009**, *235*, 293.

(371) Im, S. J.; Patel, R.; Shin, S. J.; Kim, J. H.; Min, B. R. *Korean J. Chem. Eng.* **2008**, *25*, 732.

(372) Krishnan, N. N.; Kim, H. J.; Jang, J. H.; Cho, E.; Lee, S. Y.; Lim, T. H.; Hong, S. A. *Polym. Bull.* **2009**, *62*, 457.

(373) Subbaraman, R.; Ghassemi, H.; Zawodzinski, T. *Solid State Ionics* **2009**, *180*, 1143.

(374) Roy, A.; Hickner, M. A.; Einsla, B. R.; Harrison, W. L.; Mcgrath, J. E. *J. Polym. Sci., Part A: Polym. Chem.* **2009**, *47*, 384.

(375) Yang, J.; Li, Y. X.; Roy, A.; McGrath, J. E. *Polymer* **2008**, *49*, 5300.

(376) Hasani-Sadrabadi, M. M.; Dashtimoghadam, E.; Ghaffarian, S. R.; Hasani Sadrabadi, M. H.; Heidari, M. M., H. *Renewable Energy* **2010**, *35*, 226.

(377) Choi, J.; Kim, D. H.; Kim, H. K.; Shin, C.; Kim, S. C. *J. Membr. Sci.* **2008**, *310*, 384.

(378) Zhang, Y. F.; Wang, S. J.; Xiao, M.; Bian, S. G.; Meng, Y. Z. *Int. J. Hydrogen Energy* **2009**, *34*, 4379.

(379) Wang, Z.; Ni, H. Z.; Zhang, M. Y.; Zhao, C. J.; Na, H. *Desalination* **2009**, *242*, 236.

(380) Zhu, Z.; Walsby, N. M.; Colquhoun, H. M.; Thompsett, D.; Petrucco, E. *Fuel Cells* **2009**, *9*, 305.

(381) Bae, B.; Miyatake, K.; Watanabe, M. *Macromolecules* **2009**, *42*, 1873.

(382) Bae, B.; Miyatake, K.; Watanabe, M. *J. Membr. Sci.* **2008**, *310*, 110.

(383) Tian, S. H.; Shu, D.; Wang, S. J.; Xiao, M.; Meng, Y. Z. *J. Power Sources* **2010**, *195*, 97.

(384) Kim, D. S.; Kim, Y. S.; Guiver, M. D.; Pivovar, B. S. *J. Membr. Sci.* **2008**, *321*, 199.

(385) Xu, T.; Woo, J. J.; Seo, S. J.; Moon, S. H. *J. Membr. Sci.* **2008**, *325*, 209.

(386) Wu, D.; Wu, L.; Woo, J. J.; Yun, S. H.; Seo, S. J.; Xu, T. W.; Moon, S. H. *J. Membr. Sci.* **2010**, *348*, 167.

(387) Xu, T. W.; Wu, D.; Wu, L. *Prog. Polym. Sci.* **2008**, *33*, 894.

(388) Woo, J. J.; Seo, S. J.; Yun, S. H.; Xu, T. W.; Lee, J.; Moon, S. H. *Electrochem. Commun.* **2010**, *12*, 148.

(389) Liu, Y. F.; Yu, Q. C.; Wu, Y. H. *Electrochim. Acta* **2007**, *52*, 8133.

(390) Argun, A. A.; Ashcraft, J. N.; Hammond, P. T. *Adv. Mater.* **2008**, *20*, 1539.

(391) Wu, D.; Xu, T. W.; Wu, L.; Wu, Y. H. *J. Power Sources* **2009**, *186*, 286.

(392) Jeong, Y. G.; Seo, D. W.; Lim, Y. D.; Jin, H. M.; Mollah, M. S. I.; Ur, S. C.; Pyun, S. Y.; Kim, W. G. *Electrochim. Acta* **2010**, *55*, 1425.

(393) Hasani-Sadrabadi, M. M.; Emami, S. H.; Moaddel, H. *J. Power Sources* **2008**, *183*, 551.

(394) Fu, R. Q.; Julius, D.; Hong, L.; Lee, J. Y. *J. Membr. Sci.* **2008**, *322*, 331.

(395) Schonberger, F.; Hein, M.; Kerres, J. *Solid State Ionics* **2007**, *178*, 547.

(396) Hong, Y. T.; Lee, C. H.; Park, H. N. S.; Min, K. A.; Kim, H. J.; Nam, S. Y.; Lee, Y. M. *J. Power Sources* **2008**, *175*, 724.

(397) Guo, M. M.; Liu, B. J.; Liu, Z.; Wang, L. F.; Jiang, Z. H. *J. Power Sources* **2009**, *189*, 894.

(398) Lin, H. D.; Zhao, C. J.; Cui, Z. M.; Ma, W. J.; Fu, T. Z.; Na, H.; Xing, W. *J. Power Sources* **2009**, *193*, 507.

(399) Zhang, Y.; Shao, K.; Zhao, C. J.; Zhang, G.; Li, H. T.; Fu, T. Z.; Na, H. *J. Power Sources* **2009**, *194*, 175.

(400) Peron, J.; Ruiz, E.; Jones, D. J.; Roziere, J. *J. Membr. Sci.* **2008**, *314*, 247.

(401) Qi, Y. H.; Gao, Y.; Tian, S. H.; Hlil, A. R.; Gaudet, J.; Guay, D.; Hay, A. S. *J. Polym. Sci., Part A: Polym. Chem.* **2009**, *47*, 1920.

(402) Li, N. W.; Zhang, S. B.; Liu, J.; Zhang, F. *Macromolecules* **2008**, *41*, 4165.

(403) Li, N. W.; Cui, Z. M.; Li, S. H.; Zhang, S. B.; Xing, W. *J. Membr. Sci.* **2009**, *326*, 420.

(404) Li, N. W.; Li, S. H.; Zhang, S. B.; Wang, J. H. *J. Power Sources* **2009**, *187*, 67.

(405) Wang, J. H.; Li, N. W.; Cui, Z. M.; Zhang, S. B.; Xing, W. *J. Membr. Sci.* **2009**, *341*, 155.

(406) Ding, F. C.; Wang, S. J.; Xiao, M.; Li, X. H.; Meng, Y. Z. *J. Power Sources* **2007**, *170*, 20.
(407) Zhong, S. L.; Liu, C. G.; Na, H. *J. Membr. Sci.* **2009**, *326*, 400.
(408) Feng, S. G.; Shang, Y. M.; Xie, X. F.; Wang, Y. Z.; Xu, J. M. *J. Membr. Sci.* **2009**, *335*, 13.
(409) Ishikawa, J. I.; Fujiyama, S.; Inoue, K.; Omi, T.; Tamai, S. *J. Membr. Sci.* **2007**, *298*, 48.
(410) Park, S. D.; Chang, Y. J.; Jung, J. C.; Lee, W.; Chang, H.; Kim, H. *Macromol. Symp.* **2007**, *249*, 202.
(411) Oh, Y. S.; Lee, H. J.; Yoo, M.; Kim, H. J.; Han, J.; Kim, T. H. *J. Membr. Sci.* **2008**, *323*, 309.
(412) Heo, K. B.; Lee, H. J.; Kim, H. J.; Kim, B. S.; Lee, S. Y.; Cho, E.; Oh, I. H.; Hong, S. A.; Lim, T. H. *J. Power Sources* **2007**, *172*, 215.
(413) Tsai, J. C.; Kuo, J. F.; Chen, C. Y. *J. Power Sources* **2007**, *174*, 103.
(414) Kwon, Y. H.; Kim, S. C.; Lee, S. Y. *Macromolecules* **2009**, *42*, 5244.
(415) Jeong, M. H.; Lee, K. S.; Lee, J. S. *J. Membr. Sci.* **2009**, *337*, 145.
(416) Yu, J. J.; Dong, C.; Liu, J. H.; Li, C. H.; Fang, J. H.; Guan, R. *J. Mater. Sci.* **2010**, *45*, 1017.
(417) Wu, D.; Fu, R. Q.; Xu, T. W.; Wu, L.; Yang, W. H. *J. Membr. Sci.* **2008**, *310*, 522.
(418) Shang, X. Y.; Fang, S. M.; Meng, Y. Z. *J. Membr. Sci.* **2007**, *297*, 90.
(419) Miyatake, K.; Chikashige, Y.; Higuchi, E.; Watanabe, M. *J. Am. Chem. Soc.* **2007**, *129*, 3879.
(420) Shimura, T.; Miyatake, K.; Watanabe, M. *Eur. Polym. J.* **2008**, *44*, 4054.
(421) Jeong, M. H.; Lee, K. S.; Hong, Y. T.; Lee, J. S. *J. Membr. Sci.* **2008**, *314*, 212.
(422) Matsumoto, K.; Higashihara, T.; Ueda, M. *J. Polym. Sci., Part A: Polym. Chem.* **2009**, *47*, 3444.
(423) Pang, J. H.; Zhang, H. B.; Li, X. F.; Jiang, Z. H. *Macromolecules* **2007**, *40*, 9435.
(424) Lafitte, B.; Jannasch, P. *Adv. Funct. Mater.* **2007**, *17*, 2823.
(425) Kim, D. S.; Robertson, G. P.; Guiver, M. D. *Macromolecules* **2008**, *41*, 2126.
(426) Nakabayashi, K.; Matsumoto, K.; Shibasaki, Y.; Ueda, M. *Polymer* **2007**, *48*, 5878.
(427) Kim, D. S.; Kim, Y. S.; Guiver, M. D.; Ding, J. F.; Pivovar, B. S. *J. Power Sources* **2008**, *182*, 100.
(428) Patel, R.; Im, S. J.; Ko, Y. T.; Kim, J. H.; Min, B. R. *J. Ind. Eng. Chem.* **2009**, *15*, 299.
(429) Pang, J. H.; Zhang, H. B.; Li, X. F.; Ren, D. F.; Jiang, Z. H. *Macromol. Rapid Commun.* **2007**, *28*, 2332.
(430) Pang, J. H.; Zhang, H. B.; Li, X. F.; Liu, B. J.; Jiang, Z. H. *J. Power Sources* **2008**, *184*, 1.
(431) Pang, J. H.; Zhang, H. B.; Li, X. F.; Wang, L. F.; Liu, B. J.; Jiang, Z. H. *J. Membr. Sci.* **2008**, *318*, 271.
(432) Grunzinger, S. J.; Watanabe, M.; Fukagawa, K.; Kikuchi, R.; Tominaga, Y.; Hayakawa, T.; Kakimoto, M. A. *J. Power Sources* **2008**, *175*, 120.
(433) Matsumura, S.; Hlil, A. R.; Lepiller, C.; Gaudet, J.; Guay, D.; Shi, Z. Q.; Holdcroft, S.; Hay, A. S. *Macromolecules* **2008**, *41*, 281.
(434) Matsumura, S.; Hlil, A. R.; Lepiller, C.; Gaudet, J.; Guay, D.; Hay, A. S. *Macromolecules* **2008**, *41*, 277.
(435) Park, H. S.; Seo, D. W.; Choi, S. W.; Jeong, Y. G.; Lee, J. H.; Il Kim, D.; Kim, W. G. *J. Polym. Sci., Part A: Polym. Chem.* **2008**, *46*, 1792.
(436) Yang, Z. W.; Coutinho, D. H.; Sulfstede, R.; Balkus, K. J.; Ferraris, J. R. *J. Membr. Sci.* **2008**, *313*, 86.
(437) Chaung, C. N.; Chao, L.; Huang, Y. J.; Hsieh, T. H.; Chuang, H. Y.; Lin, S. C.; Ho, K. S. *J. Appl. Polym. Sci.* **2008**, *107*, 3917.
(438) Kim, D. J.; Chang, B. J.; Kim, J. H.; Lee, S. B.; Joo, H. J. *J. Membr. Sci.* **2008**, *325*, 217.
(439) Kim, D. S.; Robertson, G. P.; Kim, Y. S.; Guiver, M. D. *Macromolecules* **2009**, *42*, 957.
(440) Sankir, M.; Kim, Y. S.; Pivovar, B. S.; McGrath, J. E. *J. Membr. Sci.* **2007**, *299*, 8.
(441) Arnett, N. Y.; Harrison, W. L.; Adami, A. S. B.; Roy, A.; Lane, O.; Cromer, F.; Dong, L.; McGrath, J. E. *J. Power Sources* **2007**, *172*, 20.
(442) Zhu, L. P.; Dong, H. B.; Wei, X. Z.; Yi, Z.; Zhu, B. K.; Xu, Y. Y. *J. Membr. Sci.* **2008**, *320*, 407.
(443) Wang, S. J.; Meng, Y. Z.; Hlil, A. R.; Hay, A. S. *Macromolecules* **2004**, *37*, 60.
(444) Shen, L. P.; Xiao, G. Y.; Yan, D. Y.; Sun, G. M.; Zhu, P. F.; Na, Z. *Polym. Bull.* **2005**, *54*, 57.
(445) Kim, D. S.; Guiver, M. D. *J. Polym. Sci., Part A: Polym. Chem.* **2008**, *46*, 989.
(446) Su, Y. H.; Liu, Y. L.; Sun, Y. M.; Lai, J. Y.; Wang, D. M.; Gao, Y.; Liu, B. J.; Guiver, M. D. *J. Membr. Sci.* **2007**, *296*, 21.
(447) Gu, S.; He, G. H.; Wu, X. M.; Guo, Y. J.; Liu, H. J.; Peng, L.; Xiao, G. K. *J. Membr. Sci.* **2008**, *312*, 48.
(448) Zhu, X. L.; Liang, Y. F.; Pan, H. Y.; Jian, X. G.; Zhang, Y. X. *J. Membr. Sci.* **2008**, *312*, 59.
(449) Yildirim, M. H.; Schwarz, A.; Stamatialis, D. F.; Wessling, M. *J. Membr. Sci.* **2009**, *328*, 127.
(450) Zhang, H. W.; Zhou, Z. T. *Solid State Ionics* **2008**, *179*, 1296.
(451) Liang, Y. F.; Zhu, X. L.; Jian, X. G. *Solid State Ionics* **2008**, *179*, 1940.
(452) Li, J. H.; Yu, H. Y. *J. Polym. Sci., Part A: Polym. Chem.* **2007**, *45*, 2273.
(453) Tan, N.; Xiao, G. Y.; Yan, D. Y. *Polym. Bull.* **2009**, *62*, 593.
(454) Gomes, D.; Marschall, R.; Nunes, S. P.; Wark, M. *J. Membr. Sci.* **2008**, *322*, 406.
(455) Gomes, D.; Roeder, J.; Ponce, M. L.; Nunes, S. P. *J. Power Sources* **2008**, *175*, 49.
(456) Gomes, D.; Nunes, S. P. *J. Membr. Sci.* **2008**, *321*, 114.
(457) Roeder, J.; Gomes, D.; Ponce, M. L.; Abetz, V.; Nunes, S. P. *Macromol. Chem. Phys.* **2007**, *208*, 467.
(458) Ponce, M. L.; Gomes, D.; Nunes, S. P. *J. Membr. Sci.* **2008**, *319*, 14.
(459) Ponce, M. L.; Boaventura, M.; Gomes, D.; Mendes, A.; Madeira, L. M.; Nunes, S. P. *Fuel Cells* **2008**, *8*, 209.
(460) Pefkianakis, E. K.; Morfopoulou, C.; Deimede, V.; Kallitsis, J. K. *Macromol. Symp.* **2009**, *279*, 183.
(461) Gourdoupi, N.; Papadimitriou, K.; Neophytides, S.; Kallitsis, J. K. *Fuel Cells* **2008**, *8*, 200.
(462) Gourdoupi, N.; Kallitsis, J. K.; Neophytides, S. *J. Power Sources* **2010**, *195*, 170.
(463) Geormezit, M.; Deimede, V.; Gourdoupi, N.; Triantafyllopoulos, N.; Neophytides, S.; Kaitsis, J. K. *Macromolecules* **2008**, *41*, 9051.
(464) Schauer, J.; Kudela, V.; Richau, K.; Mohr, R. *Desalination* **2006**, *198*, 256.
(465) Garanin, E. M.; Towers, M. S.; Toothaker, P. W.; Laali, K.; Tolmachev, Y. V. *Polym. Bull.* **2010**, *64*, 595.
(466) Yoonessi, M.; Bai, Z. W.; Dang, T. D. *J. Polym. Sci., Part B: Polym. Phys.* **2007**, *45*, 2813.
(467) Bai, Z. W.; Houtz, M. D.; Mirau, P. A.; Dang, T. D. *Polymer* **2007**, *48*, 6598.
(468) Khalfan, A. N.; Sanchez, L. M.; Kodiweera, C.; Greenbaum, S. G.; Bai, Z. W.; Dang, T. D. *J. Power Sources* **2007**, *173*, 853.
(469) Dai, H.; Zhang, H. M.; Luo, Q. T.; Zhang, Y.; Bi, C. *J. Power Sources* **2008**, *185*, 19.
(470) Lee, J. K.; Kerres, J. *J. Membr. Sci.* **2007**, *294*, 75.
(471) Bai, Z. W.; Price, G. E.; Yoonessi, M.; Juhl, S. B.; Durstock, M. F.; Dang, T. D. *J. Membr. Sci.* **2007**, *305*, 69.
(472) Zhang, C.; Guo, X. X.; Fang, J. H.; Xu, H. J.; Yuan, M. Q.; Chen, B. W. *J. Power Sources* **2007**, *170*, 42.
(473) Xu, N.; Guo, X.; Fang, J.; Yin, J.; Yuan, M.; Chen, B. *Fuel Cells* **2009**, *9*, 363.
(474) Phu, D. S.; Lee, C. H.; Park, C. H.; Lee, S. Y.; Lee, Y. M. *Macromol. Rapid Commun.* **2009**, *30*, 64.

(475) Ma, X. H.; Zhang, C. J.; Xiao, G. Y.; Yan, D. Y. *J. Power Sources* **2009**, *188*, 57.

(476) Ma, X. H.; Shen, L. P.; Zhang, C. J.; Xiao, G. Y.; Yan, D. Y.; Sun, G. M. *J. Membr. Sci.* **2008**, *310*, 303.

(477) Ma, X. H.; Zhang, C. J.; Xiao, G. Y.; Yan, D. Y.; Sun, G. M. *J. Polym. Sci., Part A: Polym. Chem.* **2008**, *46*, 1758.

(478) Park, M. J.; Nedoma, A. J.; Geissler, P. L.; Balsara, N. P.; Jackson, A.; Cookson, D. *Macromolecules* **2008**, *41*, 2271.

(479) Markova, D.; Kumar, A.; Klapper, M.; Mullen, K. *Polymer* **2009**, *50*, 3411.

(480) Takamuku, S.; Akizuki, K.; Abe, M.; Kanesaka, H. *J. Polym. Sci., Part A: Polym. Chem.* **2009**, *47*, 700.

(481) Kalapos, T. L.; Decker, B.; Every, H. A.; Ghassemi, H.; Zawodzinski, T. A. *J. Power Sources* **2007**, *172*, 14.

(482) Schonberger, F.; Kerres, J. *J. Polym. Sci., Part A: Polym. Chem.* **2007**, *45*, 5237.

(483) Roy, A.; Lee, H. S.; McGrath, J. E. *Polymer* **2008**, *49*, 5037.

(484) Lee, H. S.; Badami, A. S.; Roy, A.; Mcgrath, J. E. *J. Polym. Sci., Part A: Polym. Chem.* **2007**, *45*, 4879.

(485) Bae, B.; Miyatake, K.; Watanabe, M. *ACS Appl. Mater. Interfaces* **2009**, *1*, 1279.

(486) Li, Y. X.; Roy, A.; Badami, A. S.; Hill, M.; Yang, J.; Dunn, S.; McGrath, J. E. *J. Power Sources* **2007**, *172*, 30.

(487) Lee, H. S.; Roy, A.; Lane, O.; Dunn, S.; McGrath, J. E. *Polymer* **2008**, *49*, 715.

(488) Nakabayashi, K.; Matsumoto, K.; Higashihara, T.; Ueda, M. *J. Polym. Sci., Part A: Polym. Chem.* **2008**, *46*, 7332.

(489) Nakabayashi, K.; Matsumoto, K.; Ueda, M. *J. Polym. Sci., Part A: Polym. Chem.* **2008**, *46*, 3947.

(490) Takimoto, N.; Takamuku, S.; Abe, M.; Ohira, A.; Lee, H. S.; McGrath, J. E. *J. Power Sources* **2009**, *194*, 662.

(491) Yu, X.; Roy, A.; Dunn, S.; Badami, A. S.; Yang, J.; Good, A. S.; Mcgrath, J. E. *J. Polym. Sci., Part A: Polym. Chem*, **2009**, *47*, 1038.

(492) Yu, X.; Roy, A.; Dunn, S.; Yang, J.; McGrath, J. E. *Macromol. Symp.* **2006**, *245*, 439.

(493) Yamaguchi, T.; Zhou, H.; Nakazawa, S.; Hara, N. *Adv. Mater.* **2007**, *19*, 592.

(494) Hara, N.; Ohashi, H.; Ito, T.; Yamaguchi, T. *J. Phys. Chem. B* **2009**, *113*, 4656.

(495) Norris, B. C.; Li, W.; Lee, E.; Manthiram, A.; Bielawski, C. W. *Polymer* **2010**, *51*, 5352.

(496) Li, H. T.; Zhang, G.; Wu, J.; Zhao, C. J.; Zhang, Y.; Shao, K.; Han, M. M.; Lin, H. D.; Zhu, J.; Na, H. *J. Power Sources* **2010**, *195*, 6443.

(497) Kerres, J. A. *Fuel Cells* **2005**, *5*, 230.

(498) Garland, N. L.; Kopasz, J. P. *J. Power Sources* **2007**, *172*, 94.

(499) Galatanu, A. N.; Rollet, A. L.; Porion, P.; Diat, O.; Gebel, G. *J. Phys. Chem. B* **2005**, *109*, 11332.

(500) Marestin, C.; Gebel, G.; Diat, O.; Mercier, R. *Fuel Cells II* **2008**, *216*, 185.

(501) Hu, Z. X.; Ogou, T.; Yoshino, M.; Yamada, O.; Kita, H.; Okamoto, K. I. *J. Power Sources* **2009**, *194*, 674.

(502) Jo, T. S.; Ozawa, C. H.; Eagar, B. R.; Brownell, L. V.; Han, D. Y.; Bae, C. *J. Polym. Sci., Part A: Polym. Chem.* **2009**, *47*, 485.

(503) Chen, S. W.; Yin, Y.; Kita, H.; Okamoto, K. I. *J. Polym. Sci., Part A: Polym. Chem.* **2007**, *45*, 2797.

(504) Deligoz, H.; Vantansever, S.; Koc, S. N.; Oksuzomer, F.; Oezgumus, S.; Gurkaynak, M. A. *J. Appl. Polym. Sci.* **2008**, *110*, 1216.

(505) Guo, X. X.; Zhai, F. X.; Fang, J. H.; Laguna, M. F.; Lopez-Gonzalez, M.; Riande, E. *J. Phys. Chem. B* **2007**, *111*, 13694.

(506) Chen, X. B.; Chen, P.; Okamoto, K. *Polym. Bull.* **2009**, *63*, 1.

(507) Yin, Y.; Yamada, O.; Hayashi, S.; Tanaka, K.; Kita, H.; Okamoto, K. I. *J. Polym. Sci., Part A: Polym. Chem.* **2006**, *44*, 3751.

(508) Higuchi, E.; Asano, N.; Miyatake, K.; Uchida, H.; Watanabe, M. *Electrochim. Acta* **2007**, *52*, 5272.

(509) Shu, Y. C.; Chuang, F. S.; Tsen, W. C.; Chow, J. D.; Gong, C. L.; Wen, S. *J. Appl. Polym. Sci.* **2008**, *107*, 2963.

(510) Shu, Y. C.; Chuang, F. S.; Tsen, W. C.; Chow, J. D.; Gong, C.; Wen, S. *J. Appl. Polym. Sci.* **2008**, *108*, 1783.

(511) Jang, W.; Choi, S.; Lee, S.; Shul, Y.; Han, H. *Polym. Degrad. Stab.* **2007**, *92*, 1289.

(512) Alcaide, F.; Alvarez, G.; Ganborena, L.; Iruin, J. J.; Miguel, O.; Blazquez, J. A. *Polym. Bull.* **2009**, *62*, 813.

(513) Nguyen, T. H.; Wang, X. *Sep. Purif. Technol.* **2009**, *67*, 208.

(514) Tadanaga, K.; Michiwaki, Y.; Tezuka, T.; Hayashi, A.; Tatsumisago, M. *J. Membr. Sci.* **2008**, *324*, 188.

(515) Li, D.; Zhu, H. Y.; Ratinac, K. R.; Ringer, S. P.; Wang, H. T. *Microporous Mesoporous Mater.* **2009**, *126*, 14.

(516) Wang, L.; Yi, B. L.; Zhang, H. M.; Xing, D. M. *J. Phys. Chem. B* **2008**, *112*, 4270.

(517) Seo, J.; Jang, W.; Lee, S.; Han, H. *Polym. Degrad. Stab.* **2008**, *93*, 298.

(518) Lee, C. H.; Wang, Y. Z. *J. Polym. Sci., Part A: Polym. Chem*, **2008**, *46*, 2262.

(519) Loredo, D. E. S.; Paredes, M. L.; Sena, M. E. *Mater. Lett.* **2008**, *62*, 3319.

(520) Wang, J. L.; Lee, M. H.; Yang, J. *Polym. Bull.* **2005**, *55*, 357.

(521) Deligoz, H.; Vatansever, S.; Oeksuezoemer, F.; Koc, S. N.; Ozgumus, S.; Guerkaynak, M. A. *Polym. Adv. Technol.* **2008**, *19*, 1126.

(522) Bai, H.; Ho, W. S. W. *J. Membr. Sci.* **2008**, *313*, 75.

(523) Miyatake, K.; Yasuda, T.; Watanabe, M. *J. Polym. Sci., Part A: Polym. Chem.* **2008**, *46*, 4469.

(524) Li, Y. H.; Jin, R. Z.; Cui, Z. M.; Wang, Z.; Xing, W.; Qiu, X. P.; Ji, X. L.; Gao, L. X. *Polymer* **2007**, *48*, 2280.

(525) Hu, Z. X.; Yin, Y.; Okamoto, K.; Moriyama, Y.; Morikawa, A. *J. Membr. Sci.* **2009**, *329*, 146.

(526) Hu, Z. X.; Yin, Y.; Kita, H.; Okamoto, K. I.; Suto, Y.; Wang, H. G.; Kawasato, H. *Polymer* **2007**, *48*, 1962.

(527) Lee, C. H.; Park, C. H.; Lee, Y. M. *J. Membr. Sci.* **2008**, *313*, 199.

(528) Aoki, M.; Asano, N.; Miyatake, K.; Uchida, H.; Watanabe, M. *J. Electrochem. Soc.* **2006**, *153*, A1154.

(529) Sutou, Y.; Yin, Y.; Hu, Z.; Chen, S.; Kita, H.; Okamoto, K.; Wang, H.; Kawasato, H. *J. Polym. Sci., Part A: Polym. Chem.* **2009**, *47*, 1463.

(530) Savard, O.; Peckham, T. J.; Yang, Y.; Holdcroft, S. *Polymer* **2008**, *49*, 4949.

(531) Pan, H. Y.; Liang, Y. F.; Zhu, X. L.; Jian, X. G. *Chin. Chem. Lett.* **2007**, *18*, 1148.

(532) Zhu, X. L.; Pan, H. Y.; Liang, Y. F.; Jian, X. G. *Eur. Polym. J.* **2008**, *44*, 3782.

(533) Rabiee, A.; Mehdipour-Ataei, S.; Banihashemi, A.; Yeganeh, H. *Polym. Adv. Technol.* **2008**, *19*, 361.

(534) Kabasawa, A.; Saito, J.; Yano, H.; Miyatake, K.; Uchida, H.; Watanabe, M. *Electrochim. Acta* **2009**, *54*, 1076.

(535) Saito, J.; Miyatake, K.; Watanabe, M. *Macromolecules* **2008**, *41*, 2415.

(536) Alvarez-Gallego, Y.; Ruffmann, B.; Silva, V.; Silva, H.; Lozano, A. E.; de la Carnpa, J. G.; Nunes, S. P.; de Abajo, J. *Polymer* **2008**, *49*, 3875.

(537) Zhai, F. X.; Guo, X. X.; Fang, J. H.; Xu, H. J. *J. Membr. Sci.* **2007**, *296*, 102.

(538) Hu, Z. X.; Yin, Y.; Yaguchi, K.; Endo, N.; Higa, M.; Okamoto, K. I. *Polymer* **2009**, *50*, 2933.

(539) Yan, J. L.; Liu, C. P.; Wang, Z.; Xing, W.; Ding, M. M. *Polymer* **2007**, *48*, 6210.

(540) Li, N. W.; Cui, Z. M.; Zhang, S. B.; Li, S. H.; Zhang, F. *J. Power Sources* **2007**, *172*, 511.

(541) Zhang, F.; Li, N. W.; Cui, Z. M.; Zhang, S. B.; Li, S. H. *J. Membr. Sci.* **2008**, *314*, 24.

(542) Li, N. W.; Cui, Z. M.; Zhang, S. B.; Xing, W. *Polymer* **2007**, *48*, 7255.

(543) Chen, X. B.; Yin, Y.; Chen, P.; Kita, H.; Okamoto, K. I. *J. Membr. Sci.* **2008**, *313*, 106.

(544) Chen, X. B.; Chen, P.; Okamoto, K. I. *J. Appl. Polym. Sci.* **2009**, *112*, 3560.

(545) Li, W. M.; Cui, Z. M.; Zhou, X. C.; Zhang, S. B.; Dai, L.; Xing, W. *J. Membr. Sci.* **2008**, *315*, 172.

(546) Zhang, F.; Cui, Z. M.; Li, N. W.; Dai, L.; Zhang, S. B. *Polymer* **2008**, *49*, 3272.

(547) Qiu, Z. M.; Wu, S. Q.; Li, Z.; Zhang, S. B.; Xing, W.; Liu, C. P. *Macromolecules* **2006**, *39*, 6425.

(548) Cakir, M.; Karatas, S.; Menceloglu, Y.; Kayaman-Apohan, N.; Gungor, A. *Macromol. Chem. Phys.* **2008**, *209*, 919.

(549) Deligoz, H.; Vatansever, S.; Oksuzomer, F.; Koc, S. N.; Ozgumus, S.; Gurkaynak, M. A. *Polym. Adv. Technol* **2008**, *19*, 1792.

(550) Yamazaki, K.; Kawakami, H. *Macromolecules* **2010**, *43*, 7185.

(551) Fernandez-Carretero, F. J.; Compan, V.; Riande, E. *J. Power Sources* **2007**, *173*, 68.

(552) Kim, S. G.; Ahn, H. R.; Min, D. Y.; Nam, S. E.; Lee, K. H. *Macromol. Symp.* **2007**, *249*, 190.

(553) Kuo, P. L.; Liang, W. J.; Hsu, C. Y.; Jheng, W. H. *Polymer* **2008**, *49*, 1792.

(554) Dai, C. A.; Liu, C. P.; Lee, Y. H.; Chang, C. J.; Chao, C. Y.; Cheng, Y. Y. *J. Power Sources* **2008**, *177*, 262.

(555) Park, T. J.; Kim, S. H.; Li, G. H.; Cho, C. G.; Kim, Y. *Macromol. Symp.* **2007**, *249*, 466.

(556) El Sayed, A. M. *J. Appl. Polym. Sci.* **2007**, *104*, 3804.

(557) Navarro, A.; del Rio, C.; Acosta, J. L. *J. Membr. Sci.* **2007**, *300*, 79.

(558) Suleiman, D.; Napadensky, E.; Sloan, J. M.; Crawford, D. M. *Thermochim. Acta* **2007**, *460*, 35.

(559) Gromadzki, D.; Lokaj, J.; Cernoch, P.; Diat, O.; Nallet, F.; Stepanek, P. *Eur. Polym. J.* **2008**, *44*, 189.

(560) Saga, S.; Matsumoto, H.; Saito, K.; Minagawa, M.; Tanioka, A. *J. Power Sources* **2008**, *176*, 16.

(561) Kato, M.; Sakamoto, W.; Yogo, T. *J. Membr. Sci.* **2007**, *303*, 43.

(562) Kato, M.; Sakamoto, W.; Yogo, T. *J. Membr. Sci.* **2008**, *311*, 182.

(563) Saxena, A.; Tripathi, B. P.; Shahi, V. K. *J. Phys. Chem. B* **2007**, *111*, 12454.

(564) Fu, R. Q.; Woo, J. J.; Seo, S. J.; Lee, J. S.; Moon, S. H. *J. Power Sources* **2008**, *179*, 458.

(565) Fu, R. Q.; Woo, J. J.; Seo, S. J.; Lee, J. S.; Moon, S. H. *J. Membr. Sci.* **2008**, *309*, 156.

(566) Goktepe, F.; Bozkurt, A.; Gunday, S. T. *Polym. Int.* **2008**, *57*, 133.

(567) Itoh, T.; Hirai, K.; Tamura, M.; Uno, T.; Kubo, M.; Aihara, Y. *J. Power Sources* **2008**, *178*, 627.

(568) Caracino, P.; Ballabio, O.; Colombo, M.; Sala, E.; Cavallo, G.; Faucitano, A.; Buttafava, A.; Dondi, D. *Int. J. Hydrogen Energy* **2009**, *34*, 4653.

(569) Choi, J. K.; Lee, D. K.; Kim, Y. W.; Min, B. R.; Kim, J. H. *J. Polym. Sci., Part B: Polym. Physs* **2008**, *46*, 691.

(570) Park, M. J.; Downing, K. H.; Jackson, A.; Gomez, E. D.; Minor, A. M.; Cookson, D.; Weber, A. Z.; Balsara, N. P. *Nano Lett.* **2007**, *7*, 3547.

(571) Park, M. J.; Kim, S.; Minor, A. M.; Hexemer, A.; Bolsara, N. P. *Adv. Mater.* **2009**, *21*, 203.

(572) Mokrini, A.; Huneault, M. A.; Shi, Z. Q.; Xie, Z.; Holdcroft, S. *J. Membr. Sci.* **2008**, *325*, 749.

(573) Silva, A. L. A.; Takase, I.; Pereira, R. P.; Rocco, A. M. *Eur. Polym. J.* **2008**, *44*, 1462.

(574) Navarro, A.; del Rio, C.; Acosta, J. L. *J. Polym. Sci., Part B: Polym. Phys.* **2008**, *46*, 1684.

(575) Escribano, P. G.; Canovas, M. J.; Ojeda, M. C.; Del Rio, C.; Sanchez, F.; Acosta, J. L. *J. Polym. Sci., Part B: Polym. Phys.* **2009**, *47*, 1203.

(576) Hwang, H. Y.; Koh, H. C.; Rhim, J. W.; Nam, S. Y. *Desalination* **2008**, *233*, 173.

(577) Lee, D. K.; Lee, K. J.; Kim, Y. W.; Kim, J. H. *Desalination* **2008**, *233*, 104.

(578) Vuillaume, P. Y.; Mokrini, A.; Siu, A.; Theberge, K.; Robitaille, L. *Eur. Polym. J.* **2009**, *45*, 1641.

(579) Pu, H. T.; Ye, S.; Wan, D. C. *Electrochim. Acta* **2007**, *52*, 5879.

(580) Woudenberg, R. C.; Yavuzeetin, O.; Tuorninen, M. T.; Coughlin, E. B. *Solid State Ionics* **2007**, *178*, 1135.

(581) Park, J. K.; Kang, Y. S.; Won, J. *J. Membr. Sci.* **2008**, *313*, 217.

(582) Shaplov, A. S.; Lozinskaya, E. I.; Odinets, I. L.; Lyssenko, K. A.; Kurtova, S. A.; Timofeeva, G. I.; Iojolu, C.; Sanchez, J. Y.; Abadie, M. J. M.; Voytekunas, V. Y.; Vygodskii, Y. S. *React. Funct. Polym.* **2008**, *68*, 208.

(583) Celik, S. U.; Bozkurt, A. *Eur. Polym. J.* **2008**, *44*, 213.

(584) Yang, Z. W.; Coutinho, D. H.; Yang, D. J.; Balkus, K. J.; Ferraris, J. P. *J. Membr. Sci.* **2008**, *313*, 91.

(585) Lavorgna, M.; Fusco, L.; Piscitelli, F.; Mensitieri, G.; Agoretti, P.; Borriello, A.; Mascia, L. *Polym. Eng. Sci.* **2008**, *48*, 2389.

(586) Celik, S. U.; Aslan, A.; Bozkurt, A. *Solid State Ionics* **2008**, *179*, 683.

(587) Jithunsa, M.; Tashiro, K.; Nunes, S. P.; Chirachanchai, S. *Polym. Degrad. Stab.* **2008**, *93*, 1389.

(588) Brunklaus, G.; Schauff, S.; Markova, D.; Klapper, M.; Mullen, K.; Spiess, H. W. *J. Phys. Chem. B* **2009**, *113*, 6674.

(589) Giffin, G. A.; Castillo, F. Y.; Frech, R.; Glatzhofer, D. T.; Burba, C. M. *Polymer* **2009**, *50*, 171.

(590) Pu, H. T.; Wu, J.; Wan, D. C.; Chang, Z. H. *J. Membr. Sci.* **2008**, *322*, 392.

(591) Singh, H. P.; Kumar, R.; Sekhon, S. S. *Bull. Mater. Sci.* **2005**, *28*, 467.

(592) Itoh, T.; Sakakibara, T.; Takagi, Y.; Tamura, M.; Uno, T.; Kubo, M.; Aihara, Y. *Electrochim. Acta* **2010**, *55*, 1419.

(593) Shen, Y.; Xi, J. Y.; Qiu, X. P.; Zhu, W. T. *Electrochim. Acta* **2007**, *52*, 6956.

(594) Kruczala, K.; Szczubialka, K.; Lancucki, L.; Zastawny, I.; Gora-Marek, K.; Dyrek, K.; Sojka, Z. *Spectrochim. Acta, Part A* **2008**, *69*, 1337.

(595) Pei, H.; Hong, L.; Lee, J. Y. *J. Membr. Sci.* **2008**, *307*, 126.

(596) Choi, E. Y.; Bae, B.; Moon, S. H. *J. Phys. Chem. B* **2007**, *111*, 6383.

(597) Wang, Y. M.; Pan, Y.; Wang, Y. L.; Wu, G. P.; Wang, Y. J.; Nikitin, L. N.; Lu, X. B. *J. Supercrit. Fluids* **2008**, *44*, 62.

(598) Lee, S. W.; Bondar, Y.; Han, D. H. *React. Funct. Polym.* **2008**, *68*, 474.

(599) Li, D. R.; Chen, J. H.; Zhai, M. L.; Asano, M.; Maekawa, Y.; Oku, H.; Yoshida, M. *Nucl. Instrum. Methods, Sect. B* **2009**, *267*, 103.

(600) Fei, S. T.; Wood, R. M.; Lee, D. K.; Stone, D. A.; Chang, H. L.; Allcock, H. R. *J. Membr. Sci.* **2008**, *320*, 206.

(601) Sherazi, T. A.; Ahmad, S.; Kashmiri, M. A.; Guiver, M. D. *J. Membr. Sci.* **2008**, *325*, 964.

(602) Nguyen, T. H.; Wang, C.; Wang, X. *J. Membr. Sci.* **2009**, *342*, 208.

(603) Yamauchi, A.; Ito, T.; Yamaguchi, T. *J. Power Sources* **2007**, *174*, 170.

(604) Cho, C. G.; Kim, S. H.; Park, Y. C.; Kim, H.; Park, J. W. *J. Membr. Sci.* **2008**, *308*, 96.

(605) Fu, R. Q.; Hong, L.; Lee, J. Y. *Fuel Cells* **2008**, *8*, 52.

(606) Higa, M.; Sugita, M.; Maesowa, S. I.; Endo, N. *Electrochim. Acta* **2010**, *55*, 1445.

(607) Cui, X. J.; Zhong, S. L.; Wang, H. Y. *J. Power Sources* **2007**, *173*, 28.

(608) Lee, W.; Kim, H.; Lee, H. *J. Membr. Sci.* **2008**, *320*, 78.

(609) Aparicio, M.; Duran, A. *J. Sol-Gel Sci. Technol.* **2004**, *31*, 103.

(610) Cui, Z. M.; Liu, C. P.; Lu, T. H.; Xing, W. *J. Power Sources* **2007**, *167*, 94.

(611) Cui, Z. M.; Xing, W.; Liu, C. P.; Liao, J. H.; Zhang, H. *J. Power Sources* **2009**, *188*, 24.

(612) Yuan, W. K.; Wu, H.; Zheng, D.; Zheng, X. H.; Jiang, Z. Y.; Hao, X. P.; Wang, B. Y. *J. Power Sources* **2007**, *172*, 604.

(613) Wang, J. T.; Zheng, X. H.; Wu, H.; Zheng, B.; Jiang, Z. Y.; Hao, X. P.; Wang, B. Y. *J. Power Sources* **2008**, *178*, 9.

(614) Liu, Y. L.; Chen, W. H.; Chang, Y. H. *Carbohydr. Polym.* **2009**, *76*, 232.

(615) Wu, H.; Zheng, B.; Zheng, X. H.; Wang, J. T.; Yuan, W. K.; Jiang, Z. Y. *J. Power Sources* **2007**, *173*, 842.

(616) Wang, Y. B.; Yang, D.; Zheng, X. H.; Jiang, Z. Y.; Li, J. *J. Power Sources* **2008**, *183*, 454.

(617) Ramirez-Salgado, J. *Electrochim. Acta* **2007**, *52*, 3766.
(618) Jiang, Z. Y.; Zheng, X. H.; Wu, H.; Wang, J. T.; Wang, Y. B. *J. Power Sources* **2008**, *180*, 143.
(619) Xiang, Y.; Yang, M.; Guo, Z. B.; Cui, Z. *J. Membr. Sci.* **2009**, *337*, 318.
(620) Seo, J. A.; Koh, J. H.; Roh, D. K.; Kim, J. H. *Solid State Ionics* **2009**, *180*, 998.
(621) Goktepe, F.; Celik, S. U.; Bozkurt, A. *J. Non-Cryst. Solids* **2008**, *354*, 3637.
(622) Jin, Y. G.; da Costa, J. C. D.; Lu, G. Q. *Solid State Ionics* **2007**, *178*, 937.
(623) Seeponkai, N.; Wootthikanokkhan, J. *J. Appl. Polym. Sci.* **2007**, *105*, 838.
(624) Helen, M.; Viswanathan, B.; Murthy, S. S. *J. Membr. Sci.* **2007**, *292*, 98.
(625) Chang, Y. W.; Wang, E.; Shin, G.; Han, J. E.; Mather, P. T. *Polym. Adv. Technol.* **2007**, *18*, 535.
(626) Anis, A.; Banthia, A. K.; Bandyopadhyay, S. *J. Power Sources* **2008**, *179*, 69.
(627) Pu, H. T.; Luo, M. D.; Yang, Z. L. *Eur. Polym. J.* **2007**, *43*, 5076.
(628) Sunarso, J.; Chen, C. Y.; Wang, L. Z.; Costa, R. F. D.; Lu, G. Q.; da Costa, J. C. D. *Solid State Ionics* **2008**, *179*, 477.
(629) Sahu, A. K.; Selvarani, G.; Bhat, S. D.; Pitchumani, S.; Sridhar, P.; Shukla, A. K.; Narayanan, N.; Banerjee, A.; Chandrakumar, N. *J. Membr. Sci.* **2008**, *319*, 298.
(630) Yang, C. C.; Lee, Y. J.; Yang, J. M. *J. Power Sources* **2009**, *188*, 30.
(631) Cho, E. B.; Kim, H.; Kim, D. *J. Phys. Chem. B* **2009**, *113*, 9770.
(632) Duangkaew, P.; Wootthikanokkhan, J. *J. Appl. Polym. Sci.* **2008**, *109*, 452.
(633) Tripathi, B. P.; Saxena, A.; Shahi, V. K. *J. Membr. Sci.* **2008**, *318*, 288.
(634) Yang, T. *Int. J. Hydrogen Energy* **2009**, *34*, 6917.
(635) Yang, C. C.; Lee, Y. J. *Thin Solid Films* **2009**, *517*, 4735.
(636) Jiang, Z. Y.; Zheng, X. H.; Wu, H.; Pan, F. S. *J. Power Sources* **2008**, *185*, 85.
(637) Huang, Y. F.; Chuang, L. C.; Kannan, A. M.; Lin, C. W. *J. Power Sources* **2009**, *186*, 22.
(638) Huang, Y. F.; Hwang, B. J.; Lin, C. W. *J. Appl. Polym. Sci.* **2009**, *113*, 342.
(639) Kim, D. S.; Il Cho, H.; Kim, D. H.; Lee, B. S.; Lee, B. S.; Yoon, S. W.; Kim, Y. S.; Moon, G. Y.; Byun, H.; Rhim, J. W. *J. Membr. Sci.* **2009**, *342*, 138.
(640) Barroso-Bujans, F.; Verdejo, R.; Arroyo, M.; Lopez-Gonzalez, M. D.; Riande, E.; Lopez-Manchado, M. A. *Macromol. Rapid Commun.* **2008**, *29*, 234.
(641) Tsai, C. E.; Lin, C. W.; Hwang, B. J. *J. Power Sources* **2010**, *195*, 2166.
(642) Uma, T.; Nogami, M. *Electrochim. Acta* **2007**, *52*, 6895.
(643) Uma, T.; Nogami, M. *Fuel Cells* **2007**, *7*, 279.
(644) Uma, T.; Nogami, M. *Chem. Mater.* **2007**, *19*, 3604.
(645) Uma, T.; Nogami, M. *ChemPhysChem* **2007**, *8*, 2227.
(646) Uma, T.; Nogami, M. *J. Phys. Chem. C* **2007**, *111*, 16635.
(647) Uma, T.; Nogami, M. *J. Membr. Sci.* **2009**, *334*, 123.
(648) Uma, T.; Nogami, M. *J. Membr. Sci.* **2008**, *323*, 11.
(649) Prakash, S.; Mustain, W. E.; Park, S.; Kohl, P. A. *J. Power Sources* **2008**, *175*, 91.
(650) Ghil, L. J.; Kim, C. K.; Rhee, H. W. *Curr. Appl. Phys.* **2009**, *9*, E56.
(651) Aparicio, M.; Mosa, J.; Duran, A. *J. Sol-Gel Sci. Technol.* **2006**, *40*, 309.
(652) Colomer, M. T.; Rubio, F.; Jurado, J. R. *J. Power Sources* **2007**, *167*, 53.
(653) Tsui, E. A.; Wiesner, M. R. *J. Membr. Sci.* **2008**, *318*, 79.
(654) Marschall, R.; Sharifi, M.; Wark, M. *Microporous Mesoporous Mater.* **2009**, *123*, 21.
(655) Cavalcanti, W. L.; Marschall, R.; Tolle, P.; Kohler, C.; Wark, M.; Frauenheim, T. *Fuel Cells* **2008**, *8*, 244.
(656) Wilhelm, M.; Jeske, M.; Marschall, R.; Cavalcanti, W. L.; Tolle, P.; Kohler, C.; Koch, D.; Frauenheim, T.; Grathwohl, G.; Caro, J.; Wark, M. *J. Membr. Sci.* **2008**, *316*, 164.
(657) Mika, M.; Paidar, M.; Klapste, B.; Masinova, M.; Bouzek, K.; Vondrak, J. *J. Phys. Chem. Solids* **2007**, *68*, 775.
(658) Kato, M.; Katayama, S.; Sakamoto, W.; Yogo, T. *Electrochim. Acta* **2007**, *52*, 5924.
(659) Athens, G. L.; Ein-Eli, Y.; Chmelka, B. F. *Adv. Mater.* **2007**, *19*, 2580.
(660) Munakata, H.; Sasajima, K.; Kanamura, K. *Fuel Cells* **2009**, *9*, 226.
(661) Inoue, T.; Uma, T.; Nogami, M. *J. Membr. Sci.* **2008**, *323*, 148.
(662) Tezuka, T.; Tadanaga, K.; Hayashi, A.; Tatsumisago, M. *Solid State Ionics* **2008**, *179*, 1151.
(663) Yazawa, T.; Shojo, T.; Mineshige, A.; Yusa, S.; Kobune, M.; Kuraoka, K. *Solid State Ionics* **2008**, *178*, 1958.
(664) Onizuka, H.; Kato, M.; Shimura, T.; Sakamoto, W.; Yogo, T. *J. Sol-Gel Sci. Technol.* **2008**, *46*, 107.
(665) Tezuka, T.; Tadanaga, K.; Hayashi, A.; Tatsumisago, M. *Solid State Ionics* **2007**, *178*, 705.
(666) Nakanishi, T.; Norisuye, T.; Sato, H.; Takemori, T.; Tran-Cong-Miyata, Q.; Sugimoto, T.; Nomura, S. *Macromolecules* **2007**, *40*, 4165.
(667) Vaivars, G.; Mokrani, T.; Hendricks, N.; Linkov, V. *J. Solid State Electrochem.* **2004**, *8*, 882.
(668) Horan, J. L.; Genupur, A.; Ren, H.; Sikora, B. J.; Kuo, M. C.; Meng, F. Q.; Dec, S. F.; Haugen, G. M.; Yandrasits, M. A.; Hamrock, S. J.; Frey, M. H.; Herring, A. M. *ChemSusChem* **2009**, *2*, 226.
(669) Kumbharkar, S. C.; Islam, M. N.; Potrekar, R. A.; Kharul, U. K. *Polymer* **2009**, *50*, 1403.
(670) Mader, J.; Xiao, L.; Schmidt, T. J.; Benicewicz, B. C. *Fuel Cells II* **2008**, *216*, 63.
(671) Li, Q. F.; Jensen, J. O.; Savinell, R. F.; Bjerrum, N. J. *Prog. Polym. Sci.* **2009**, *34*, 449.
(672) He, R. H.; Li, Q. F.; Jensen, J. O.; Bjerrum, N. J. *J. Polym. Sci., Part A: Polym. Chem.* **2007**, *45*, 2989.
(673) Zhang, J. L.; Tang, Y. H.; Song, C. J.; Zhang, J. J. *J. Power Sources* **2007**, *172*, 163.
(674) Lobato, J.; Canizares, P.; Rodrigo, M. A.; Linares, J. J. *Electrochim. Acta* **2007**, *52*, 3910.
(675) Jespersen, J. L.; Schaltz, E.; Kaer, S. K. *J. Power Sources* **2009**, *191*, 289.
(676) Kim, J. H.; Kim, H. J.; Lim, T. H.; Lee, H. I. *J. Power Sources* **2007**, *170*, 275.
(677) Oono, Y.; Sounai, A.; Hori, M. *J. Power Sources* **2009**, *189*, 943.
(678) Kwon, Y.; Kim, T. Y.; Yoo, D. Y.; Hong, S. G.; Park, J. O. *J. Power Sources* **2009**, *188*, 463.
(679) Matar, S.; Higier, A.; Liu, H. T. *J. Power Sources* **2010**, *195*, 181.
(680) Kongstein, O. E.; Berning, T.; Borresen, B.; Seland, F.; Tunold, R. *Energy* **2007**, *32*, 418.
(681) Lobato, J.; Canizares, P.; Rodrigo, M. A.; Linares, J. J.; Aguilar, J. A. *J. Membr. Sci.* **2007**, *306*, 47.
(682) Lobato, J.; Canizares, P.; Rodrigo, M. A.; Linares, J. J.; Lopez-Vizcaino, R. *Energy Fuels* **2008**, *22*, 3335.
(683) Sukumar, P. R.; Wu, W. C.; Markova, D.; Unsal, O.; Klapper, M.; Mullen, K. *Macromol. Chem. Phys.* **2007**, *208*, 2258.
(684) Li, M. Q.; Shao, Z. G.; Scott, K. *J. Power Sources* **2008**, *183*, 69.
(685) Quartarone, E.; Mustarelli, P.; Carollo, A.; Grandi, S.; Magistris, A.; Gerbaldi, C. *Fuel Cells* **2009**, *9*, 231.
(686) Mustarelli, P.; Quartarone, E.; Grandi, S.; Carollo, A.; Magistris, A. *Adv. Mater.* **2008**, *20*, 1339.
(687) Suryani; Liu, Y. L. *J. Membr. Sci.* **2009**, *332*, 121.
(688) Li, Q. F.; Hjuler, H. A.; Bjerrum, N. J. *J. Appl. Electrochem.* **2001**, *31*, 773.
(689) Lin, H. L.; Chen, Y. C.; Li, C. C.; Cheng, C. P.; Yu, T. L. *J. Power Sources* **2008**, *181*, 228.
(690) Lin, H. L.; Hsieh, Y. S.; Chiu, C. W.; Yu, T. L.; Chen, L. C. *J. Power Sources* **2009**, *193*, 170.

(691) Kerres, J.; Schonberger, F.; Chromik, A.; Haring, T.; Li, Q.; Jensen, J. O.; Pan, C.; Noye, P.; Bjerrum, N. J. *Fuel Cells* **2008**, *8*, 175.

(692) Li, Q.; Jensen, J. O.; Pan, C.; Bandur, V.; Nilsson, M. S.; Schonberger, F.; Chromik, A.; Hein, M.; Haring, T.; Kerres, J.; Bjerrum, N. J. *Fuel Cells* **2008**, *8*, 188.

(693) Li, M. Q.; Scott, K. *Electrochim. Acta* **2010**, *55*, 2123.

(694) Larson, J. M.; Hamrock, S. J.; Haugen, G. M.; Pham, P.; Lamanna, W. M.; Moss, A. B. *J. Power Sources* **2007**, *172*, 108.

(695) Noy, P.; Li, Q. F.; Pan, C.; Bjerrurn, N. J. *Polym. Adv. Technol.* **2008**, *19*, 1270.

(696) Jiang, F. J.; Pu, H. T.; Meyer, W. H.; Guan, Y. S.; Wan, D. C. *Electrochim. Acta* **2008**, *53*, 4495.

(697) Ye, H.; Huang, J.; Xu, J. J.; Kodiweera, N. K. A. C.; Jayakody, J. R. P.; Greenbaum, S. G. *J. Power Sources* **2008**, *178*, 651.

(698) Hong, S. G.; Kwon, K.; Lee, M. J.; Yoo, D. Y. *Electrochem. Commun.* **2009**, *11*, 1124.

(699) Kim, T. H.; Lim, T. W.; Lee, J. C. *J. Power Sources* **2007**, *172*, 172.

(700) Yu, S.; Xiao, L.; Benicewicz, B. C. *Fuel Cells* **2008**, *8*, 165.

(701) Yu, S.; Zhang, H.; Xiao, L.; Choe, E. W.; Benicewicz, B. C. *Fuel Cells* **2009**, *9*, 318.

(702) Diaz, L. A.; Abuin, G. C.; Corti, H. R. *J. Power Sources* **2009**, *188*, 45.

(703) Wannek, C.; Kohnen, B.; Oetien, H. F.; Lippert, H.; Mergel, J. *Fuel Cells* **2008**, *8*, 87.

(704) Wannek, C.; Lehnert, W.; Mergel, J. *J. Power Sources* **2009**, *192*, 258.

(705) Kim, T. H.; Lim, T. W.; Park, Y. S.; Shin, K.; Lee, J. C. *Macromol. Chem. Phys.* **2007**, *208*, 2293.

(706) Kim, S. K.; Kim, T. H.; Jung, J. W.; Lee, J. C. *Macromol. Mater. Eng.* **2008**, *293*, 914.

(707) Qian, G. Q.; Benicewicz, B. C. *J. Polym. Sci., Part A: Polym. Chem.* **2009**, *47*, 4064.

(708) Chuang, S. W.; Hsu, S. L. C.; Hsu, C. L. *J. Power Sources* **2007**, *168*, 172.

(709) Chuang, S. W.; Hsu, S. L. C.; Yang, M. L. *Eur. Polym. J.* **2008**, *44*, 2202.

(710) Chuang, S. W.; Hsu, S. L. C.; Liu, Y. H. *J. Membr. Sci.* **2007**, *305*, 353.

(711) Qian, G. Q.; Smith, D. W.; Benicewicz, B. C. *Polymer* **2009**, *50*, 3911.

(712) Kim, T. H.; Kim, S. K.; Lim, T. W.; Lee, J. C. *J. Membr. Sci.* **2008**, *323*, 362.

(713) Xu, H. J.; Chen, K. C.; Guo, X. X.; Fang, J. H.; Yin, J. *Polymer* **2007**, *48*, 5556.

(714) Kang, S.; Zhang, C. J.; Xiao, G. Y.; Yan, D. Y.; Sun, G. M. *J. Membr. Sci.* **2009**, *334*, 91.

(715) Bai, H.; Ho, W. S. W. *J. Taiwan Inst. Chem. Eng.* **2009**, *40*, 260.

(716) Potrekar, R. A.; Kulkarni, M. P.; Kulkarni, R. A.; Vernekar, S. P. *J. Polym. Sci., Part A: Polym. Chem.* **2009**, *47*, 2289.

(717) Quartarone, E.; Magistris, A.; Mustarelli, P.; Grandi, S.; Carollo, A.; Zukowska, G. Z.; Garbarczyk, J. E.; Nowinski, J. L.; Gerbaldi, C.; Bodoardo, S. *Fuel Cells* **2009**, *9*, 349.

(718) Lee, H. S.; Roy, A.; Lane, O.; McGrath, J. E. *Polymer* **2008**, *49*, 5387.

(719) Weber, J.; Kreuer, K. D.; Maier, J.; Thomas, A. *Adv. Mater.* **2008**, *20*, 2595.

(720) Yang, J. S. A.; He, R. H.; Che, Q. T.; Gao, X. L.; Shi, L. L. *Polym. Int.* **2010**, *59*, 1695.

(721) Bhadra, S.; Kim, N. H.; Lee, J. H. *J. Membr. Sci.* **2010**, *349*, 304.

(722) Lu, S. F.; Pan, J.; Huang, A. B.; Zhuang, L.; Lu, J. T. *Proc. Natl. Acad. Sci. U. S. A.* **2008**, *105*, 20611.

(723) Shen, P. K.; Xu, C. W.; Meng, H.; Zeng, R. Anion exchange membrane fuel cells. In *Advances in Fuel Cells*; Research Signpost: India, 2005; p 149.

(724) Wang, Y.; Li, L.; Hu, L.; Zhuang, L.; Lu, J. T.; Xu, B. Q. *Electrochem. Commun.* **2003**, *5*, 662.

(725) Varcoe, J. R.; Slade, R. C. T.; Wright, G. L.; Chen, Y. L. *J. Phys. Chem. B* **2006**, *110*, 21041.

(726) Jagur-Grodzinski, J. *Polym. Adv. Technol.* **2007**, *18*, 785.

(727) Zhang, H. W.; Zhou, Z. T. *J. Appl. Polym. Sci.* **2008**, *110*, 1756.

(728) Varcoe, J. R.; Slade, R. C. T.; Yee, E. L. H.; Poynton, S. D.; Driscoll, D. J. *J. Power Sources* **2007**, *173*, 194.

(729) Modestov, A. D.; Tarasevich, M. R.; Leykin, A. Y.; Filimonov, V. Y. *J. Power Sources* **2009**, *188*, 502.

(730) Li, Y. S.; Zhao, T. S.; Liang, Z. X. *J. Power Sources* **2009**, *187*, 387.

(731) Bianchini, C.; Bambagioni, V.; Filippi, J.; Marchionni, A.; Vizza, F.; Bert, P.; Tampucci, A. *Electrochem. Commun.* **2009**, *11*, 1077.

(732) Kong, X.; Wadhwa, K.; Verkade, J. G.; Schmidt-Rohr, K. *Macromolecules* **2009**, *42*, 1659.

(733) Chempath, S.; Einsla, B. R.; Pratt, L. R.; Macomber, C. S.; Boncella, J. M.; Rau, J. A.; Pivovar, B. S. *J. Phys. Chem. C* **2008**, *112*, 3179.

(734) Hou, H. Y.; Sun, G. Q.; He, R. H.; Wu, Z. M.; Sun, B. Y. *J. Power Sources* **2008**, *182*, 95.

(735) Gu, S.; Cai, R.; Luo, T.; Chen, Z. W.; Sun, M. W.; Liu, Y.; He, G. H.; Yan, Y. S. *Angew. Chem., Int. Ed.* **2009**, *48*, 6499.

(736) Varcoe, J. R.; Slade, R. C. T. *Fuel Cells* **2005**, *5*, 187.

(737) Tang, D. P.; Pan, J.; Lu, S. F.; Zhuang, L.; Lu, J. T. *Sci. China Chem.* **2010**, *53*, 357.

(738) Nikolic, V. M.; Krkljes, A.; Popovic, Z. K.; Lausevic, Z. V.; Miljanic, S. S. *Electrochem. Commun.* **2007**, *9*, 2661.

(739) Yang, C. C.; Chiu, S. J.; Lin, C. T. *J. Power Sources* **2008**, *177*, 40.

(740) Hou, H. Y.; Sun, G. Q.; He, R. H.; Sun, B. Y.; Jin, W.; Liu, H.; Xin, Q. *Int. J. Hydrogen Energy* **2008**, *33*, 7172.

(741) Fujiwara, N.; Siroma, Z.; Yamazaki, S. I.; Ioroi, T.; Senoh, H.; Yasuda, K. *J. Power Sources* **2008**, *185*, 621.

(742) Leykin, A. Y.; Shkrebko, O. A.; Tarasevich, M. R. *J. Membr. Sci.* **2009**, *328*, 86.

(743) Sollogoub, C.; Guinault, A.; Bonnebat, C.; Bennjima, M.; Akrour, L.; Fauvarque, J. F.; Ogier, L. *J. Membr. Sci.* **2009**, *335*, 37.

(744) Yang, C. C.; Lin, C. T.; Chiu, S. J. *Desalination* **2008**, *233*, 137.

(745) Yang, C. C.; Chiu, S. J.; Lee, K. T.; Chien, W. C.; Lin, C. T.; Huang, C. A. *J. Power Sources* **2008**, *184*, 44.

(746) Qiao, J. L.; Fu, J.; Lin, R.; Ma, J. X.; Liu, J. S. *Polymer* **2010**, *51*, 4850.

(747) Suzuki, S.; Nagai, M. *Mater. Sci. Eng., B* **2009**, *161*, 138.

(748) Wu, Y. G.; Wu, C. M.; Yu, F.; Xu, T. W.; Fu, Y. X. *J. Membr. Sci.* **2008**, *307*, 28.

(749) Wu, Y. H.; Wu, C. M.; Xu, T. W.; Yu, F.; Fu, Y. X. *J. Membr. Sci.* **2008**, *321*, 299.

(750) Xiong, Y.; Fang, J.; Zeng, Q. H.; Liu, Q. L. *J. Membr. Sci.* **2008**, *311*, 319.

(751) Xiong, Y.; Liu, Q. L.; Zhu, A. M.; Huang, S. M.; Zeng, Q. H. *J. Power Sources* **2009**, *186*, 328.

(752) Xiong, Y.; Liu, Q. L.; Zhang, Q. G.; Zhu, A. M. *J. Power Sources* **2008**, *183*, 447.

(753) Wan, Y.; Peppley, B.; Creber, K. A. M.; Bui, V. T.; Halliop, E. *J. Power Sources* **2008**, *185*, 183.

(754) Yang, J. M.; Wang, H. Z.; Yang, C. C. *J. Membr. Sci.* **2008**, *322*, 74.

(755) Stoica, D.; Ogier, L.; Akrour, L.; Alloin, F.; Fauvarque, J. F. *Electrochim. Acta* **2007**, *53*, 1596.

(756) Matsuoka, K.; Chiba, S.; Iriyama, Y.; Abe, T.; Matsuoka, M.; Kikuchi, K.; Ogumi, Z. *Thin Solid Films* **2008**, *516*, 3309.

(757) Hong, J. H.; Li, D.; Wang, H. T. *J. Membr. Sci.* **2008**, *318*, 441.

(758) Scott, K.; Yu, E.; Vlachogiannopoulos, G.; Shivare, M.; Duteanu, N. *J. Power Sources* **2008**, *175*, 452.

(759) Poynton, S. D.; Kizewski, J. P.; Slade, R. C. T.; Varcoe, J. R. *Solid State Ionics* **2010**, *181*, 219.

(760) Vinodh, R.; Ilakkiya, A.; Elamathi, S.; Sangeetha, D. *Mater. Sci. Eng., B* **2010**, *167*, 43.

(761) Wan, Y.; Peppley, B.; Creber, K. A. M.; Bui, V. T. *J. Power Sources* **2010**, *195*, 3785.

(762) Park, J. S.; Park, S. H.; Yim, S. D.; Yoon, Y. G.; Lee, W. Y.; Kim, C. S. *J. Power Sources* **2008**, *178*, 620.

(763) Xiong, Y.; Liu, Q. L.; Zeng, Q. H. *J. Power Sources* **2009**, *193*, 541.

(764) Wang, G. G.; Weng, Y. M.; Zhao, J.; Chen, R. R.; Xie, D. *J. Appl. Polym. Sci.* **2009**, *112*, 721.

(765) Zhou, J. F.; Unlu, M.; Vega, J. A.; Kohl, P. A. *J. Power Sources* **2009**, *190*, 285.

(766) Xing, D. B.; Zhang, S. H.; Yin, C. X.; Yan, C.; Jian, X. *Mater. Sci. Eng., B* **2009**, *157*, 1.

(767) Wu, L.; Xu, T. W.; Wu, D.; Zheng, X. *J. Membr. Sci.* **2008**, *310*, 577.

(768) Wu, L.; Xu, T. W. *J. Membr. Sci.* **2008**, *322*, 286.

(769) Wu, Y. H.; Wu, C. M.; Xu, T. W.; Lin, X. C.; Fu, Y. X. *J. Membr. Sci.* **2009**, *338*, 51.

(770) Pan, J.; Li, Y.; Zhuang, L.; Lu, J. T. *Chem. Commun.* **2010**, *46*, 8597.

(771) Pan, J.; Lu, S. F.; Li, Y.; Huang, A. B.; Zhuang, L.; Lu, J. T. *Adv. Funct. Mater.* **2010**, *20*, 312.

(772) Zhou, J. F.; Unlu, M.; Anestis-Richard, I.; Kohl, P. A. *J. Membr. Sci.* **2010**, *350*, 286.

(773) Lin, B. C.; Cheng, S.; Qiu, L. H.; Yan, F.; Shang, S. M.; Lu, J. M. *Chem. Mater.* **2010**, *22*, 1807.

(774) Hickner, M. A.; Tudryn, G. J.; Alam, T. M.; Hibbs, M. R.; Fujimoto, C. H. *Macromol. Symp.* **2009**, *279*, 59.

(775) Hibbs, M. R.; Hickner, M. A.; Alam, T. M.; McIntyre, S. K.; Fujimoto, C. H.; Cornelius, C. J. *Chem. Mater.* **2008**, *20*, 2566.

(776) Valade, D.; Boschet, F.; Roualdes, S.; Ameduri, B. *J. Polym. Sci., Part A: Polym. Chem.* **2009**, *47*, 2043.

(777) Gu, S.; Cai, R.; Luo, T.; Jensen, K.; Contreras, C.; Yan, Y. S. *ChemSusChem* **2010**, *3*, 555.

(778) Unlu, M.; Zhou, J. F.; Kohl, P. A. *J. Phys. Chem. C* **2009**, *113*, 11416.